DETERMINATION OF PHOTOCHEMICAL PRODUCTION OF HYDROXYL RADICAL IN WHOLE (BULK) EFFLUENT USING CAFFEINE AS A PHOTOCHEMICAL PROBE

Undergraduate Research Thesis
Submitted in partial fulfillment of the requirements for graduation
With research distinction in Earth Sciences
in the undergraduate colleges of
The Ohio State University

By

Lindsey N. White
The Ohio State University
2017

Approved by

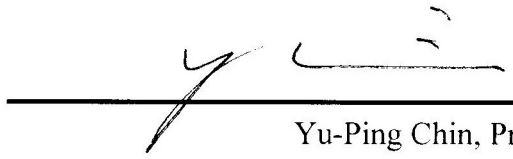

Yu-Ping Chin, Project Advisor

School of Earth Sciences

TABLE OF CONTENTS

ABSTRACT

Hydroxyl radical (•OH) acts as strong oxidizer in wastewater effluent and in natural water systems. Hydroxyl radical is a highly reactive, non-selective reactive oxygen species (ROS) that is generated in photochemical systems primarily from organic matter (OM) and nitrate (NO_3^-) and is primarily scavenged by organic matter (OM) and carbonate species. Previous research has shown that indirect photolysis via reaction with •OH is the primary pathway of caffeine degradation in effluent and natural surface water samples. An objective of this project is the support or rejection of using caffeine as a photochemical probe for measuring $[•OH]_{ss}$ in the presence of varying levels of effluent organic matter (EfOM), NO_3^-, and carbonate chemical species (measured as alkalinity) in five whole (bulk) wastewater effluent samples collected from cities surrounding Columbus, Ohio. An initial rates method was used to determine photochemical values. Alkalinity, dissolved organic carbon (DOC), nitrate, specific UV absorbance ($SUVA_{254nm}$), the absorbance at 254 nm to 365 nm (E_2/E_3 ratios) were also experimentally determined to provide additional data in this current field of research. Values for steady state ($[•OH]_{ss}$ (in units of fM)) were obtained to be 1.01±14.16 for DEL, 1.95±4.63 for MAR, 1.24±1.89 for PIC, 0.99±2.38 for NEW, and 1.14±12.57 for LON, which were within expected ranges for effluent waters (0.2-1.5 fM) via photochemical generation. This work supported research into using caffeine as a photochemical probe for hydroxyl radical with some qualifiers. Precision of the data was found to be significantly impacted based on minor adjustments to how some variables were calculated using the initial rates method.

ACKNOWLEDGEMENTS

First, I would like to thank my thesis project advisor, Yo Chin, for accepting me into his research group, and my thesis research supervisor, Molly Semones, for mentoring me in the laboratory for the experimental portion of this project. I would also like to thank Christine Pelletier for her many thoughtful reviews of my thesis. My thanks also go to Sue Welch who spent a long day teaching me how to utilize her laboratory's nutrient analyzer, Effie Miller for assistance with my UV-Vis spectra, and Anne Carey who served as my thesis course advisor. I sincerely thank the directors, superintendents and employees from Delaware, Marysville, Pickerington, Newark, and London wastewater treatment facilities who assisted me with sample acquisition. My undergraduate thesis research was supported by the Marcus J. and Lottie C. Lieberman Scholarship Fund of the School of Earth Sciences and the Swink Theatre Scholarship of the Department of Theatre, both of which I received in support of my academic education.

Further, I express my wholehearted and heartfelt thanks to Jim Knapp of the Department of Theatre. Support from him for the past five-and-a-half years has been essential to my success today. He has been one of my strongest advocates throughout my undergraduate career and I greatly appreciate his contributions to further my academic and professional development.

My appreciation also goes to all of the educators I've had who have encouraged my intellectual pursuits. I am particularly thankful for the strong female role models I have encountered in the sciences, including Rosemary Bartoszek-Loza, my introductory chemistry professor; Ava Nickerson, my high school's awesome "Ms. Frizzle"; and Beverley McMillan, my middle school science teacher who was one of the first people to make science "cool" for me. I would also like to thank a presumably non-female mentor of mine, T.P., whose guidance on the written word and whose recommendation that I apply to The Ohio State University for my undergraduate degree really influenced the direction of my educational experience and personal life path for the better.

Additionally, I would like to thank my family for supporting my educational experience. My mother, Peggy; stepfather, Robert; sisters, Season and Delaney; nieces and nephew, Alia, Raely, and Jace; Grandma Joy; and the rest of my extended family have always encouraged me to pursue my academic endeavors. Knowing that I have their support has hardened my resolve and helped me push through the challenges I have encountered along the way. My family laid the foundation for who I am today and, while they are not with us anymore, I am grateful for my Grandpa Cliff and my dad, Frank, who enriched my life in the time they were here.

I am also thankful for my friends and coworkers for the memories made and camaraderie shared over the years. My thanks go to those on The Two Towers MUD (t2tmud.org) who listened to me recount my struggles and successes throughout the thesis writing process. I would also like to thank my pets for their contributions of surprisingly intellectual personalities and cute antics. Also, a sincere thanks to CampusParc for ensuring I didn't stay too late on campus too often.

Last, but not least, I am exceedingly grateful and thankful for David Pelletier. He has been my champion, my critic, and my conversational sounding board. His unfailing support and continuous encouragement have been monumental to my success. I significantly admire and respect his ability to brighten my life on a daily basis. Thank you for everything that you do.

List of Figures

List of Tables

INTRODUCTION

Effluent discharged from municipal wastewater treatment plants (WWTPs) often introduces low levels of pollutants into natural surface waters. These micro-pollutants, including trace levels of pharmaceuticals and personal care products, can have adverse effects on downstream environmental and ecological health (Bodhipaksha et al., 2015). Wastewater treatment plants do not fully remove all contaminants before effluent discharge or reuse, and the treatment processes themselves can introduce biological and chemical contaminants that were not present in influent water, such as bacteria from activated sludge processes or elevated nitrate (NO_3^-) levels from nitrification/denitrification (Murray et al., 2010; Brooks et al., 2006).

A current area of interest in Earth Science, environmental engineering, and other fields of environmental study is the use of photochemically produced reactive intermediates, such as hydroxyl radical (•OH), that can act as strong oxidizers to degrade micro-pollutants during water treatment and through photolysis in natural water systems (Bodhipaksha et al., 2015; Dong et al., 2010). Hydroxyl radical is a highly reactive oxygen species that can be generated in photochemical systems primarily from organic matter and NO_3^- and is primarily scavenged by organic matter and carbonate species (Brezonik & Brekken, 1998; Dalrymple et al., 2010; Jacobs et al., 2011; Lee et al., 2013; Dong et al., 2010). Because it reacts quickly, •OH is often present in low steady state concentrations (10^{-18} to 10^{-15} M) and can be difficult to measure directly (White, 2000). Prior studies have used chemical probes, such as benzene and terephthalic acid (TPA), to indirectly measure hydroxyl radical steady state concentrations ($[•OH]_{ss}$) in water samples (Semones, 2017; Jacobs et al., 2011; Zhou & Mopper, 1990). Benzene, TPA, and similar probes often require additional experimental steps to use effectively, due to complications from reaction pathways and product generation, and can be hazardous to human health with prolonged use. Finding a cheap, quick, and easy way to measure $[•OH]_{ss}$ in environmental samples is part of ongoing research to help characterize the importance and impact of •OH in water systems.

Caffeine is inexpensive, non-toxic, easily obtained, highly soluble in water, and selective for measuring •OH, based on previous studies (Semones, 2017; Dong et al., 2010). Other studies using caffeine as a photochemical probe for •OH have focused on such topics as characterizing effluent and dissolved organic matter, studying quantum yields, and determining chemical

kinetics information, usually with regard to natural freshwater and seawater samples (Dong et al., 2010; Bodhipaksha et al., 2015; Lee et al., 2013). In the current study, caffeine is used as an indirect photochemical probe in whole (bulk) wastewater effluent samples for measuring $[\bullet OH]_{ss}$ with an initial rates kinetics approach. Whole water effluent samples, rather than isolates, were analyzed to support whether caffeine works as a photochemical probe in the presence of heterogeneous chemical species typically present in treated wastewater. Effluent water samples were collected after final treatment processes and before release into local waterways. Effluent samples were not chemically altered after collection other than to adjust the acidity of samples prepared for irradiation in photolysis experiments to pH 7.

This study includes comparison of $[\bullet OH]_{ss}$ values to reported literature values, and notes each samples' relative effluent organic matter (EfOM) as characterized by each sample's optical properties, NO_3^-, and alkalinity. Values for $[\bullet OH]_{ss}$ were experimentally determined via an initial rates kinetics approach using caffeine as the photochemical probe, which was quantified with high performance liquid chromatography (HPLC) instrumentation. The relationship of $[\bullet OH]_{ss}$ to EfOM was explored by assessing each effluent sample's dissolved organic carbon (DOC) and optical properties from ultraviolet-visible spectrophotometry (UV-Vis). Alkalinity information was obtained from titration with sulfuric acid (H_2SO_4) solution using Gran Titration and other computational methods. Nitrate was measured on nutrient analyzer instrumentation.

An objective of this project is the support or rejection of using caffeine as a photochemical probe for measuring $[\bullet OH]_{ss}$ in the presence of varying levels of EfOM, NO_3^-, and carbonate chemical species (measured as alkalinity). Both EfOM and NO_3^- are important •OH generating species, while organic matter and carbonate species are important natural scavengers of •OH (Dong & Rosario-Ortiz, 2012; Lee et al., 2013; Bodhipaksha et al., 2015; Brezonik & Brekken, 1998; Gligorovski et al., 2015). This study could support research in water quality monitoring, advanced oxidation processes, and in helping to characterize the fate and transport of chemically complex effluent water during treatment and after release into natural waterways.

BACKGROUND INFORMATION

WASTEWATER EFFLUENT

Wastewater effluent, as characterized in this study, is water that has been treated through physical, chemical, and biological treatment processes by wastewater treatment plants (WWTPs). For this study, effluent was collected for experimentation after final treatment and before release into local waterways from five different WWTPs serving cities surrounding Columbus, Ohio. Wastewater can come from a variety of municipal, industrial, and agricultural origins and can include contributions from storm and surface water. These sources introduce a number of pollutants into wastewater, such as household chemicals, raw sewage, leaf litter, fertilizers, solid trash, and more.

Wastewater treatment facilities utilize primary, secondary, and tertiary treatment processes to remove unwanted contaminants (Office of Water, 1998). A standard for most WWTPs during primary treatment is to remove solid waste from water entering the treatment facility (influent water). Secondary treatment removes dissolved and suspended organic matter and other nutrients using a variety of biological, chemical, and physical processes. Tertiary treatments can vary and are not used in all WWTPs, but typically encompass disinfection processes, such as chlorination and ultraviolet radiation. Many WWTPs operate tertiary disinfection only during the recreational season from May through October (Batt et al., 2007). The WWTPs in this study all use some variation of the following treatment steps: screening, grit removal, pre-treatment aeration, flow equalization, primary clarifiers, secondary treatment (activated sludge processes, nitrification and denitrification, and other chemical and biological treatments), final settling tanks, ultraviolet disinfection/chlorination, and post-aeration.

Screening removes large solid objects, such as cans, branches, and plastics from influent. Grit removal removes smaller solid particles, such as food waste, sand, and gravel through sedimentation by slowing the velocity of incoming water to allow larger particles to settle out of suspension. Pre-treatment aeration adds oxygen to decrease the biochemical oxygen demand (BOD—the amount of dissolved oxygen needed by aerobic organisms to break down organic material) to aid in the breakdown of ammonia and other chemical species. Equalization basins retain influent and release it at a steady flow into the next parts of the treatment process, which

can be important during times of heavy rain to avoid flooding the system. Primary clarifiers remove suspended solids by reducing the speed of the flow even more to allow the suspended solids to settle out of suspension. Some facility designs support skimming the top of the water at the primary clarifying stage to remove oil and grease that has risen to the top of the tank due to having a lower density than water. Secondary treatment usually consists of activated sludge processes where water is aerated and mixed with bacteria after primary treatment to allow bacteria to break down organic matter. Any products that settle out with the bacteria form the activated sludge, which can be re-used to introduce bacterial loads to fresh influent or can be removed and treated as solid waste. Secondary clarifiers and/or final settling tanks assist with removing excess bacteria and any remaining sedimentation. Ultraviolet disinfection or chlorination kills harmful bacteria if tertiary disinfection processes are present (Office of Water, 1998). The effluent water is then released into local waterways, usually nearby streams or rivers.

However, even primary, secondary, and tertiary treatment processes do not fully remove all contaminants from wastewater and the impacts of these contaminants on human health and on fresh and salt water environments is of current interest in research (Murray et al., 2010; Brooks et al., 2006). As a result, effluent from WWTPs into local waterways consists of a complex heterogeneous mixture containing low concentrations of contaminants, such as pharmaceuticals, personal care products and other synthetic organic compounds, which could potentially have adverse ecological and environmental effects downstream (Bodhipaksha et al., 2015; Batt et al., 2007; Lee et al., 2013). These contaminants enter local waterways where effluent is discharged from WWTPs and can accumulate, attenuate (be reduced/lost), or otherwise be transformed by biological and/or chemical means in ways that could potentially be hazardous or beneficial to the local environment (Semones, 2017). Dissolved organic matter (DOM) can heavily influence the fate of these contaminants (Semones, 2017).

Effluent organic matter (EfOM) forms the bulk of this complex heterogeneous mixture. Effluent organic matter is of particular interested because it is similar to, and yet different from, DOM present in natural water systems. Effluent organic matter is composed of refractory organic matter originating from drinking water sources, soluble microbial products derived during biological treatment of wastewater, and trace organic contaminants (Lee et al., 2013). Dissolved organic matter has been characterized as a complex mixture of aromatic and aliphatic

hydrocarbon structures that have attached amide, carboxyl, hydroxyl, ketone, and various minor functional groups derived from plant detritus and algal precursors (Leenheer & Croué, 2003). Aromatic compounds are those that form cyclic or planar molecules that have a ring of resonance bonds that exhibit more stability than other geometric configurations of the same set of molecules. Aliphatic compounds form open chains, rather than aromatic rings.

Effluent organic matter has previously been characterized as being relatively hydrophilic with a high proportion of protein-like substances and can include fractions of polysaccharides, proteins, amino sugars, nucleic acids, humic and fulvic acids, organic acids, and cell components (Lee et al., 2013). Humic and fulvic acids are relatively hydrophobic acids that are components of soil and dissolved organic matter (Dalrymple et al., 2010). Degradation of organic matter forms humic substances, which are a complex mixture of many different acids that are generally resistant to further transformation. These include fulvic acids that generally have a lower molecular mass and remain in solution at all pH and humic acids that are insoluble under acidic conditions. Operationally defined humic substances typically compose about 50% of the DOM of an average river (Leenheer & Croué, 2003).

Total organic carbon (TOC) has been shown to be the most comprehensive measurement to quantify organic matter in aquatic systems (Leenheer & Croué, 2003). Total organic carbon is often measured as dissolved organic carbon (DOC), which represents the fraction of organic carbon that remains soluble after filtration through a 0.45 μm pore-size filter. The utilization of DOC measurements as a proxy for TOC can be done due to the fact that particulate organic carbon (organic carbon filtered out of solution using a 0.45 μm pore-sized membrane) usually represents a minor fraction (below 10%) of the TOC and due to organic contaminants representing an insignificant fraction of TOC (Leenheer & Croué, 2003). DOC concentrations range from 0.1 mg-C L^{-1} in groundwater to 50 mg-C L^{-1} in bogs. DOC concentrations are typically within the range of 5 to 20 mg-C L^{-1} for water samples, with an average for WWTP samples between 6 to 8 mg-C L^{-1} (Bodhipaksha et al., 2015; Dong et al., 2010; Dong & Rosario-Ortiz, 2012; Lee et al., 2013).

The optical properties for effluent samples can help describe the photoreactivity of organic matter and can help characterize complex EfOM by complementing measured DOC values (Bodhipaksha et al., 2015; Leenheer & Croué, 2003). Optical spectra (absorbance of the

analyte at different wavelengths present in light) are generally broad and featureless, due to the variety of chromophores that do not possess easily distinguishable spectra when analyzed (Leenheer & Croué, 2003). However, specific ultraviolet absorbance at 254 nm ($SUVA_{254nm}$) values can describe the attenuation, or absorbance, of light on a per carbon basis in the water column and have been strongly correlated with the hydrophobic organic acid fraction of DOM (Bodhipaksha et al., 2015; Hansen et al., 2016). Weishaar et al. (2003) and Leenheer and Croué (2003) noted that $SUVA_{254nm}$ is a good indicator of the hydrophobic humic fraction of DOC in water samples and thus is a useful proxy for DOM aromatic content, where a higher number is typically associated with greater aromatic content. As noted by Leenheer et al. (2003) high nitrate content in low DOC waters may interfere with SUVA measurements as does dissolved iron (Weishaar et al., 2003). Values for $SUVA_{254nm}$ for effluent samples have been measured in other studies to fall within the range of 1 to 2 L mg^{-1} m^{-1} (Dong & Rosario-Ortiz, 2012; Hansen et al., 2016; Lee et al., 2013).

Another measurement obtained from optical spectra is the ratio of DOM absorbance at 254 nm divided by the absorbance at 365 nm (E_2/E_3 ratio). The E_2/E_3 ratio in water samples has been related to quantum yields of photochemically produced reaction intermediates (Bodhipaksha et al., 2015). The correlation of quantum yields with other chemical, photochemical, and optical properties of DOM is also a current area of research in looking into the possibility of using spectroscopic data to provide insight into photochemical reaction rates of DOM and EfOM (Dalrymple et al., 2010). Quantum yield values of a chemical species indicate the percentage of light absorbed by the chemical species, which results in a specific reaction (or photophysical process such as fluorescence). Characterizing the complex heterogeneous mixture that effluent is composed of is important for understanding how effluent interacts with natural waterways and could help shape designs for new water treatment processes (Leenheer & Croué, 2003). Reported literature values for effluent samples range from 0.41 to 8, with most falling between 4.8 and 5.7 (Bodhipaksha et al., 2015; Lee et al., 2013).

Hydroxyl Radical

One current area of interest is the characterization of photochemically produced reactive intermediates that are known to break down lingering low-level contaminants through indirect

photolysis (Bodhipaksha et al., 2015). Photolysis refers to the degradation or breakdown of molecules due to the presence of light. Indirect photolysis refers to the degradation of a molecule through a photochemically generated intermediate that was likely formed from the direct photolysis of DOM or other chemical species, e.g., nitrate, whereas direct photolysis refers to the transformation of a compound through the absorption of photons, generally from sunlight, as shown in Figure 1 (Dong & Rosario-Ortiz, 2012; Semones, 2017).

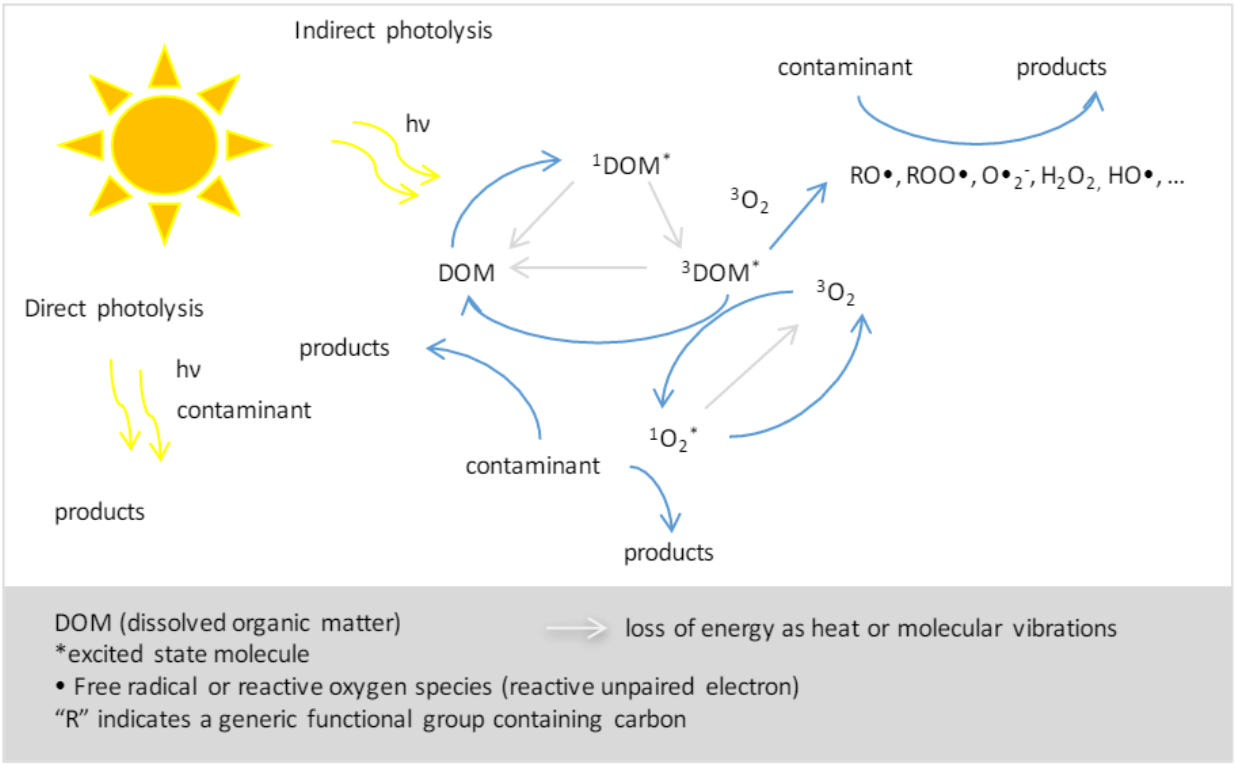

Figure 1. Illustration of direct photolysis (left) and indirect photolysis (right) processes via sorption of light by EfOM/DOM (Semones, 2017).

These photochemically produced reactive intermediates can be generated from DOM and EfOM via irradiation in the lab or in sunlit natural surface waters and include reactive intermediates such as triplet-state excited organic matter ($^3OM^*$), singlet oxygen ($^1O_2$), superoxide anion ($O_2•^-$), peroxyl (ROO•), phenoxyl (RO•), and hydroxyl radicals (•OH) (Bodhipaksha et al., 2015; Brezonik & Brekken, 1998; Dalrymple et al., 2010; Jacobs et al., 2011; Lee et al., 2013; Gligorovski et al., 2015). These reactive intermediates are of interest

because of their impact on the photochemistry taking place in natural waterways and of their use in advanced oxidation processes (AOPs) to remove contaminants from wastewater during water treatment (Dong & Rosario-Ortiz, 2012). Advanced oxidation processes are a set of chemical treatment procedures designed to degrade the more difficult to remove organic matter from aqueous solutions by oxidation through reactions with such species as hydroxyl radical.

Of particular interest is the study of •OH in whole water effluent. Hydroxyl radical is known to be a highly reactive oxidant and one of the more important intermediates in water photochemistry (Brezonik & Brekken, 1998; Dong et al., 2010). Because it is a highly reactive and non-selective oxidizing species, •OH is present at very low concentrations and is usually measured indirectly using a chemical probe (Dong & Rosario-Ortiz, 2012). As •OH is produced, it is also being scavenged/consumed by other chemical species. Hydroxyl radical production can occur from photolysis of organic matter and NO_3^-, in addition to several other mechanisms (Bodhipaksha et al., 2015; Brezonik & Brekken, 1998; Brinkmann et al., 2003; Jacobs et al., 2011). Previous studies have indicated that humic substances in DOM and EfOM are good sources for •OH via highly photo-reactive chromophores (an atom or group of atoms capable of absorbing a photon), which can produce hydroxyl radicals (Lee et al., 2013). EfOM/DOM, carbonate, and bicarbonate have been shown to scavenge hydroxyl radical (Bodhipaksha et al., 2015; Brezonik & Brekken, 1998; Dong & Rosario-Ortiz, 2012). Organic matter can thus be a major sink for •OH as well as a major producer, especially in waters with low NO_3^- levels (Semones, 2017).

Alkalinity measurements can help explain high natural scavenging rates, as alkalinity corresponds to and is affected by levels of carbonate, bicarbonate and hydroxide in water samples (Rounds & Wilde, 2002). Dong et al. (2012) reported two alkalinity values for effluent samples at 1.2 and 1.8 $m_{eq}\ L^{-1}$. Alkalinity is essentially a measurement of a solution's ability to neutralize acids to a specific endpoint defined by the carbonate system. Alkalinity is an important parameter for WWTPs as it can help determine the effectiveness of the treatment process on wastewater and can help indicate how the processes could be controlled for the wastewater to be more receptive to various types of treatments (Rounds & Wilde, 2002).

Measurements for •OH are of interest not only because of its potential use in AOPs, but also because effluent released into local waterways typically has higher than normal surface

water concentrations of NO_3^- due to wastewater treatment processes. This can lead to a potential increase in oxidation taking place within effluent and within the receiving surface water due to increased levels of •OH upon irradiation. Literature values for NO_3^- found in effluent have been reported in the range from <0.01 to 15.8 $mg_N\ L^{-1}$ (Dong et al., 2010; Lee et al., 2013). Nitrate as low as 0.1 mM has been shown to contribute significantly to •OH production (Semones, 2017).

CAFFEINE

Previous research has found that caffeine degrades slowly through direct photolysis, and that indirect photolysis via reaction with •OH is the primary pathway of caffeine degradation in sunlit effluent and natural surface water samples (Jacobs et al., 2011). Caffeine is non-toxic, inexpensive, selective for •OH, soluble, and is easily measured. This makes caffeine a good •OH probe for research in characterizing •OH in water samples assuming that research into its use as a photochemical probe proves that it does indeed measure accurately without interfering factors. Previous probes for •OH include such compounds as cumene, benzene, benzoic acid, butylchloride, methanol, and terephthalic acid (White, 2000). Other methods to measure •OH have included electron paramagnetic resonance, laser-induced fluorescence, and long-path optical spectroscopies, however these methods can only measure •OH qualitatively due to the low steady state concentrations and quick reaction time of hydroxyl radical (White, 2000).

Zhou and Mopper (1990) first established the initial rates method used to measure the steady-state concentration of ($[•OH]_{ss}$) in seawater and freshwaters, which is noted in Appendix B and in the methodology section. Parameters measured by the initial rates method include the overall production rate for •OH ($P_{•OH}$, units of Ms^{-1}) and the overall natural scavenging rate (k'_{ns}, units of s^{-1}). The second order (bimolecular) rate constant (k_p) used for caffeine and •OH is described in literature as 5.9E09 $M^{-1}s^{-1}$ and is similar to other reported literature values (Shi & Dalal, 1991). The production rate in whole (bulk) water effluent samples takes into account the heterogeneous variety of chemical species that can produce •OH, and by the same token the natural scavenging rate takes into account all of the chemical species that react with or use up hydroxyl radical.

In this work five municipal wastewater effluent samples were analyzed for $[•OH]_{ss}$, $P_{•OH}$, and k'_{ns} using caffeine as a photochemical probe in bulk effluent samples containing organic

matter, NO_3^-, carbonate, bicarbonate, and other chemical and biological species. Several assumptions are entertained during this experiment.

It was assumed that (Semones, 2017):

- caffeine attenuation primarily comes from selective reaction with •OH
- direct photolysis to caffeine minimally changes the caffeine system
- caffeine probe concentration affects scavenging and measured $[•OH]_{ss}$ values
- the presence of DOM/EfOM impacts the production of •OH from NO_3^- thus resulting in a co-dependent relationship from these two sources

In this study, experimentally obtained $[•OH]_{ss}$ was compared with reported literature values and differences between the effluent samples were compared from the other measured water parameters.

EXPERIMENTAL METHODOLOGY

CHEMICALS

Caffeine (99.7%) was obtained from Alfa Aesar. HPLC-grade methanol, concentrated hydrochloric acid (Certified ACS Plus, 36-37%), and sulfuric acid (Certified ACS Plus, 95–98%) were obtained from Fisher Chemical. Total Organic Carbon (TOC) Calibration Standard (Certified Reference Material, 1000 $mg_C\ L^{-1}$) was obtained from Sigma-Aldrich. Milli-Q water (18.2 MΩ, Millipore Inc.) and Reverse Osmosis water (Millipore Inc.) were obtained from on-site instrumentation.

SAMPLING METHODOLOGY

Five full-scale WWTPs surrounding Columbus, Ohio were selected for this study. The facilities of Delaware (DEL), London (LON), Marysville (MAR), Newark (NEW), and Pickerington (PIC) were chosen due to their radial distribution from Columbus, Ohio (Fig. 2). Schematic diagrams of these facilities and WWTP characteristics are recorded in Appendix A. A grab sample was collected from one facility each week spanning approximately 1.5 months. Grab samples were collected due to limited access to WWTPs and due to experimental photolysis design space limitations. Sample collection, filtration, and titration occurred on the same day to minimize pH errors due to possible changes in the samples during storage.

Effluent collection occurred at each facility's designated sampling location, after final wastewater treatment and before release into local waterways. A 1-L Pyrex media storage bottle was rinsed with sample effluent from a continuously flowing collection location before the container was filled with sample. Effluent temperature, pH, and dissolved oxygen values were recorded in Appendix A as provided by each facility on the day of collection. Effluent samples were transported from facility to laboratory out of direct sunlight.

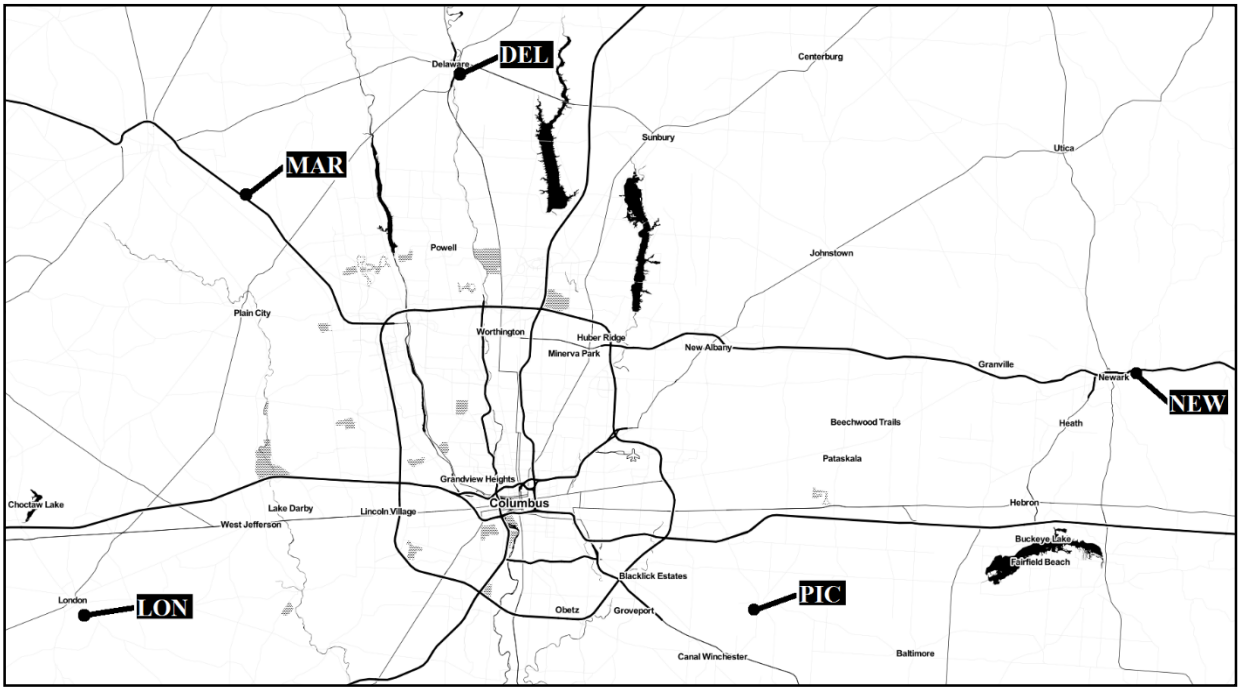

Figure 2. An adapted Stamen Standard Toner map showing effluent sampling locations at WWTPs surrounding Columbus, Ohio.[1] Delaware (DEL), Newark (NEW), Pickerington (PIC), London (LON), and Marysville (MAR) treatment facility locations are shown.

FILTRATION

Samples were filtered through 0.7 µm pore-size glass fiber filters (Grade GF/F, Whatman) after rinsing the filters with 1000 mL Milli-Q water. Filtration of each effluent sample was completed within five hours of sample collection. Filtered effluent samples were kept in the dark at room temperature during use and in the dark at 4°C when stored. Aliquots of filtered effluent were frozen and analyzed later for nitrate.

ALKALINITY

Titrations to measure alkalinity were performed using the Gran Function Plot Method as specified by the United States Geological Survey for burette titrations (Rounds & Wilde, 2002). An effluent sample of approximately 100 mL was used for each titration with 0.01703 N H_2SO_4 (prepared and standardized by Semones, M. on 9/7/2016). A pH detection probe was calibrated

[1] *Source:* Map tiles by Stamen Design, under CC BY 3.0. Data by OpenStreetMap, under ODbL. http://maps.stamen.com

with pH 4 and 7 standard buffers. The Gran Function F_1 and alkalinity equations were used to determine the bicarbonate equivalence point and alkalinity in Excel manually. The Excel-based LINEST function was used to calculate titrant volume used to reach the bicarbonate equivalence point. From the bicarbonate equivalence point, alkalinity was calculated in milliequivalents per litre ($m_{eq}\,L^{-1}$).

Five additional alkalinity values were obtained from computational analysis of the titration data using the advanced speciation method for Inflection Point, Theoretical Carbonate Titration Method 1, Theoretical Carbonate Titration Method 2, and Gran Functions F_1 and F_3 provided by the U.S. Geological Survey and U.S. Department of the Interior Online Alkalinity Calculator (Rounds S., Web-based Alkalinity Calculator, 2013). All alkalinity calculations assume that carbonate and bicarbonate account for all of the alkalinity measured in the sample (Rounds S., Methods for Alkalinity Calculator, 2013). Other chemical species with acid/base properties in the effluent samples could introduce error into the calculations if present in significant concentrations. It was assumed that the chemistry of carbonic acid is the primary contributor to alkalinity and that concentrations of additional chemical species are small relative to the magnitude of carbonate species.

Dissolved Organic Carbon

Each effluent sample was analyzed for its concentration of dissolved organic carbon (DOC) with a Shimadzu TOC-V_{CPN} instrument in NPOC (non-purgeable organic carbon) mode. In this mode, inorganic carbon is purged from the sample before measuring the total organic carbon (TOC). Because the samples were filtered, TOC is the same as DOC concentration, expressed in milligrams carbon per litre (mg-C L^{-1}). A Milli-Q water calibration blank was used before each analysis to monitor for potential contamination and to monitor the calibration curve baseline. Check standards of approximately 6 mg-C L^{-1} were made from TOC Calibration Standard (1000 mg-C L^{-1}). Check standard concentrations were within 2.5% of calculated values. At least two measurements were taken for each sample and the values averaged to give the final DOC concentrations.

Optical Properties

Absorption spectra were collected from 190 to 800 nm in 1-cm quartz cuvettes on a dual-beam Ultraviolet/Visible (UV-Vis) Shimadzu UV-1800 Series spectrophotometer with a 1-nm spectral bandwidth. Cuvettes were stored in and cleaned with methanol and rinsed with Milli-Q water between scans. Two aliquots of each sample were measured to obtain two independent spectra per sample. Samples included both effluent filtered on the day of collection and working solution effluent exposed to eight hours of irradiation, as detailed in the photolysis procedure.

Specific ultraviolet absorbance ($SUVA_{254nm}$) values (L mg^{-1} m^{-1}) were calculated by dividing the calculated UV absorbance in the sample in absorbance units (UV-Abs (UVA as a variable, not to be confused with types of ultraviolet radiation like UVA, UVB, etc.) in cm^{-1}) at 254 nm by the DOC concentration of each effluent sample (Potter & Wimsatt, 2009). UVA was determined by dividing the measured UV absorbance at 254 nm of the filtered sample (A) by the quartz cell path length (d in cm). E_2/E_3 ratios were obtained by dividing the absorbance at 254 nm by the absorbance at 365 nm.

$$\text{SUVA (L mg}^{-1}\text{M}^{-1}) = \frac{\text{UVA (cm}^{-1})}{\text{DOC (mg L}^{-1})} * 100 \text{ cm m}^{-1}$$

$$\text{UVA (cm}^{-1}) = \frac{\text{A}}{\text{d (cm)}}$$

$$\frac{E_2}{E_3} = \frac{A_{254\text{ nm}}}{A_{365\text{nm}}}$$

Nitrate Determination

A Skalar San^{++} System was used to obtain ion concentrations of nitrite and nitrate plus nitrite (nitrate+nitrite) following methods provided by the manufacturer (Analysis: Nitrite, 2008; Analysis: Nitrate+Nitrite, 2008). An aliquot of each effluent sample was frozen the day of sample collection to help preserve nutrient concentrations for analysis. Tested samples included both frozen effluent samples and non-frozen effluent samples stored at 4°C. Calibration solutions for nitrite analysis were 0, 100, 200, and 500 ppb nitrite as nitrogen. Calibration solutions for nitrate+nitrite analysis were 0, 500, 1000, and 2000 ppb nitrite as nitrogen. Due to the high concentration of nitrate in effluent samples, samples were diluted by a factor of ten for nitrate

plus nitrite analysis. Undiluted samples were used for nitrite analysis. Two vials of each sample type were measured in duplicate. This resulted in four measurements per type of sample. Reported nitrate values were obtained by subtraction of nitrite from nitrate+nitrite values and conversion of units to milligrams per litre as nitrogen ($mg_N\ L^{-1}$) and millimoles per litre as nitrate ion (mM) for comparison to other studies that used one or the other reporting methods.

Photolysis Procedure

The initial rates photolysis method was adapted with permission from the Semones, M. paper on the "Dynamics in the reactivity and photochemical production of hydroxyl radical in treated wastewater effluent and aquatic dissolved organic matter" (Semones, 2017).

A stock solution of caffeine (10 mM) was made from powdered caffeine reagent and Milli-Q water and was used to generate calibration standards for photolysis experiments. Calibration standards created for each experiment ranged from 5 to 20 µM. The stock caffeine solution was also used to add ("spike") caffeine into working solutions to act as a probe for hydroxyl radical. Three diluted HCl solutions (1 M, 0.1 M, and 0.01 M) were prepared from concentrated hydrochloric acid to adjust working solutions to pH 7 for photolysis experiments. All solutions were prepared using Milli-Q water and stored in a dark refrigerator at 4°C. Caffeine stock solution was added to aliquots of the Delaware (DEL) working solution to yield caffeine probe concentrations of 5, 10, and 15 µM. Caffeine stock solution was added to the other four effluent sample working solutions (LON, MAR, NEW, and PIC) to yield probe concentrations of 10, 15, and 20 µM.

Aliquots of the spiked solutions were transferred to quartz phototubes (i.d. = 0.9 mm), sealed with Teflon tape-wrapped O-rings and ground quartz lids, and clamped shut. Dark controls in 1-mL borosilicate HPLC vials for all three caffeine levels, for each time point, were wrapped in foil and irradiated along with the phototubes. Irradiation occurred in an Atlas Suntest CPS^+ equipped with a solar sunlight filter (Filter H, Atlas Technologies) and a Xenon arc lamp set to 500 Wm^{-2} and temperature monitored at an average of 23.4°C (range: 19–25°C) across all experiments. Irradiance was monitored using a radiometer (VWR Ultraviolet Light Meter 21800-016) during experiments, with measurements taken at each time point. Light intensity varied less than ±8% from the average of all intensity measurements taken for all photolysis experiments.

Two phototubes containing aliquots for each caffeine level and respective dark controls were removed at one, four, and eight hours elapsed time and stored in the dark at 4°C for next day HPLC analysis. Phototubes and dark controls were rotated within the Atlas Suntest CPS$^+$ at 30 minutes and two hours elapsed time to help ensure homogenous exposure to irradiation.

Irradiated samples were measured with a Waters 1515 Isocratic HPLC Pump connected in line with a Waters 717plus Autosampler and Waters 2487 Dual λ Absorbance Detector. Caffeine was separated on a Restek Pinnacle DB C18 column (150 x 4.6 mm, 5 µm) using a 30:70 methanol:Milli-Q water mobile phase, 50 µL injection volume, 1 mL min^{-1} flow rate, a detection wavelength of 275 nm, and a 6 minute retention time. Each measurement of peak area and retention time for unreacted caffeine was taken in duplicate.

Data collected from this experiment were analyzed with permission using the initial rates method detailed in Semones, M.'s paper as noted in Appendix B, first established by Zhou and Mopper (Semones, 2017; Zhou & Mopper, 1990). Peak areas were averaged from duplicate injections of each vial and converted to concentration of caffeine (M) using a calibration curve respective for each effluent sample. Peak area values that were clearly the result of instrumental or preparatory error were removed from analysis and are noted in Appendix C. The calibration curve for each effluent sample was created using the Excel-based LINEST function, where the linear regression was forced through zero (intercept = 0). This reflects that at a caffeine concentration of zero, no peak area should be observed. The concentration of each vial for the three different time points was plotted against the time of those time points (concentration (M) vs time (s) for each caffeine spike level) with the irradiated vials as one data set and the non-irradiated "dark vials" as a second data set on the same graph. Linear regressions were performed for each data set using the Excel-based LINEST function. The linear regressions for the dark vials were used to calculate the initial concentration at time point T0. The rate of caffeine consumption (R_p) was calculated from the linear regression of the irradiated caffeine vials, where y-values equaled the concentration of probe as measured after irradiation, x-values equaled the length of irradiation time in seconds, and intercept was determined by the LINEST function. Thus, the slope of the line (m) in units of Ms^{-1} was calculated. The consumption of probe, R_p, was found by multiplying the slope by a factor of -1. As the values used in this calculation result

in a negative rate, this multiplication factor is needed to convert the rate into a positive number, which denotes consumption of the probe.

Once all three R_p values were obtained for each of the three caffeine levels for the effluent sample, 1/Rp (sM^{-1}) was plotted versus 1/[probe] (M^{-1}). Using the LINEST function, the parameters of intercept (b in units of sM^{-1}) and slope (m in units of s) were found. The production rate of hydroxyl radical ($P_{\bullet OH}$ in units of Ms^{-1}), natural scavenging rate (k'_{ns} in units of s^{-1}), and hydroxyl radical steady state concentration ($[\bullet OH]_{ss}$ in units of M) were found by the following equations:

$$P_{\bullet OH} = \frac{1}{b}$$

$$k'_{ns} = \frac{m\, k_p}{b}$$

$$[\bullet\, OH]_{ss} = \frac{P_{\bullet OH}}{k'_{ns}}$$

The variable k_p is the bimolecular rate constant of caffeine and hydroxyl radical as described in literature at 5.9E+9 $M^{-1}s^{-1}$ (Shi & Dalal, 1991). Error for the slope and intercept of curves generated and used for $P_{\bullet OH}$, k'_{ns}, and $[\bullet OH]_{ss}$ calculations were determined using the Excel-based LINEST function and arithmetic error propagation, rather than as standard deviation of multiple experimental measurements or standard error (SE).

Additional Notes

Comparative information regarding the WWTPs is provided in Appendix A. Supplemental methodology can be found in Appendix B. Raw data are recorded in Appendix C.

RESULTS

CHARACTERIZATION OF SAMPLES

The water quality parameters for the five collected effluent samples are presented in Table 1. Values for reported pH as provided by each WWTP on the day of collection compared to pH values recorded during titration for alkalinity were within ±0.9 units of each other, with the largest difference being a higher pH measured for the LON sample in the lab as compared to the reported value. Alkalinity ($m_{eq}\ L^{-1}$) was recorded as 2.26±0.03 (range: 2.59:2.68) for DEL, 2.78±0.10 (range: 2.71:2.99) for MAR, 8.67±0.16 (range: 8.57:8.99) for PIC, 4.14±0.20 (range: 3.76:4.29) for NEW, and 3.55±0.06 (range: 3.50:3.67) for LON effluent, where the range lists the lowest and highest alkalinity values calculated from each titration using six different computational methods. Statistical error was reported as the standard deviation among different calculation methods for each sample rather than as standard deviation of multiple titrations of each sample. Therefore, it should be noted that the six different computational methods may not have a normal distribution, which is why the range was provided.

Values for the MAR Gran Function F_3 and NEW Gran Function F_1 from the Online Alkalinity Calculator indicated warnings that the carbonate titration curve and method assumptions did not fit the data well, giving a mean absolute titrant volume error of 1.04 and 1.18 mL respectively. These results indicate that other chemical species could have been neutralized in the titrations and that these values should be treated as estimates, as recommended by the Online Alkalinity Calculator. Due to the potential presence of non-carbonate species in whole water samples, alkalinity results are treated as estimates for relative comparison, and it is assumed that carbonate and bicarbonate contribute predominantly to measured alkalinity values. Other computational methods that take into account additional titratable chemical species contributing to alkalinity, especially considering the complex heterogeneous mixture of wastewater effluent and EfOM, are recommended for more detailed analysis, but were not used in this experiment.

The DOC values (mg-C L^{-1}) were recorded as 5.8 for DEL, 7.4 for MAR, 28.2 for PIC, 6.7 for NEW, and 4.5 for LON. Check standard (~6 mg-C L^{-1}) error measurements were used to report DOC error as percent error for the experimental method by comparison of theoretical

values for check standard solutions to measured instrumental values. Percent error for DOC values was determined to be 2.5%. DOC values were used in finding SUVA values as noted in the Optical Properties section in the methodology.

Alkalinity and DOC values for the Pickerington facility were noted to be higher than values from the other four WWTPs, with percent differences from the Pickerington effluent values to the next highest alkalinity and DOC values being 70.7% and 116.9% respectively. [2]

Concentrations for nitrate+nitrite and nitrite were calculated for frozen and non-frozen effluent samples from the five WWTP effluent samples and were converted to NO_3^- concentrations as nitrogen and as nitrate ion for each effluent sample. Nitrate values were reported in these two different units for comparison to other studies that used one or the other unit for reporting their results. Nitrate ($mg_{NO3\text{-}N}\,L^{-1}$) was found as 6.87±0.03 for DEL, 12.37±0.16 for MAR, 4.18±0.02 for PIC, 10.11±0.28 for NEW, and 10.29±0.07 for LON effluent samples. Error was calculated as the standard deviation of eight replicate measurements (four per frozen and four per non-frozen sample type per effluent sample), arithmetically propagated for the subtraction of nitrite and unit conversion. Nitrate ion (mM) was found as 0.48 for DEL, 0.88 for MAR, 0.30 for PIC, 0.72 for NEW, and 0.73 for LON. Pickerington effluent resulted in the lowest nitrate concentration levels, but had significantly higher nitrite concentrations for both frozen and non-frozen samples, the data for which can be found in Appendix B.

Nitrate+nitrite and nitrite measurements were analyzed for the impact of storage (frozen vs non-frozen effluent samples) by finding the percent change between the two averaged measurements of each sample type through calculations of percent difference. Frozen samples were considered the "original" sample, as frozen samples were likely to have less concentration drift over time as compared to samples stored in the liquid phase at 4°C. The percent difference for DEL samples could not be determined because no frozen DEL sample was analyzed. The frozen to non-frozen nitrate+nitrite averages had percent differences of ±5% in parts per billion. The percent differences for nitrite were ±40% in parts per billion. However, at such low concentrations (ppb) these variances were considered negligible for this study, and as such both

[2] Percent difference defined as $|V_1\text{-}V_2| \div [(V_1+V_2) / (2)] * 100\%$ from NEW alkalinity and MAR DOC values.

frozen and non-frozen values were averaged together for each effluent sample for calculations to find the reported nitrate values. Nitrate analysis occurred outside of the recommended period as established in literature, approximately three months after the general sample collection period. As such, reported ion measurements are for relative comparison, rather than direct quantitative analysis, but should be a good indicator of high, moderate, and low nitrate levels.

Optical Properties

Table 2 shows the optical properties of the five effluent samples. Optical spectra were generally featureless, with absorptivity increasing noticeably toward saturation at wavelengths lower than 250 nm and flattening out toward the baseline at higher wavelengths, examples of which can be found in Appendix C. $SUVA_{254nm}$ and E_2/E_3 ratios (254 nm/365 nm) were measured for both filtered, non-irradiated effluent samples and filtered, 8-h irradiated effluent working solutions that were adjusted to pH 7.

$SUVA_{254nm,Non\text{-}Irradiated}$ values for filtered, non-irradiated effluent samples ranged from 0.4 to 2.7 L mg^{-1} m^{-1}, where the low SUVA values are characteristic of wastewater samples (Lee et al., 2013). However, removing the much lower PIC value, $SUVA_{254nm,Non\text{-}Irradiated}$ ranges from 2.2 to 2.7 L mg^{-1} m^{-1}. This trend continues for the filtered, 8-h irradiated effluent working solution sample set. The $SUVA_{254nm,Irradiated}$ values for filtered, 8-h irradiated working solution effluent samples adjusted to pH 7 ranged from 1.7 to 2.5 L mg^{-1} m^{-1} for four of the effluent samples and was 0.3 L mg^{-1} m^{-1} for the PIC sample. $SUVA_{254nm,Irradiated}$ values decreased by 3.8-25% compared to filtered, non-irradiated effluent measurements.

Table 2 also shows E_2/E_3 ratios calculated at 254 nm divided by 365 nm for both types of irradiated and non-irradiated samples. There was an inverse increase in E_2/E_3 values with irradiation, ranging from 22.4-87.3% as a percent increase. E_2/E_3 ratios ranged from 4.3 to 5.8 in non-irradiated effluent samples and from 6.0 to 10.3 in irradiated working solutions.

Initial Rates Values

Table 3 shows experimentally determined hydroxyl radical production rate ($P_{\bullet OH}$), background natural scavenging rate (k'_{ns}), and hydroxyl radical steady state concentration ($[\bullet OH]_{ss}$) for all five WWTP effluent samples through the photolysis of caffeine, as discussed

above. The error in the $[\bullet OH]_{ss}$ measurements represents the error in fitting the parameters used to calculate $[\bullet OH]_{ss}$ from the LINEST function with arithmetic propagation rather than the standard deviation based on multiple experimental measurements. Peak area measurements for injection vials that were clearly the result of instrumental error, such as a failed or incomplete injection, were removed from analysis and are noted in Appendix C.

Dark controls, foil-wrapped and irradiated along with their respective phototube counterparts, showed relatively small changes in caffeine concentration. This indicates that the primary decrease in caffeine concentration was due to photolysis. However, some caffeine concentration drift was observed, with both positive and negative slopes, for different caffeine levels for different effluent samples. In addition, effluent working solutions not containing caffeine probe, both vials that were non-irradiated and irradiated for eight hours, exhibited no peak areas in the retention time detection window for caffeine, verifying that the only chemical species analyzed in this area was due to the addition of the caffeine probe. The potential for species other than •OH to react with caffeine was considered in previous research and so it was assumed in this experiment that caffeine was selective for •OH radical (Semones, 2017).

Hydroxyl radical steady state concentrations were reported in units of femto-molar (fM) for the five effluent samples. Values for $[\bullet OH]_{ss}$ were obtained to be 1.01±14.16 for DEL, 1.95±4.63 for MAR, 1.24±1.89 for PIC, 0.99±2.38 for NEW, and 1.14±12.57 for LON. Error for $[\bullet OH]_{ss}$ was an order of magnitude larger than the calculated result for the DEL and LON effluent samples. The overall hydroxyl radical production rates for the bulk effluent samples were reported in units of nano-molar per second (nMs^{-1}). Values for $P_{\bullet OH}$ were recorded as 0.8±10.6 for DEL, 0.3±0.7 for MAR, 0.5±0.7 for PIC, 0.3±0.6 for NEW, and 3.7±0.3 for LON. Error for the DEL sample was of a significantly higher magnitude compared to the other four samples. The overall background scavenging rates from natural scavengers in the effluent samples were reported in units of inverse seconds (s^{-1}). Values for k'_{ns} ranged from $2x10^5$ to $3x10^6$ s^{-1} with error ranging from $5x10^4$ to $4x10^7$ s^{-1}. Error was obtained from arithmetic propagation of error from the LINEST linear regression for all three variables for each caffeine level of each effluent sample.

Table 1. Summary of five WWTP effluent samples' water quality parameters for pH, alkalinity, DOC, and nitrate.

Chemical Characterization of Effluent Samples						
Samples	pH [a]	pH [b]	Alkalinity [c] (m_{eq} L^{-1})	DOC [d] (mg_C L^{-1})	NO_3^- [e] ($mg_{NO3\text{-}N}$ L^{-1})	NO_3^- [f] (mM)
DEL	7.96	7.92	2.26 ± 0.03	5.8	6.78 ± 0.03	0.48
MAR	7.44	7.30	2.78 ± 0.10	7.4	12.37 ± 0.16	0.88
PIC	7.80	7.86	8.67 ± 0.16	28.2	4.18 ± 0.02	0.30
NEW	7.12	7.52	4.14 ± 0.20	6.7	10.11 ± 0.28	0.72
LON	6.95	7.89	3.55 ± 0.06	4.5	10.29 ± 0.07	0.73

Notes: [a] pH as reported by WWTP at time of collection. [b] pH as initially measured at the start of alkalinity titrations on day of collection. [c] Alkalinity error reported as the standard deviation between computational methods for each sample, rather than as standard deviation of multiple titrations. : [d] DOC error reported as 2.5% as determined by comparison to check standards. [e] Nitrate values are reported in two different units for comparison with other studies. This column is reported as nitrate as nitrogen, with standard deviation arithmetically propagated to reach the displayed units. [f] This column reports nitrate as nitrate ion (mM).

Table 2. Characterization of optical data via specific ultraviolet absorbance (SUVA) and E_2/E_3 ratios for five WWTP samples.

Characterization of Optical Data						
	$SUVA_{254nm}$ [a] ($L\ mg^{-1}\ m^{-1}$)	$SUVA_{254nm}$ [b] ($L\ mg^{-1}\ m^{-1}$)	% Dec	E_2/E_3 [c] Non-Irr.	E_2/E_3 [d] Irrad.	% Dec
DEL	2.4	1.9	20.8	4.9	6.2	-26.5
MAR	2.2	1.7	22.7	5.8	8.9	-53.4
PIC	0.4	0.3	25.0	5.5	10.3	-87.3
NEW	2.6	2.5	3.8	4.9	6.0	-22.4
LON	2.7	2.2	18.5	4.3	6.1	-41.9

Notes: [a] SUVA at 254nm for filtered, non-irradiated effluent samples. [b] SUVA taken at 254 nm for filtered, 8-h irradiated effluent working solutions (pH 7). [c] E_2/E_3 ratio taken at 254 nm/365 nm for non-irradiated effluent. [d] E_2/E_3 ratio taken at 254 nm/365 nm for 8-h irradiated effluent working solution.

Table 3. Initial rates method results for $P_{\bullet OH}$, k'_{ns}, and $[\bullet OH]_{ss}$ using caffeine as a photochemical probe.

Initial Rates: Caffeine Probe Results						
Samples	$[\bullet OH]_{ss}$ (fM)	±	$P_{\bullet OH}$ (nMs^{-1})	±	k'_{ns} (s^{-1})	±
DEL	1.01	14.16	0.8	10.6	7.48E+05	5.36E+04
MAR	1.95	4.63	0.3	0.7	1.52E+05	7.45E+04
PIC	1.24	1.89	0.5	0.7	4.04E+05	3.13E+05
NEW	0.99	2.38	0.3	0.6	2.63E+05	1.16E+05
LON	1.14	12.57	3.7	0.3	3.22E+06	3.54E+07

Notes: $P_{\bullet OH}$ is the hydroxyl radical production rate.
k'_{ns} is the background scavenging rate of natural scavengers.
$[\bullet OH]_{ss}$ is the hydroxyl radical steady state concentration.
k_p of 5.9E9 $M^{-1}s^{-1}$ was the caffeine probe bimolecular rate constant used in these calculations (Shi & Dalal, 1991).

Discussion

The hypothesis that caffeine could be an effective photochemical probe for •OH in whole (bulk) effluent samples in the presence of nitrate was supported by the data collected. Based on measured •OH production and scavenging rates in wastewaters studied by Dong and Rosario-Ortiz (2012) known to be higher for EfOM than DOM, the expected overall $[•OH]_{ss}$ should be on the order of $1x10^{-15}$ M. This expectation was met using caffeine as a photochemical probe for •OH, with calculated values ranging within $1x10^{-15}$ to $2x10^{-15}$ M. The effluent samples measured in this study also corresponded to other reported literature values. Zhou and Mopper (1990) reported $[•OH]_{ss}$ ranging from 10^{-17} to 10^{-15} M in nitrate and DOM rich lake and river water. The findings in this study are on the upper end of the range reported by Zhou and Mopper, likely due to generally higher EfOM and nitrate concentrations in effluent water, which are the primary producers of •OH from photolysis. To further support nitrate's role in production of •OH, Dong and coworkers observed $[•OH]_{ss}$ values for effluent without nitrate contribution to be in the range of $0.2x10^{-15}$ to $0.4x10^{-15}$ M. Nitrate was present in the tested effluent samples in this study and the individual contribution of nitrate for production of •OH was not removed from the initial rates calculations in this study. This follows research that indicates that a higher $[•OH]_{ss}$ value would be observed in the presence of nitrate in effluent samples due to increases in caffeine's rate of phototransformation due to increased production of •OH from nitrate (Dong & Rosario-Ortiz, 2012; Jacobs et al., 2011).

Observed •OH production rates for the five effluent samples were determined to be several orders of magnitude higher than noted for literature values for natural surface waters. Values for $P_{•OH}$ in this study were on the order of $1x10^{-10}$ Ms^{-1}, however formation rates for •OH have been observed through other experiments for many surface waters to be at a lower scale of 10^{-15} to 10^{-11} Ms^{-1} and in river water from DOM at $1.1x10^{-11}$ Ms^{-1} (Dong & Rosario-Ortiz, 2012; Zhou & Mopper, 1990). Values for $P_{•OH}$ through nitrate photolysis only have been reported at 10^{-14} to 10^{-15} Ms^{-1}, with discrepancies likely indicating a potential major unknown •OH source, such as from DOM (Zepp & Cline, 1977; Zhou & Mopper, 1990). Dong et al. (2010) reported $P_{•OH}$ values for three effluent samples to be in the range of 0.23 to 0.38 nMs^{-1}, which more closely corresponds to values measured in this experiment. This, again, is likely attributable to higher concentrations of organic matter, nitrate, and other •OH producing species in effluent water

compared to natural surface waters. Semones (2017) reported $P_{\bullet OH}$ values for bulk, non-isolated effluent using benzene as a probe to be on the order of 0.199 nMs^{-1} and in an isolate solution of that same effluent to be 0.178 nMs^{-1} for a large-scale WWTP south of Columbus, Ohio using caffeine as a photochemical probe. Lee and coworkers observed formation rates for •OH, considering H_2O_2 independent pathways only, to be 0.48 and 0.096 nMs^{-1} for two respective WWTP effluent samples (Lee et al., 2013). Thus, compared to literature values using caffeine and other probes, the overall production of hydroxyl radical was similar to literature values.

Table 4. Comparison of $[\bullet OH]_{ss}$ and $P_{\bullet OH}$ results to literature values.

Comparison to Literature Values			
Samples	$[\bullet OH]_{ss}$ (fM)	$P_{\bullet OH}$ (nMs^{-1})	Source
DEL	1.01	0.8	
MAR	1.95	0.3	
PIC	1.24	0.5	
NEW	0.99	0.3	
LON	1.14	3.7	
Wastewaters in general	1.00		(Dong & Rosario-Ortiz, 2012)
Nitrate & DOM rich freshwater	0.001-1		(Zhou & Mopper, 1990)
Wastewaters without nitrate	0.2-0.4		(Dong & Rosario-Ortiz, 2012)
Old Woman Creek Fulvic Acid	0.242		(Jacobs, Weavers, Houtz, & Chin, 2011)
Caffeine probe, whole effluent	1.32		(Semones, 2017)
Caffeine probe, isolate	1.50		(Semones, 2017)
Wastewater samples		0.2-0.4	(Dong & Rosario-Ortiz, 2012)
Benzene probe, non-isolated effluent		0.20	(Semones, 2017)
Benzene probe, isolate effluent		0.18	(Semones, 2017)
H_2O_2 independent pathways		0.1-0.5	(Lee, Glover, & Rosario-Ortiz, 2013)

Notes: $P_{\bullet OH}$ is the hydroxyl radical production rate. $[\bullet OH]_{ss}$ is the hydroxyl radical steady state concentration.

The idea presented by Semones that the relationship between organic matter and NO_3^- production of •OH are co-dependent was considered. The MAR effluent sample had the highest nitrate concentration and highest observed $[\bullet OH]_{ss}$. However, just using a general high, medium, low relationship between •OH producers and scavengers proved to be too simplistic to characterize the complex interactions between chemical species. Effluent samples with relatively higher natural scavenging rates and lower nitrate concentrations compared to the other effluent samples did not necessarily have the lowest observed $[\bullet OH]_{ss}$, such as in the case of the PIC effluent sample. The PIC effluent sample had the second highest $[\bullet OH]_{ss}$ even though it had the highest alkalinity value (more scavenging) and lowest nitrate concentration (less •OH

production) out of the five samples studied. This is likely due to the complex relationship of EfOM and due to the nature and high concentration of the organic matter itself. As such, no apparent linear correlations between $[\bullet OH]_{ss}$ and any of the other measured parameters could be reported. Three of the effluent samples (DEL, NEW, and LON) exhibited similar relationships when plotting $[\bullet OH]_{ss}$ against the different parameters of nitrate, alkalinity, and $SUVA_{254nm}$ values. However, the samples of MAR and PIC were both significantly different from the three similar effluent samples and different from each other in all of these comparisons. A slight correlation between nitrate and DOC was observed, but ultimately not reported due to the behavior of the PIC sample and low R^2 value which indicated a loose fit of the data.

Effluent organic matter varies depending on influent water sources and wastewater treatment processes. Effluent organic matter in comparison to DOM exhibits lower $SUVA_{254nm}$ and therefore absorbs less light per carbon in the water column than DOM (Bodhipaksha et al., 2015). These major differences in the PIC and MAR samples could be explained by the chemical makeup of the effluent itself. Specific ultraviolet absorption (SUVA) has been shown to be a useful parameter for estimating the dissolved aromatic carbon content in aquatic systems (Weishaar et al., 2003). The $SUVA_{254nm,Non\text{-}irradiated}$ values for PIC (0.4 L mg^{-1} m^{-1}) and MAR (2.2 L mg^{-1} m^{-1}) were the two lowest values for this parameter in the effluent samples and had the highest percent decreases in $SUVA_{254nm}$ after eight hours of irradiation. SUVA values for effluent and natural waters typically range from 1 to 6 L mg^{-1} m^{-1} (Hansen et al., 2016). Lee and coworkers reported that lower $SUVA_{254nm}$ values are characteristic of effluent samples, and previous research has noted effluent samples as having $SUVA_{254nm}$ values around 2 L mg^{-1} m^{-1} (Lee et al., 2013; Dong & Rosario-Ortiz, 2012). While the MAR sample $SUVA_{254nm}$ values are close to the values recorded by Lee, the PIC sample exhibited much lower $SUVA_{254nm}$ values than expected.

Weishaar et al. noted that $SUVA_{254nm}$ is a good indicator of the hydrophobic humic fraction of DOC in water samples and thus is a useful proxy for DOM aromatic content, where a higher number is typically associated with greater aromatic content (Weishaar et al., 2003; Leenheer & Croué, 2003). This should indicate that the PIC effluent had a much smaller fraction of aromatic content compared to the other wastewater samples. However, DOC for the PIC sample was on an order of a magnitude higher than the other effluent samples and much higher

than typical DOC measurements reported in literature for effluent and natural waters. Typical DOC concentrations as reported in previous studies for water samples range from 5-20 mg-C L^{-1} where the higher end of the range corresponds to measurements taken in bogs (Bodhipaksha et al., 2015). A typical range for treated wastewater effluent samples specifically is generally within the 5-11 mg-C L^{-1} range and usually within the 6-8 mg-C L^{-1} range (Dong & Rosario-Ortiz, 2012; Dong et al., 2010; Lee et al., 2013). It could be that while the fraction of aromatic content in the PIC sample is small, the high DOC value actually makes the absolute amount of aromatic content in the PIC sample relatively higher than the other four effluent samples. This could also indicate potential problems at time of collection with regard to the wastewater treatment process itself at that facility. However, the nitrate concentration for the PIC effluent sample (4.18 mg_{NO3-N} L^{-1}) did fall within an expected range for effluent samples (<0.01 to 16 mg_{NO3-N} L^{-1}) (Dong et al., 2010; Lee et al., 2013).

Another measurement obtained from optical spectra is the ratio of DOM absorbance at 254 nm divided by the absorbance at 365 nm (E_2/E_3 ratio). Reported literature values for effluent samples range from 0.41 to 8, with most falling between 4.8 and 5.7 (Bodhipaksha et al., 2015; Lee et al., 2013). Dalrymple and coworkers (2010) suggested that low E_2/E_3 ratios could indicate that DOM photochemistry will be influenced by charge-transfer interactions and that high E_2/E_3 ratios will indicate reactions via non-charge-transfer interactions, such as by energy transfer. All effluent samples had relatively similar E_2/E_3 ratios.

Of particular note with regard to kinetic values obtained from experimentation is the necessity of clearly defining the method of calculation for these values. In this study, an initial rates method was used to calculate $[\bullet OH]_{ss}$, $P_{\bullet OH}$, and k'_{ns} values. Especially with regard to the values on the order of 10^{-15} to 10^{-10} it is important to clearly define certain parameters during calculations. Namely, some of the dark control vials for each caffeine level that were foil covered exhibited positive or negative slopes depending on the effluent sample and caffeine level. This could indicate confounding factors, such as reactions taking place between caffeine and chemical species in the effluent samples that could introduce a larger error into $[\bullet OH]_{ss}$ results. In particular, this study determined the initial probe concentration (caffeine spike levels for working solutions) for each effluent sample by using the Excel-based LINEST function to create a linear regression from the dark control vials for each caffeine level. This allowed for the

calculation of the initial probe concentration by finding the concentration of probe in solution at time zero. This method was utilized to present the information here. However, other calculation pathways were considered, including calculation of initial probe concentration by direct creation of the solution (the direct measurement of caffeine in the volume of working solution created). This method ended up not being utilized because the direct calculation of initial probe concentration did not reflect measurements taken for the vials recorded at T0 for each caffeine level in each effluent sample. Directly measured probe concentrations are noted in the supporting information, however.

One method considered for this analysis included the subtraction of probe left in solution after irradiation from the initial probe concentration as measured at each time point ([initial probe concentration as determined from the dark control vial linear regression line at each time point] minus [the concentration of caffeine at each time point]). This resulted in data showing caffeine loss over time (positive slope, denoting the consumption of probe, R_p, without having to multiply by -1 as mentioned in the methodology) while also taking into account potential caffeine concentration drift not due to attenuation from •OH via irradiation. While all of these methods resulted in more or less similar $[\bullet OH]_{ss}$ values, depending on which method was used the values for $P_{\bullet OH}$ and k'_{ns} varied significantly. Even slight deviations in how initial variables are calculated can introduce significant reductions in the precision and accuracy of the data obtained.

CONCLUSIONS

The purpose of this study was to provide data to support or reject the use of caffeine as a photochemical probe for hydroxyl radical in whole (bulk) wastewater effluent samples containing varying amount of EfOM, nitrate, carbonate, bicarbonate, and other chemical species. This objective was met through using an initial rates method to determine hydroxyl radical steady state concentration, overall production rate, and overall natural scavenging rate, in addition to gathering water quality parameters, for each effluent sample. This work supported research into using caffeine as a photochemical probe for hydroxyl radical with some qualifiers. Reported values for hydroxyl radical steady state concentration for each of the effluent samples (1–2 fM) were within expected ranges for effluent waters (0.2–1.5 fM). However, the precision of the data was found to be significantly affected by minor adjustments to how some variables were calculated using the initial rates method.

RECOMMENDATIONS FOR FUTURE WORK

Additional study is warranted to explore further the relationship between the photochemical properties of effluent samples to the characterization of effluent and natural dissolved organic matter. Specifically, correlations between quantum yields for hydroxyl radical to E_2/E_3 ratios for repeated measurements of effluent samples could help further current research that suggests E_2/E_3 ratios could be a simple parameter for estimating apparent quantum yields, production rates, and steady state reactive species concentrations.

Further, research into the co-dependency of effluent organic matter and nitrate as the two primary producers of hydroxyl radical should be explored, as suggested by Semones, M. This study looked at using caffeine as a photochemical probe in bulk effluent water containing such species as nitrate without calculating the individual contributions of the primary chemical species responsible for hydroxyl radical production and scavenging.

Finally, due to the extremely low hydroxyl radical steady state concentrations present in effluent samples, detailed analysis of the initial rates method to further support caffeine as a photochemical probe for hydroxyl radical is necessary to obtain accurate steady state results. In this study, the decrease of caffeine due to irradiation was taken at face-value with assumptions that caffeine is primarily reacting with hydroxyl radical. However, this study did not explore the slight drift in the initial caffeine concentrations at each caffeine level for each effluent sample. Namely, some of the dark control vials for each caffeine level that were foil covered exhibited positive or negative slopes depending on the effluent sample and caffeine level. This could indicate confounding factors, such as reactions taking place between caffeine and chemical species in the effluent samples not due to irradiation that could introduce a larger error into hydroxyl radical steady state concentration results. Future work should be directed at careful analysis of these samples to account for the drift of caffeine not due to irradiation.

REFERENCES

———. (2008, September 23). Analysis: Nitrate+Nitrite. *Skalar Methods* (Catnr. 461-032 issue 092308/TL/99252980). Retrieved 2017

———. (2008, September 23). Analysis: Nitrite. *Skalar Methods* (Catnr. 467-033 issue 092308/TL/99252980). Retrieved 2017

Adams, C., Wang, Y., Loftin, K., & Meyer, M. (2002). Removal of Antibiotics from Surface and Distilled Water in Conventional Water Treatment Processes. *Journal of Environmental Engeineering, 128*(3), 253-260. doi:10.1061/(ASCE)0733-9372(2002)128:3(253)

Batt, A. L., Kim, S., & Aga, D. S. (2007). Comparison of the occurence of antibiotics in four full-scale wastewater treatment plants with varying designs and operations. *Chemosphere, 68*, 428-435. doi:10.1016/j.chemosphere.2007.01.008

Bodhipaksha, L. C., Sharpless, C. M., Chin, Y.-P., Sander, M., Langston, W. K., & MacKay, A. A. (2015). Triplet Photochemistry of Effluent and Natural Organic Matter in Whole Water and Isolates from Effluent-Receiving Rivers. *Environmental Science & Technology*, 3453-3463. doi:10.1021/es505081w

Brezonik, P. L., & Brekken, J. F. (1998). Nitrate-Induced Photolysis in Natural Waters: Controls on Concentrations of Hydroxyl Radical Intermediates by Natrual Scavenging Agents. *Environmental Science & Technology*, 3004-3010.

Brinkmann, T., Sartorius, D., & Frimmel, F. H. (2003). Photobleaching of humic rich dissolved organic matter. *Aquatic Sciences, 65*, 415-424. doi:10.1007/s00027-003-0670-9

Brooks, B. W., Riley, T. M., & Taylor, R. D. (2006). Water quality of effluent-dominated ecosystems: ecotoxilogical, hydrological, and management considerations. *Hydrobiologia*, 365-379. doi:10.1007/s10750-004-0189-7

Dalrymple, R. M., Carfagno, A. K., & Sharpless, C. M. (2010). Correlations between Dissolved Organic Matter Optical Properties and Quantum Yields of Singlet Oxygen and Hydrogen Peroxide. *Environmental Science & Technology, 44*, 5824-5829. doi:10.1021/es101005u

Dong, M. M., & Rosario-Ortiz, F. L. (2012). Photochemical Formation of Hydroxyl Radical from Effluent Organic Matter. *Environmental Science & Technology* (46(7)), 3788-3794. doi:10.1021/es2043454

Dong, M., Mezyk, S. P., & Rosario-Ortiz, F. L. (2010). Reactivity of Effluent Organic Matter (EfOM) with Hydroxyl Radical as a Function of Molecular Weight. *Environmental Science & Technology*, 5714-5720.

Gligorovski, S., Strekowski, R., Barbati, S., & Vione, D. (2015). Environmental Implications of Hydroxyl Radicals (•OH). *Chemical Reviews, 115(24)*, 13051-13092. doi:10.1021/cr500310b

Hansen, A. M., Kraus, T. E., Pellerin, B. A., Fleck, J. A., Downing, B. D., & Bergamaschi, B. A. (2016). Optical properties of dissolved organic matter (DOM): Effects of biological and photolytic degradation. *Limnology and Oceanography*, 1015-1032. doi:10.1002/lno.10270

Jacobs, L. E., Weavers, L. K., Houtz, E. F., & Chin, Y.-P. (2011). Photosensitized degradation of caffeine: Role of fulvic acids and nitrate. *Chemosphere*, 124-129. doi:10.1016/j.chemosphere.2011.09.052

Lee, E., Glover, C. M., & Rosario-Ortiz, F. L. (2013). Photochemical Formation of Hydroxyl Radical from Effluent Organic Matter: Role of Composition. *Environmental Science & Technology, 47*, 12073-12080. doi:10.1021/es402491t

Leenheer, J. A., & Croué, J. (2003). Peer Reviewed: Characterizing Aquatic Dissolved Organic Matter. *Environmental Science & Technology, 37(1)*. doi:10.1021/es032333c

Murray, K. E., Thomas, S. M., & Bodour, A. A. (2010, August 13). Prioritizing research for trace pollutants and emerging contaminants in the freshwater environment. *Environmental Pollution*, 3462-3471. doi:10.1016/j.envpol.2010.08.009

Office of Water. (1998, May). How Wastewater Treatment Works... The Basics. *(EPA 833-F-98-002)*. United States Environmental Protection Agency. Retrieved March 24, 2017, from https://www3.epa.gov/npdes/pubs/bastre.pdf

Potter, B., & Wimsatt, J. (2009, September). *Determination of Total Organic Carbon and Specific UV Absorbance at 254 nm in Source Water and Drinking Water.* Cincinnati, Ohio: National Exposure Research Laboratory and U.S. Environmental Protection Agency. Retrieved 2017, from National Service Center for Environmental Publications (NSCEP)

Rounds, S. (2013, January 4). *Methods for Alkalinity Calculator*. (U.S. Department of the Interior and U.S. Geological Survey) Retrieved February 2017, from Oregon Water Science Center: https://or.water.usgs.gov/alk/methods.html

Rounds, S. (2013, January 4). *Web-based Alkalinity Calculator*, 2.22. (U.S. Department of Interior and U.S. Geological Survey) Retrieved February 2017, from Oregon Water Science Center: https://or.water.usgs.gov/alk/index.html

Rounds, S., & Wilde, F. (2002). *Chapter A6. Section 6.6. Alkalinity and Acid Neutralizing Capacity.* Geological Survey (U.S.). Retrieved 2016, from http://water.usgs.gov/owq/FieldManual/Chapter6/section6.6/

Semones, M. C. (2017). Dynamics in the reactivity and photochemical production of hydroxyl radical in treated wastewater effluent and aquatic dissolved organic matter. *Manuscript in preparation (The Ohio State University PhD Dissertation).*

Semones, M. C., Sharpless, C. M., MacKay, A. A., & Chin, Y. P. (2017). Photodegradation of UV filters oxybenzone and sulisobenzone in wastewater effluent and by dissolved organic matter. *Applied Geochemistry*. http://doi.org/10.1016/j.apgeochem.2017.02.008

Shi, X., & Dalal, N. (1991). Antioxidant behavior of caffeine: Efficient scavenging of hydroxyl radicals. *Food and Chemical Toxicology, 29 (1)*, 1-6.

Weishaar, J. L., Aiken, G. R., Bergamaschi, B. A., Fram, M. S., Fujii, R., & Mopper, K. (2003). Evaluation of specific ultraviolet absorbance as an indicator of the chemical composition and reactivity of dissolved organic carbon. *Environmental Science and Technology, 37*(20), 4702-4708. Retrieved 2017, from 10.1021/es030360x

White, E. M. (2000). Determination of Photochemical Production of Hydroxyl Radical by Dissolved Organic Matter and Associated Iron Complexes in Natural Waters. *The Ohio State Unviersity (Master's thesis)*.

Zepp, R. G., & Cline, D. M. (1977). Rates of direct photolysis in aquatic environment. *Environmental Science & Technology* (11(4)), 359-366. doi:10.1021/es60127a013

Zhou, X., & Mopper, K. (1990). Determination of photochemically produced hydroxyl radicals in seawater and freshwater. *Marine Chemistry* (30), 71-88. doi:10.1016/0304-4203(90)90062-h

SUPPORTING INFORMATION

APPENDIX A

WASTEWATER TREATMENT FACILITIES

COMPARATIVE FACILITY INFORMATION

Site specific effluent sample collection information is listed for each WWTP below. The approximate distance from The Ohio State University where laboratory testing took place, average design flow, and design peak flow are listed.

MGD = million of gallons per day.

Effluent Facility	Acronym	Approx. Distance from OSU (mi)	Design Flow (MGD)	Peak Flow (MGD)
Delaware	(DEL)	24	10.0	30.0
Marysville	(MAR)	34	8.0	21.5
Pickerington	(PIC)	21	3.2	-
Newark	(NEW)	44	8.0	20.0
London	(LON)	30	5.8	17.1
Jackson-Pike (not tested, for comparison only)		8	68	102
Southerly (not tested, for comparison only)		17	96	114

Effluent sample location, date, temperature, pH, and dissolved oxygen data provided by each wastewater treatment facility from data collected for use in water treatment monitoring.

Sampling Site and Date		Temperature (°C)	pH	Dissolved O_2 (mg L^{-1})
Delaware, OH (DEL)				
10:15AM	10/17/16	22.4	7.96	~ 9 [a]
Marysville, OH (MAR)				
11:00AM	10/24/16	21.7	7.44	7.61
Pickerington, OH (PIC)[b]				
10:15AM	10/31/16	18.9	7.80	10.09
Newark, OH (NEW)[b]				
10:45AM	11/07/16	19.7	7.12	8.22
London, OH (LON)[b, c]				
11:13AM	11/14/16	18.2	6.95	9.45

[a] Average dissolved oxygen level as reported by facility. Probe was non-functional during sample collection.

[b] Subsequent to sample collection at the Newark facility it was raised that wastewater treatment facilities are not required to disinfect effluent, such as with ultraviolet light, during the recreational off-season (October 31st-May 1st). As such, these facilities may or may not have had their disinfection process active during sample collection.

[c] Additional levels for nitrate (NO_3^-) and ammonia-nitrate (NH_3-NO_3^-) were recorded as 11.6 mg L^{-1} and 16.8 mg L^{-1} respectively.

Google Earth Overhead View

Overhead views of each facility indicate current facility size and layout. A yellow pin on the Google Earth overhead view marks the specific sample collection location used in this experiment. The letter A pin marks the latitude and longitude coordinates as provided in the *Source* section for the overhead maps. Facility design schematics and flow charts as provided by each facility have been included for reference.

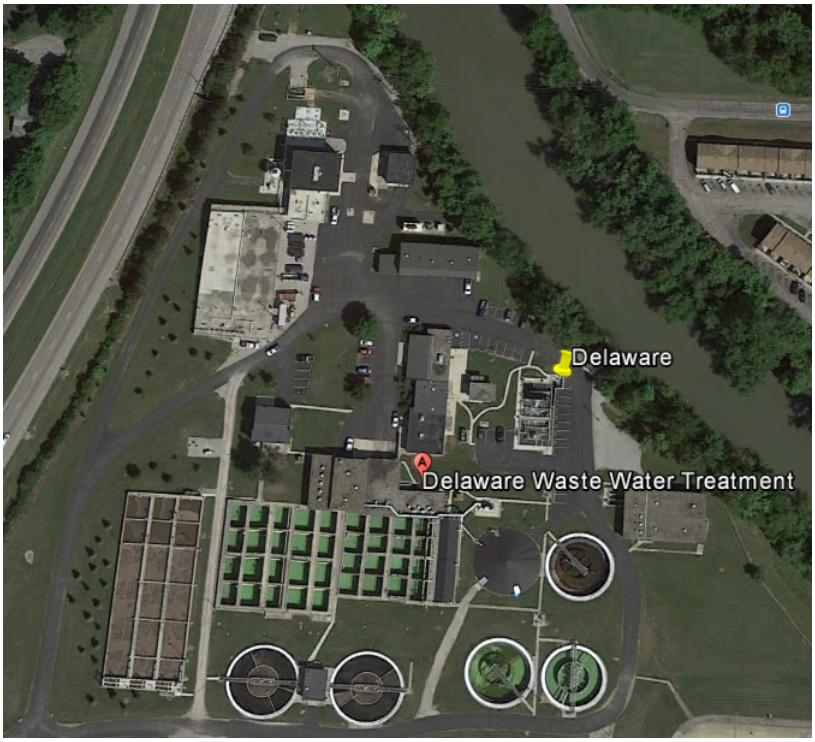

Google Earth view of the Upper Olentangy Water Reclamation Center of Delaware, Ohio near the Olentangy River.[a]

Google Earth view of the Marysville Water Reclamation Facility near Mill Creek. .[b]

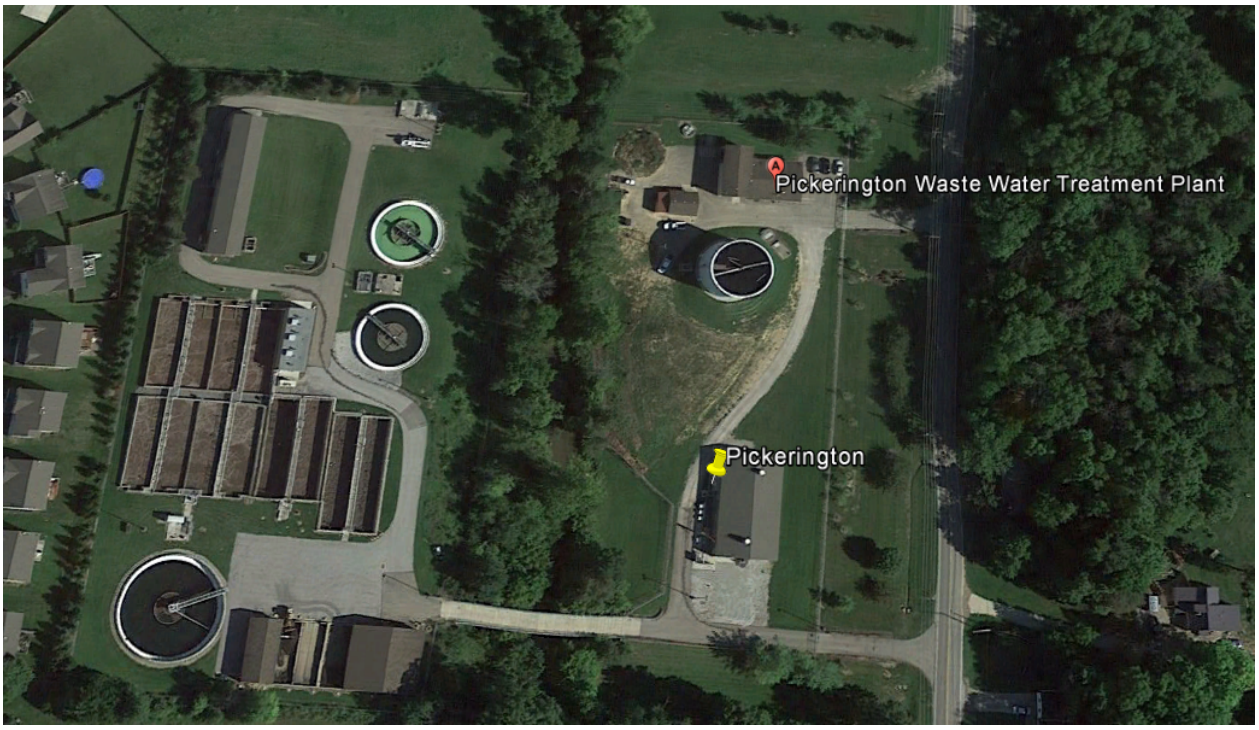

Google Earth view of the Pickerington Waste Water Treatment Plant near Sycamore Creek. [c]

Google Earth view of the Newark Wastewater Treatment Plant near the Licking River. [d]

Google Earth view of the London Sewage Treatment Plant near Oak Run Stream. [e]

[a] *Source:* Google Earth 7.0. *Delaware Waste Water Treatment Facility, 40.2913835,-83.0607819.* Viewed 2016. <http://www.google.com/earth/index.html>.

[b] *Source:* Google Earth 7.0. *Marysville Water Reclamation Facility, 40.1947379,-83.2690204.* Viewed 2016. <http://www.google.com/earth/index.html>.

[c] *Source:* Google Earth 7.0. *Pickerington Waste Water Treatment Plant, 39.873064,-82.7610918.* Viewed 2016. .<http://www.google.com/earth/index.html>.

[d] *Source:* Google Earth 7.0. *Newark Wastewater Treatment Plant, 40.0575655,-82.3622277.* Viewed 2016. .<http://www.google.com/earth/index.html>.

[e] *Source:* Google Earth 7.0. *London Sewage Treatment Plant, 39.8754504,-83.435712.* Viewed 2016. .<http://www.google.com/earth/index.html>.

Glory to the Valacirca! Cheers to all of Middle-Earth!

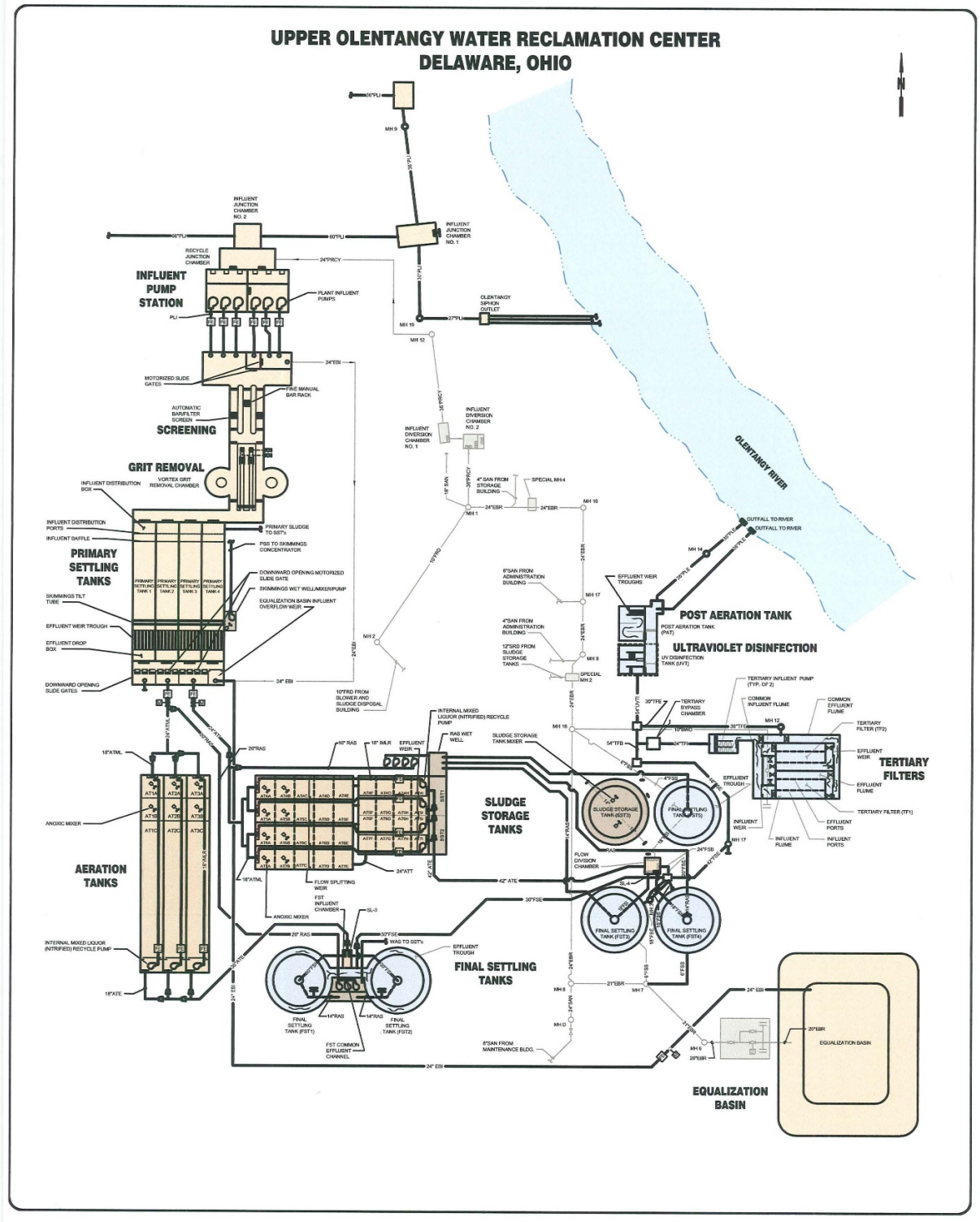

Upper Olentangy Water Reclamation Center of Delaware, Ohio system design schematic.

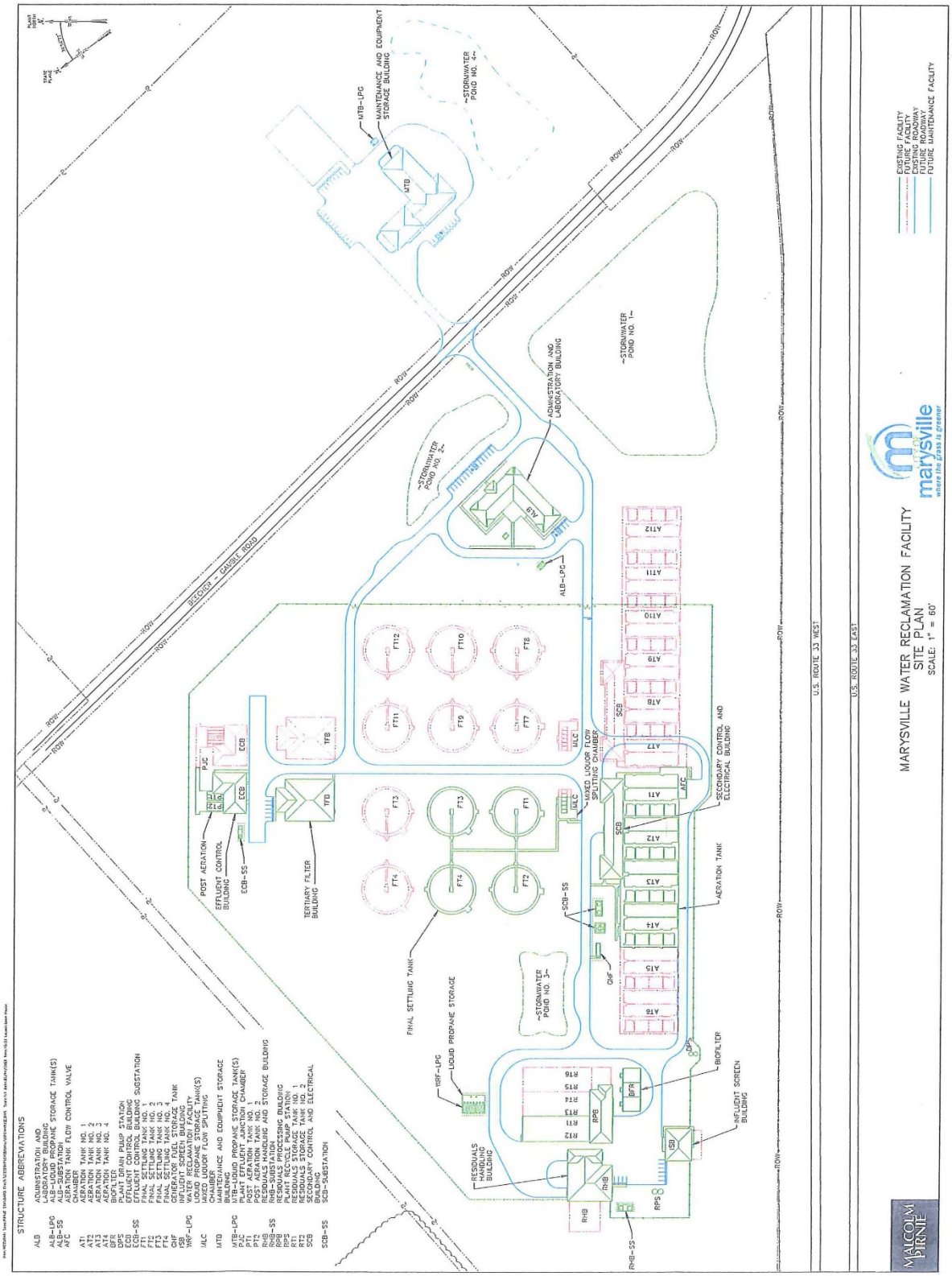

Marysville Water Reclamation Center of Marysville, Ohio system design schematic.

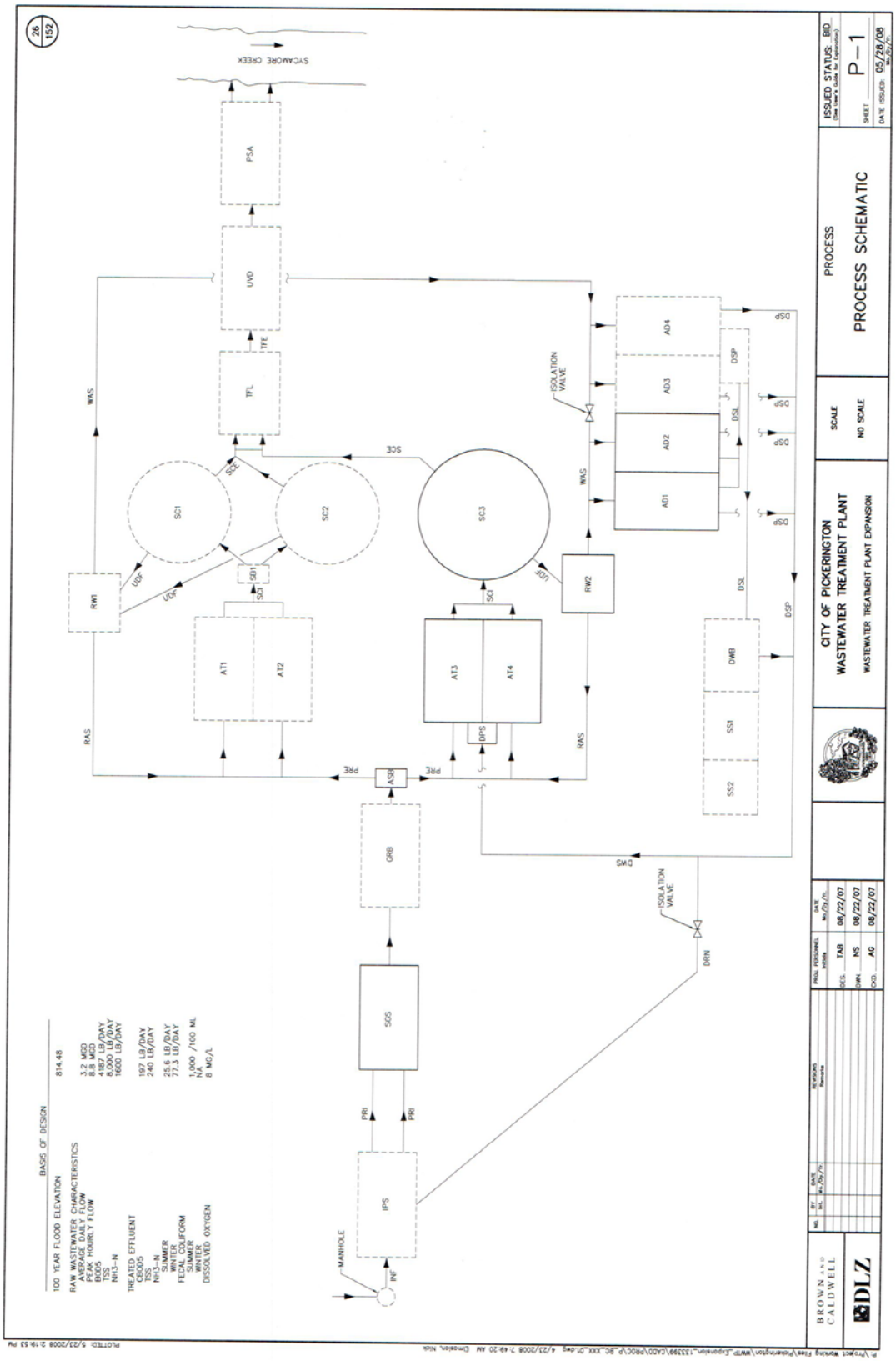

City of Pickerington Wastewater Treatment Plant of Pickerington, Ohio system schematic.

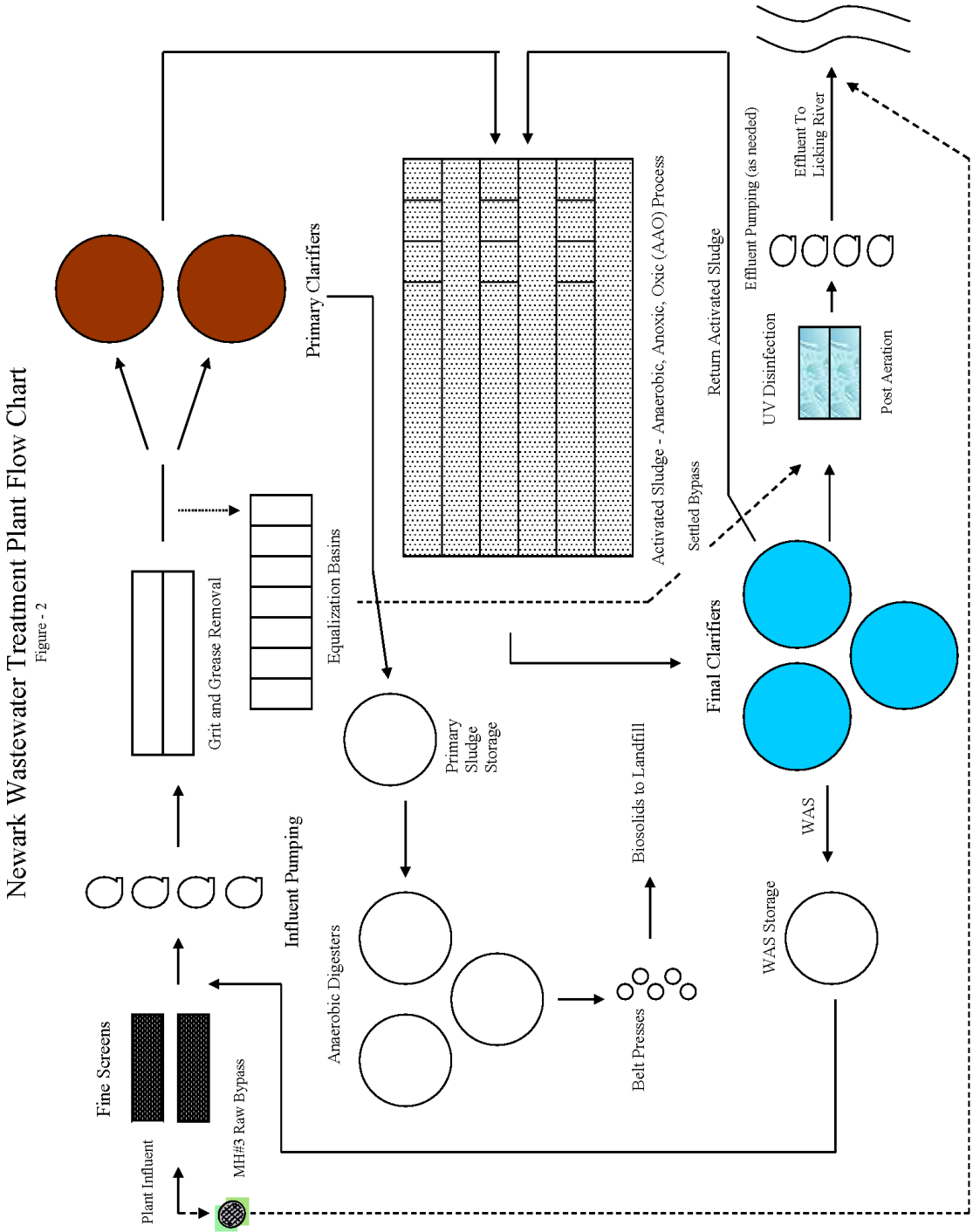

Newark Water Treatment Plant of Newark, Ohio system flow chart design schematic.

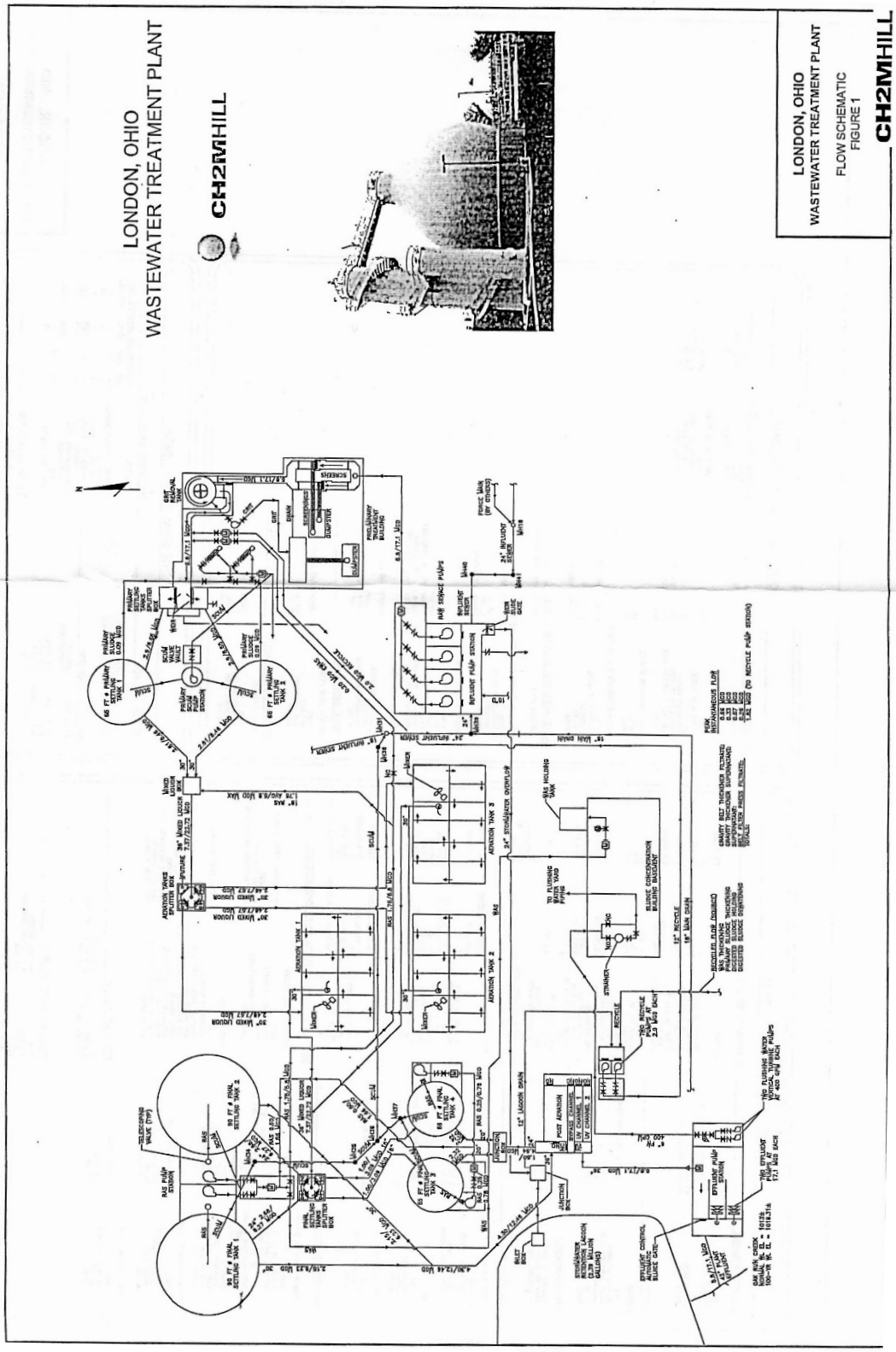

London Wastewater Treatment Plant of London, Ohio system design schematic.

APPENDIX B

SUPPLEMENTAL METHODOLOGY

Solution Preparation and Filtration

The general method used to determine how much reagent would be needed in each stock solution preparation was determined by the following equations as needed, where V_1 and C_1 are the initial volume and initial concentration, respectively, and V_2 and C_2 are the final volume and final concentration, respectively, and FW is the formula weight of a dry reagent. Additionally, all volumes were obtained on an analytical or top loading mass balance.

$$V_1 C_1 = V_2 C_2$$

$$\frac{\text{dry reagent } [g]}{\text{desired volume } [L]} = \text{desired molarity } \left[\frac{mol}{L}\right] * \text{FW } \left[\frac{g}{mol}\right]$$

An example calculation was included below for the caffeine stock solution created from a dry reagent to highlight the use of estimation before preparation.

Caffeine Stock Solution

To determine how much caffeine was needed for the stock solution, the following calculation was employed:

$$\frac{\text{dry reagent } [g]}{\text{desired volume } [L]} = \left(\text{desired molarity } \left[\frac{mol}{L}\right]\right) * \left(\text{FW } \left[\frac{g}{mol}\right]\right)$$

$$\text{Need: } \left(\text{desired molarity } \left[\frac{mol}{L}\right]\right)\left(\text{FW } \left[\frac{g}{mol}\right]\right)(\text{desired volume } [L]) = \text{dry reagent } [g]$$

$$\text{Want: } \left(0.01 \frac{mol}{L}\right)\left(194.19 \frac{g}{mol}\right)(0.1\ L) = 0.19419\ g \text{ caffeine goal amount}$$

To prepare the caffeine stock solution, an amber vial was placed on a mass balance and tared. Caffeine (99.7%) was added via a spatula to the vial, and the mass of caffeine added was weighed. The vial was tared and Milli-Q water added until the desired total volume was reached. The mass of the water was recorded. The vial was sealed with a Teflon protected cap.

$$\text{Actual Measurement Calculation: } \left(\frac{\text{caffeine used } [g]}{\text{FW } \left[\frac{g}{mol}\right]}\right) * \left(\frac{1000 \left[\frac{mL}{L}\right]}{\text{total MQ used } [mL]}\right) * \left(\frac{1000\ mmol}{1\ mol}\right) = \text{final concentration} \left[\frac{mmol}{L}\right] = \text{final concentration}[mM]$$

$$\text{Used: } \frac{0.1965\ g \text{ caffeine}}{194.19 \frac{g}{mol}} * \frac{\frac{1000\ mL}{1\ L}}{101.35\ mL\ MQ} * \frac{1000\ mmol}{1\ mol} = 9.98 \frac{mmol}{L} = 9.98\ mM$$

HCl Stock Solution and Diluted HCl Vials

To calculate the approximate molarity of solution in stock bottle of HCl (Certified ACS Plus, Trace Metal Grade, 36-37%):

$$\frac{\%\frac{w}{w} * \rho}{MW} * 10 = M$$

$$\frac{36\% * 1.2\ g/mL}{36.46\ g/mol} * 10 = 12\ M$$

To obtain three diluted HCl vials, a serial dilution method was used. Solutions were made at approximately 1, 0.1, and 0.01 M HCl in Milli-Q water. The 1 M HCl solution was made from concentrated HCl stock, the 0.1 M solution was made from the 1 M solution, and the 0.01 M solution was made from the 0.01 M HCl solution. These solutions were utilized during photolysis experiments to create filtered effluent working solutions by adjustment to pH 7.

Filtration

A 1-L sidearm flask; 0.7-µm pore-size filters (Grade GF/F, Whatman); Millipore glass filter assembly with funnel, fritted base, stopper, and clamp; sidearm flask reservoir for backflow; rubber tubing; and sink suction were utilized for filtration. The equipment was assembled and four washes of 250 mL Milli-Q water were used to rinse each filter. Effluent samples were filtered and stored in clean 1-L Pyrex media storage bottles. Used filters were saved for visual comparison.

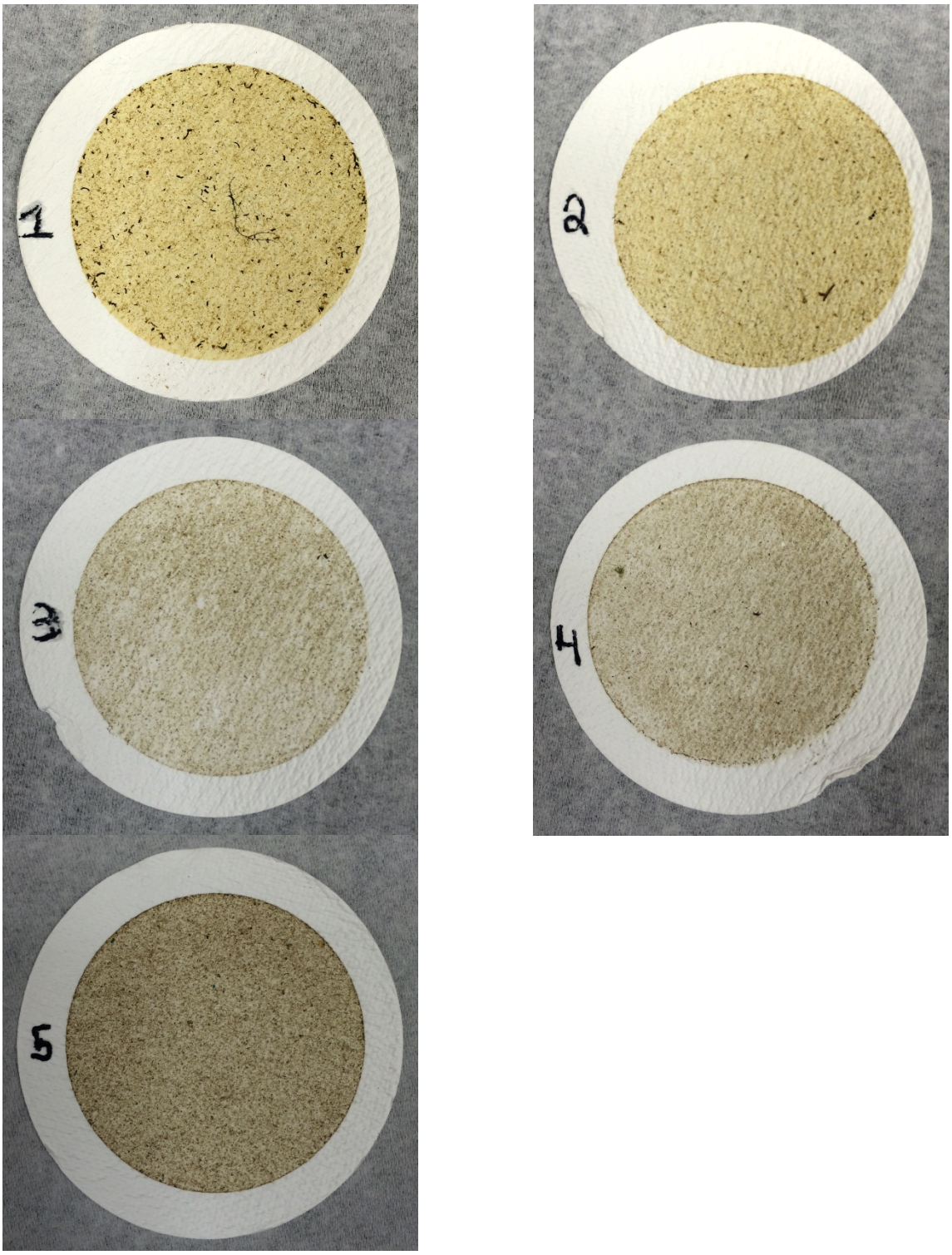

Images of material filtered from effluent samples. 1 = DEL, 2 = MAR, 3 = PIC, 4 = NEW, 5 = LON

ALKALINITY: GRAN FUNCTION PLOT AND ONLINE ALKALINITY CALCULATOR METHODS

A 250 mL beaker, 25 mL burette, Teflon stir bar, stir apparatus, pH electrode and instrument, 0.01703 N H_2SO_4 titrant (prepared by Semones, M. on 9/7/2016), ~ 100 mL effluent sample, burette clamp, stand, Milli-Q water, and analytical balance were used to perform titrations for alkalinity.

Equation for Bicarbonate Equivalence Point:

$$F_1 Gran\ Function\colon (V_0 + V_t)(10^{-pH})/\gamma = (V_t - B)C_a$$

Equation for Alkalinity:

$$Alk\left(\frac{m_{eq}}{L}\right) = \frac{B(mL)\times C_a\left(\frac{m_{eq}}{ml}\right)\times CF}{V_s(mL)\times\left(\frac{1\ L}{1000\ mL}\right)} = \frac{1000(B)(C_a)(CF)}{V_s}$$

where

V_0	is the initial volume of sample
V_t	is the volume of acid titrant added
B	is the titrant volume added from the initial pH to the bicarbonate equivalence point
γ	is the activity coefficient for H^+ which is assumed to be 1.0
C_a	is the normality of acid titrant
CF	is the correction factor that is equal to 1.0 when using the burette titration method
Alk	is the alkalinity of the sample

The initial volume of effluent sample used in alkalinity calculations were recorded as 100.4597 mL for DEL, 100.0265 mL for MAR, 100.1125 mL for PIC, 96.9366 mL for NEW, and 99.3444 mL for LON.

To manually calculate the alkalinity for each sample, $(V_0 + V_t)(10^{-pH})$ was plotted against V_t using pH and titrant measurements that occur after the bicarbonate equivalence point. These points were determined by graphing $(V_0 + V_t)(10^{-pH})$ against V_t and identifying the linear area immediately to the right of the slope change (data points should more or less linearly increase along the $(V_0 + V_t)(10^{-pH})$ and V_t axes to a pH less than 3.5). By selecting these data points a linear equation can be created using the LINEST function on values for $(V_0 + V_t)(10^{-pH})$ vs V_t. The straight line can then be extrapolated through the region beyond the bicarbonate equivalence point to where it meets the x-axis. The point where it meets the x-axis is the bicarbonate equivalence point [B=(0-intercept)/slope]. This point can then be used to calculate alkalinity

using the alkalinity equation. Data points selected to find the bicarbonate equivalence point are indicated in Appendix C.

A visual comparison of computational methods to determine alkalinity in the five effluent samples is included below. Values for the MAR Gran Function F_3 and NEW Gran Function F_1 from the Online Alkalinity Calculator indicated warnings that the carbonate titration curve and method assumptions did not fit the data well, giving a mean absolute titrant volume error of 1.04 and 1.18 mL respectively. These results indicate that other chemical species could have been neutralized in the titrations and that these values should be treated as estimates, as recommended by the Online Alkalinity Calculator.

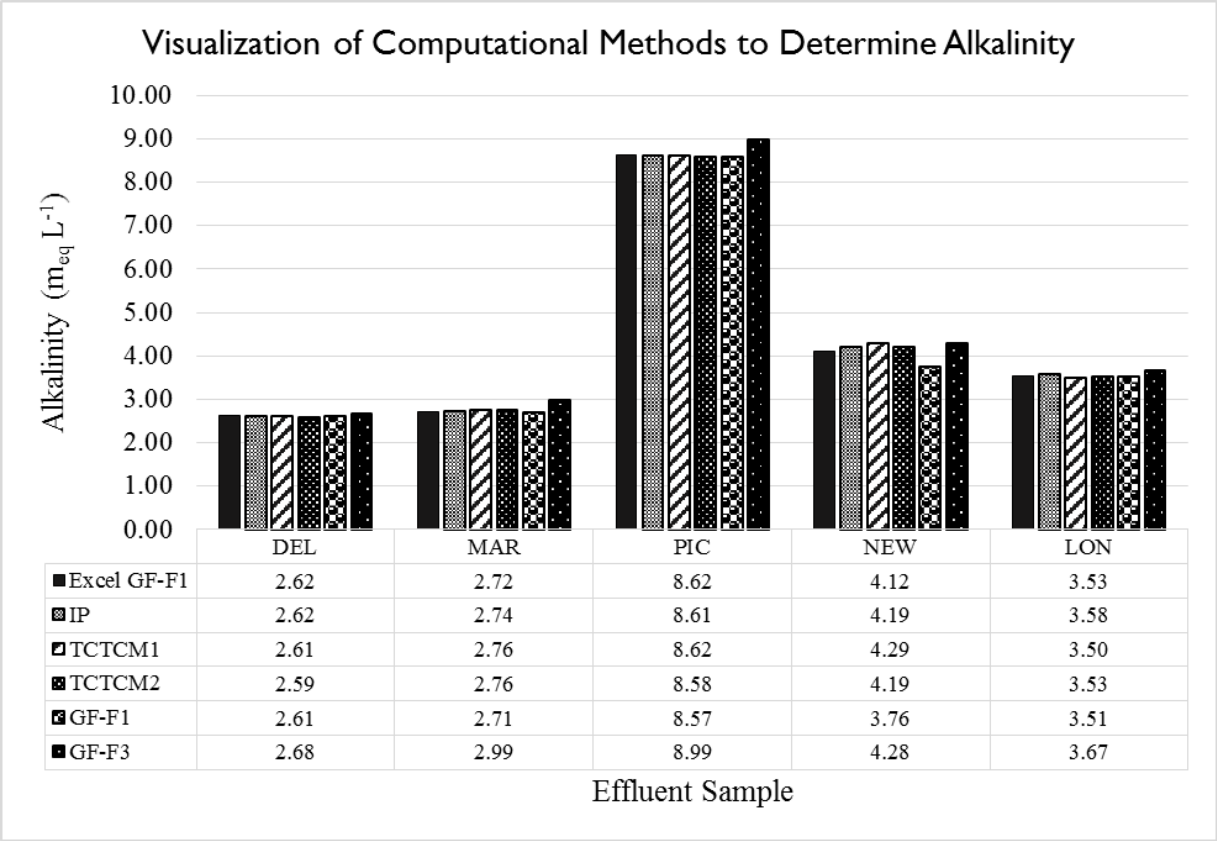

	DEL	MAR	PIC	NEW	LON
Excel GF-F1	2.62	2.72	8.62	4.12	3.53
IP	2.62	2.74	8.61	4.19	3.58
TCTCM1	2.61	2.76	8.62	4.29	3.50
TCTCM2	2.59	2.76	8.58	4.19	3.53
GF-F1	2.61	2.71	8.57	3.76	3.51
GF-F3	2.68	2.99	8.99	4.28	3.67

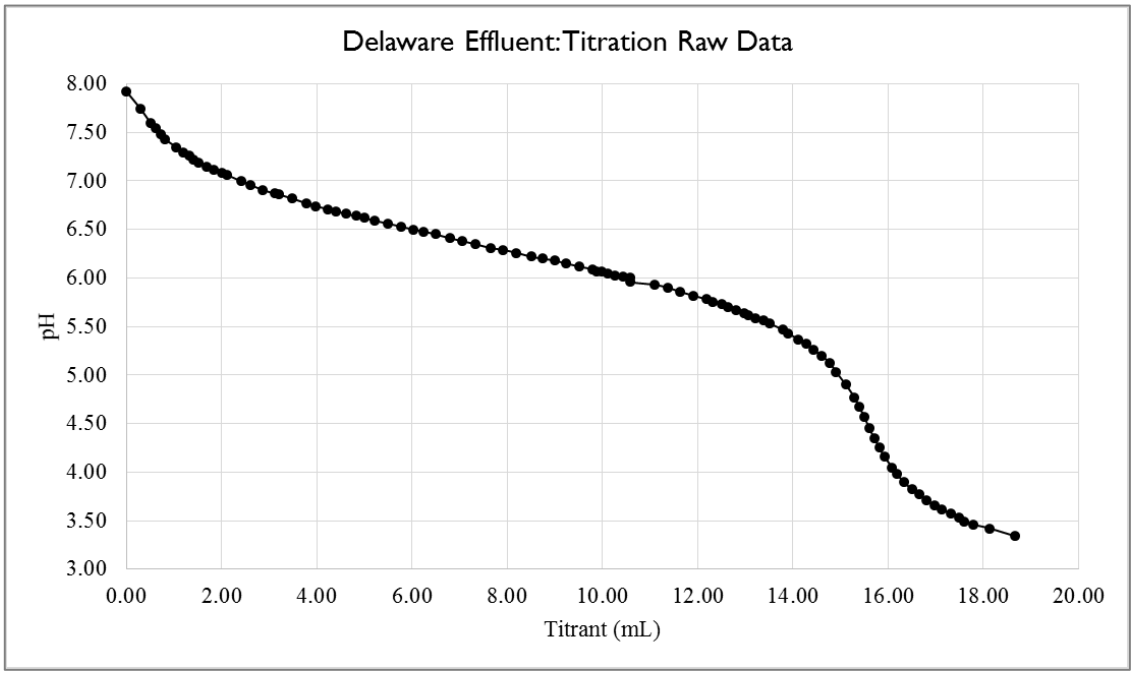
Delaware Effluent: Titration Raw Data
8.00
7.50
7.00
6.50
6.00
5.50
5.00
4.50
4.00
3.50
3.00
pH
0.00
2.00
4.00
6.00
8.00
10.00
12.00
14.00
16.00
18.00
20.00
Titrant (mL)

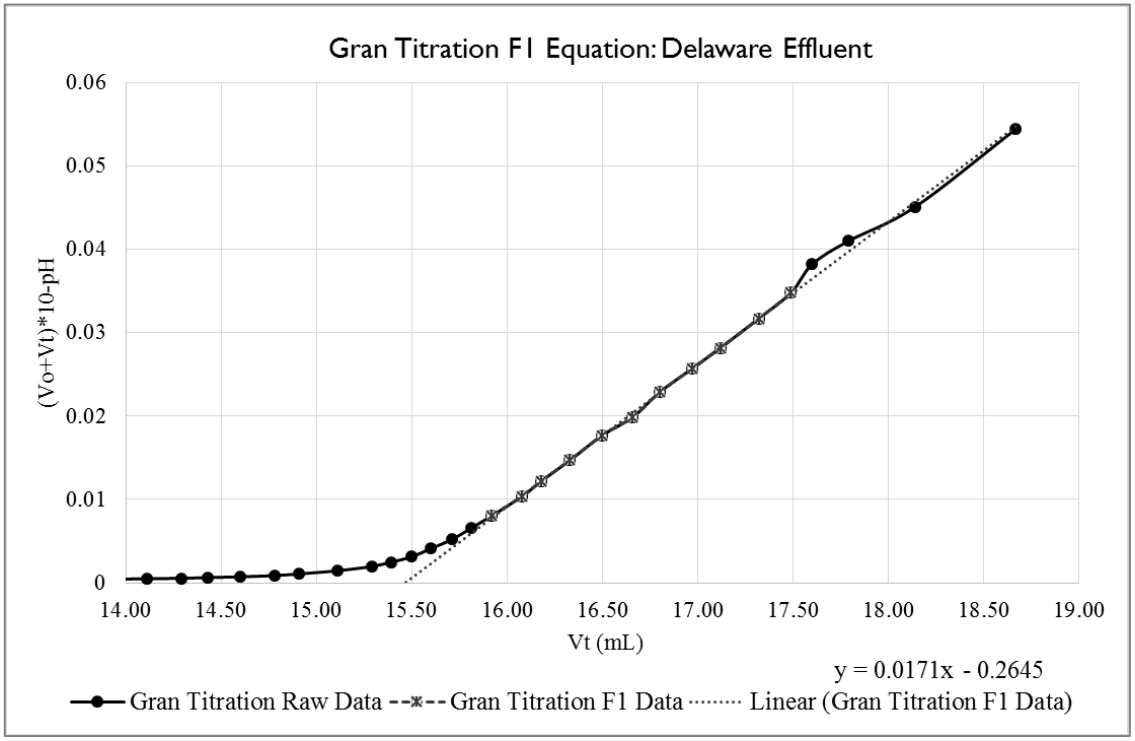
Gran Titration F1 Equation: Delaware Effluent
0.06
0.05
0.04
0.03
0.02
0.01
0
(Vo+Vt)*10-pH
14.00
14.50
15.00
15.50
16.00
16.50
17.00
17.50
18.00
18.50
19.00
Vt (mL)
y = 0.0171x - 0.2645
Gran Titration Raw Data
Gran Titration F1 Data
Linear (Gran Titration F1 Data)

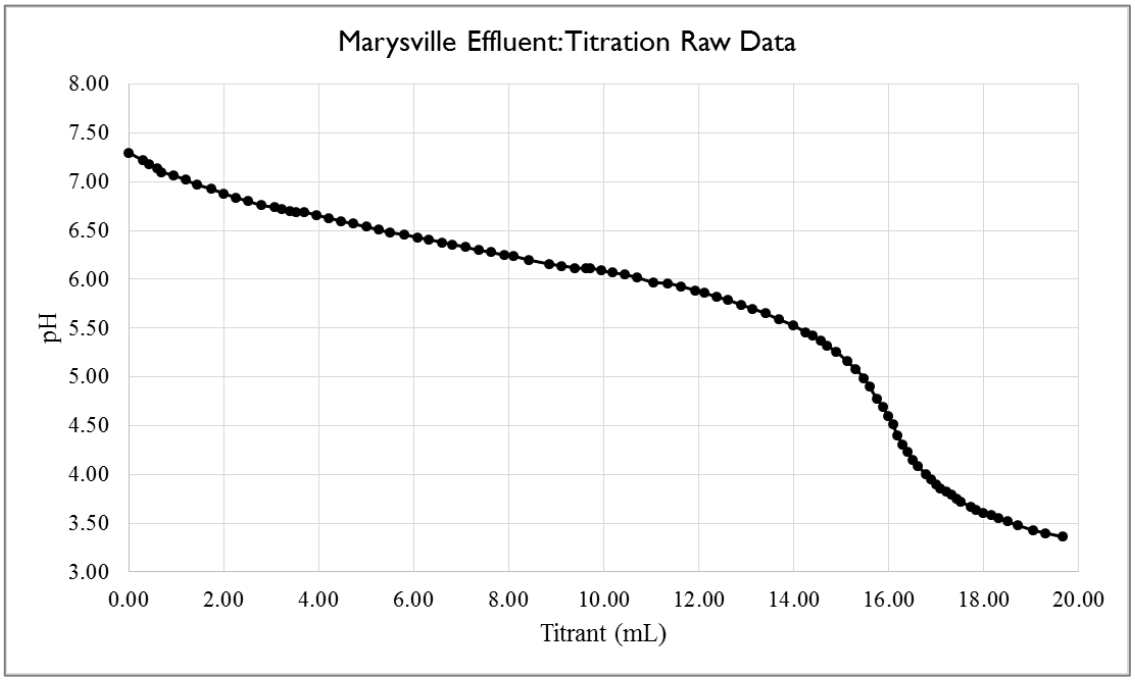
Marysville Effluent: Titration Raw Data
8.00
7.50
7.00
6.50
6.00
5.50
5.00
4.50
4.00
3.50
3.00
pH
0.00
2.00
4.00
6.00
8.00
10.00
12.00
14.00
16.00
18.00
20.00
Titrant (mL)

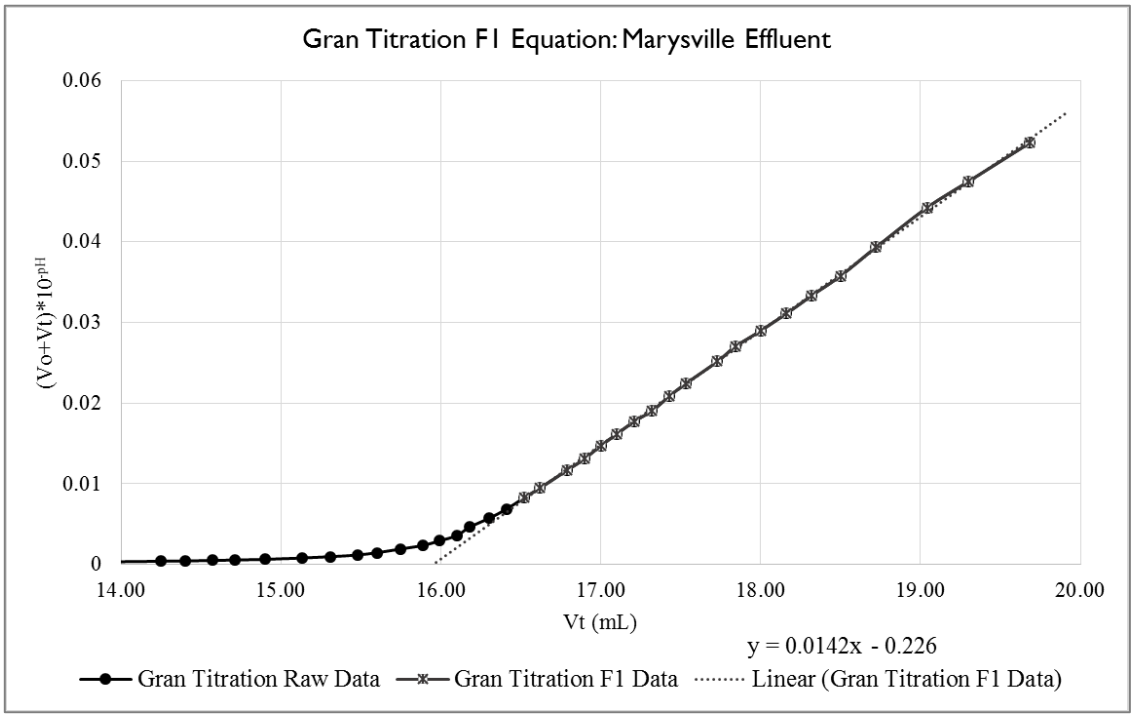
Gran Titration F1 Equation: Marysville Effluent
0.06
0.05
0.04
0.03
0.02
0.01
0
(Vo+Vt)*10^pH
14.00
15.00
16.00
17.00
18.00
19.00
20.00
Vt (mL)
y = 0.0142x - 0.226
Gran Titration Raw Data
Gran Titration F1 Data
Linear (Gran Titration F1 Data)

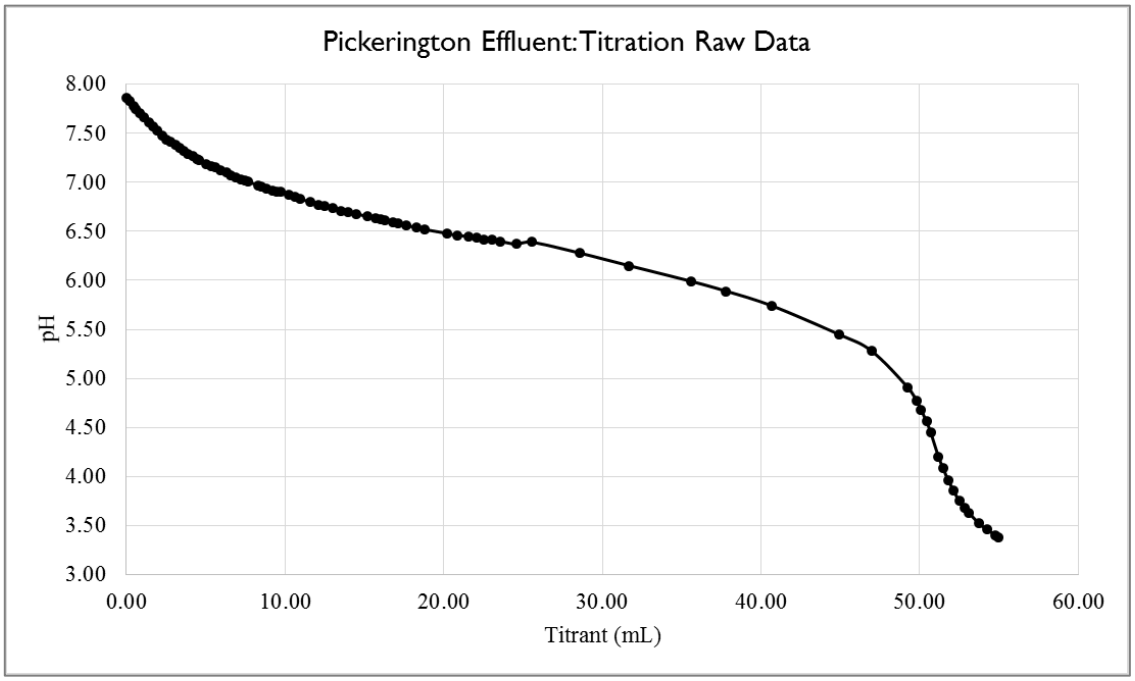
Pickerington Effluent: Titration Raw Data
8.00
7.50
7.00
6.50
6.00
5.50
5.00
4.50
4.00
3.50
3.00
pH
0.00
10.00
20.00
30.00
40.00
50.00
60.00
Titrant (mL)

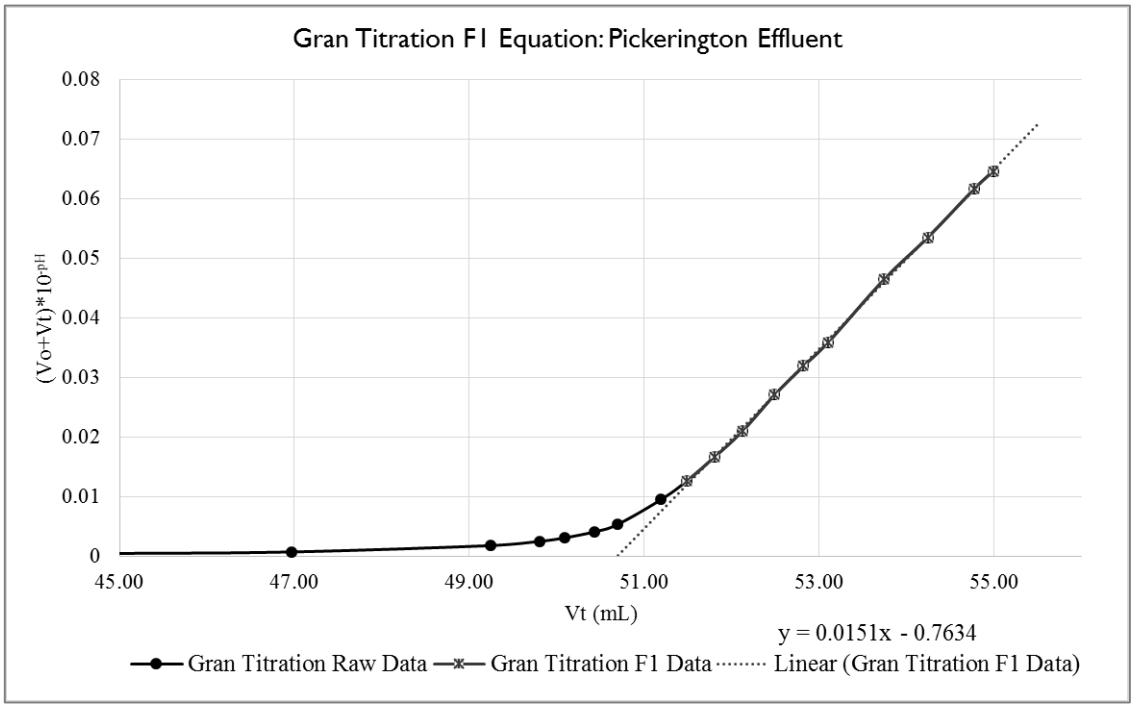
Gran Titration F1 Equation: Pickerington Effluent
0.08
0.07
0.06
0.05
0.04
0.03
0.02
0.01
0
(Vo+Vt)*10^pH
45.00
47.00
49.00
51.00
53.00
55.00
Vt (mL)
y = 0.0151x - 0.7634
Gran Titration Raw Data
Gran Titration F1 Data
Linear (Gran Titration F1 Data)

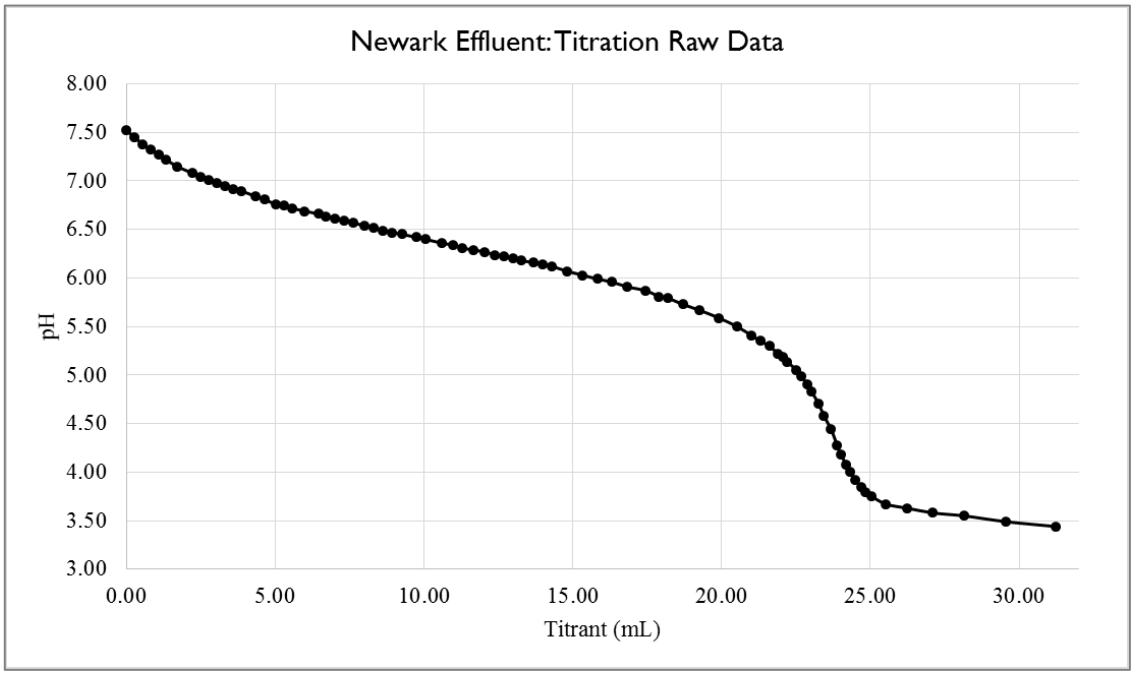
Newark Effluent: Titration Raw Data
8.00
7.50
7.00
6.50
6.00
5.50
5.00
4.50
4.00
3.50
3.00
pH
0.00
5.00
10.00
15.00
20.00
25.00
30.00
Titrant (mL)

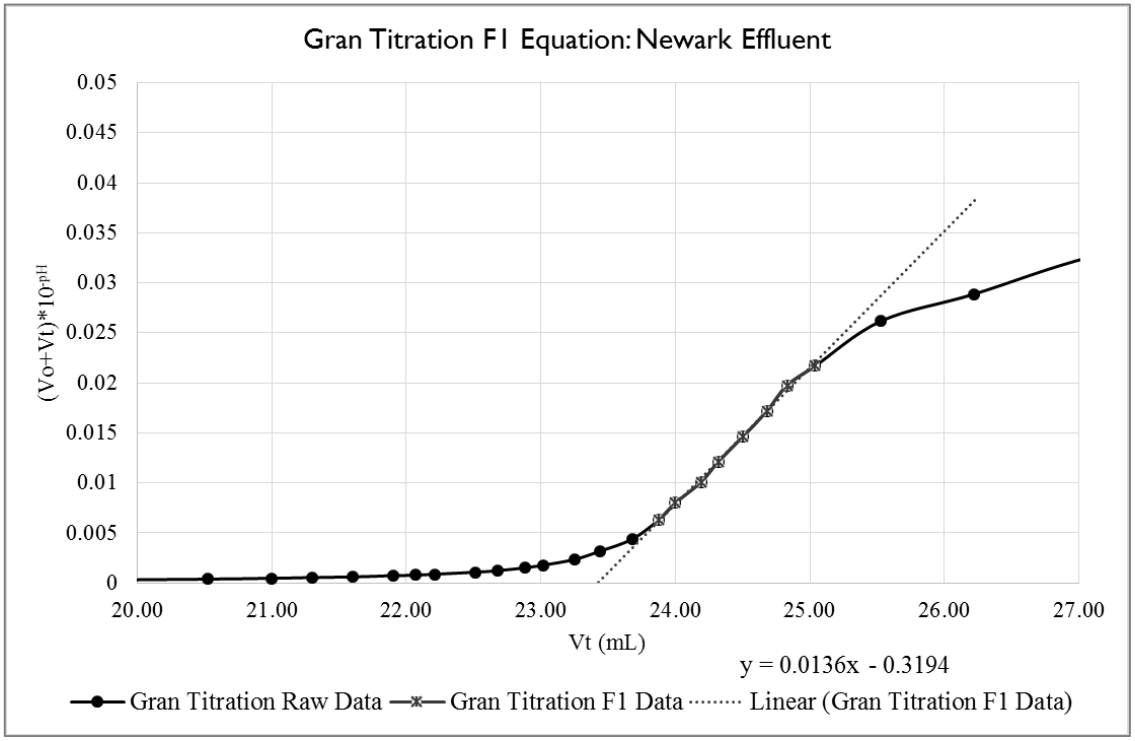
Gran Titration F1 Equation: Newark Effluent
0.05
0.045
0.04
0.035
0.03
0.025
0.02
0.015
0.01
0.005
0
(Vo+Vt)*10^pH
20.00
21.00
22.00
23.00
24.00
25.00
26.00
27.00
Vt (mL)
y = 0.0136x - 0.3194
Gran Titration Raw Data
Gran Titration F1 Data
Linear (Gran Titration F1 Data)

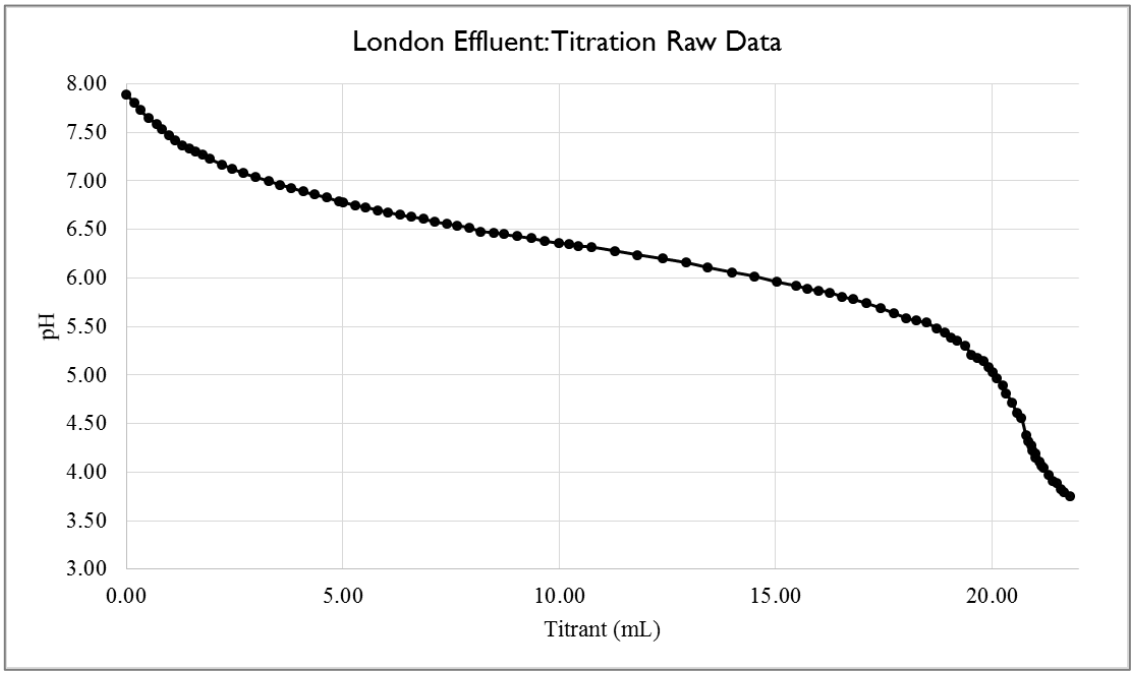
London Effluent: Titration Raw Data
8.00
7.50
7.00
6.50
6.00
5.50
5.00
4.50
4.00
3.50
3.00
pH
0.00
5.00
10.00
15.00
20.00
Titrant (mL)

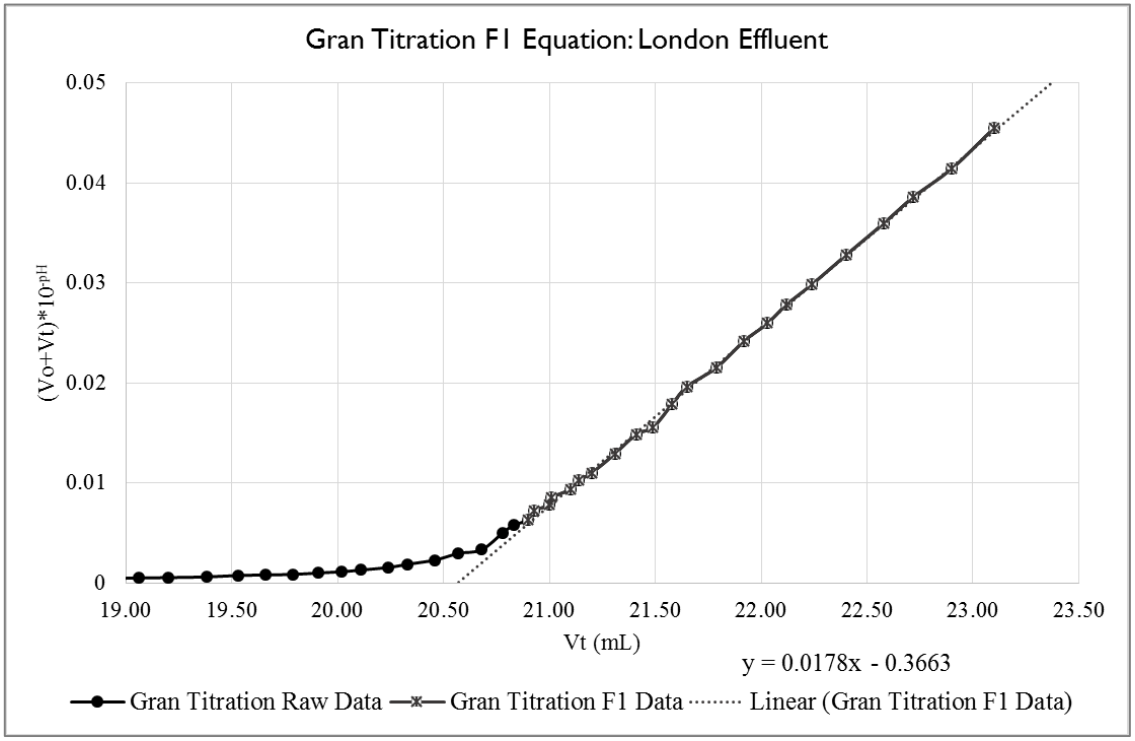
Gran Titration F1 Equation: London Effluent
0.05
0.04
0.03
0.02
0.01
0
(Vo+Vt)*10^pH
19.00
19.50
20.00
20.50
21.00
21.50
22.00
22.50
23.00
23.50
Vt (mL)
y = 0.0178x - 0.3663
Gran Titration Raw Data
Gran Titration F1 Data
Linear (Gran Titration F1 Data)

Online Alkalinity Calculator methods are detailed on the USGS Oregon Water Science Center website (Rounds S., Methods for Alkalinity Calculator, 2013). For each computation, parameters were modified as noted. Alkalinity values for each method for each sample are listed, with the average and standard deviation recorded as reported in the Results section. A graph visually showing the relative outputs of each method is included for reference.

Site Name – Effluent sample name
Collection Date – Date of collection & titration
Sample Temperature - Assumed to be 20°C
Sample Volume – Volume of sample in mL
Filtered Sample – Yes
Acid Concentration – Other
Specify other acid concentration – 0.01703 N
Titration Data Field – Input titration data
Acid Correction Factor – 1.00
Stirring Method – Magnetic
Titration Type – Burette
Order of titration data – pH in 1st column, titrant volume in 2nd column
Analysis Methods – Selected Inflection Point, Gran Function Plot, and Theoretical Carbonate Titration Curve

Alkalinity values for effluent samples from six computational methods: Gran Function F1 done manually in Excel and from the online calculator using the advanced speciation method: Inflection Point, Theoretical Carbonate Titration Curve Methods 1 and 2, and Gran Functions F1 and F3.

Alkalinity Values for Effluent Samples from Six Computational Methods

	Effluent Sample Alkalinity (meq/L)				
Methods	DEL	MAR	PIC	NEW	LON
Excel GF-F1*	2.62	2.72	8.62	4.12	3.53
IP	2.62	2.74	8.61	4.19	3.58
TCTCM1	2.61	2.76	8.62	4.29	3.50
TCTCM2	2.59	2.76	8.58	4.19	3.53
GF-F1	2.61	2.71	8.57	3.76[b]	3.51
GF-F3	2.68	2.99[a]	8.99	4.28	3.67
Average	2.62	2.78	8.67	4.14	3.55
Std Dev	0.03	0.10	0.15	0.18	0.06
Median	2.62	2.74	8.62	4.19	3.53

a,b Online Alkalinity calculator warning that the carbonate titration curve does not fit the data well, giving a mean absolute titrant volume error of 1.04 mL and 1.18 mL respectively, indicating that something else was neutralized in this titration. These values are estimates.

* This manual Excel-based calculation did not utilize the advanced speciation method.

GF = Gran Function Plot Method
IP = Inflection Point Method
TCTCM – Theoretical Carbonate Titration Curve Method

DEL Graphed Titration & Inflection Point

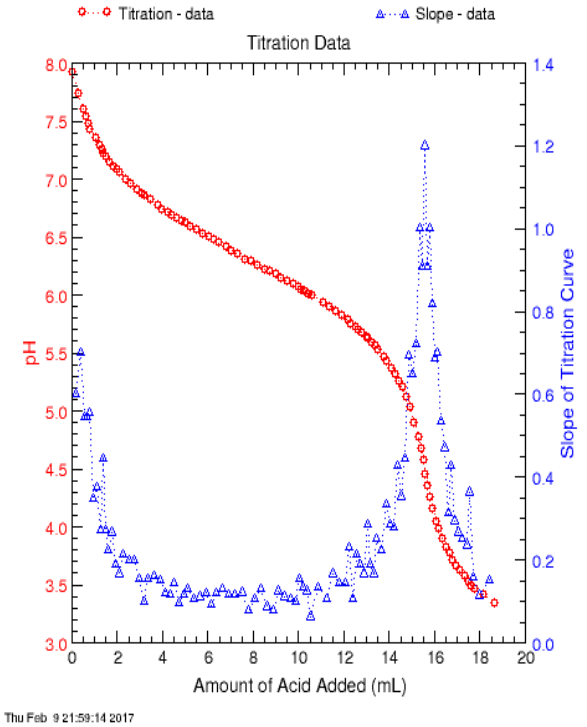

Gran Functions F1 and F3

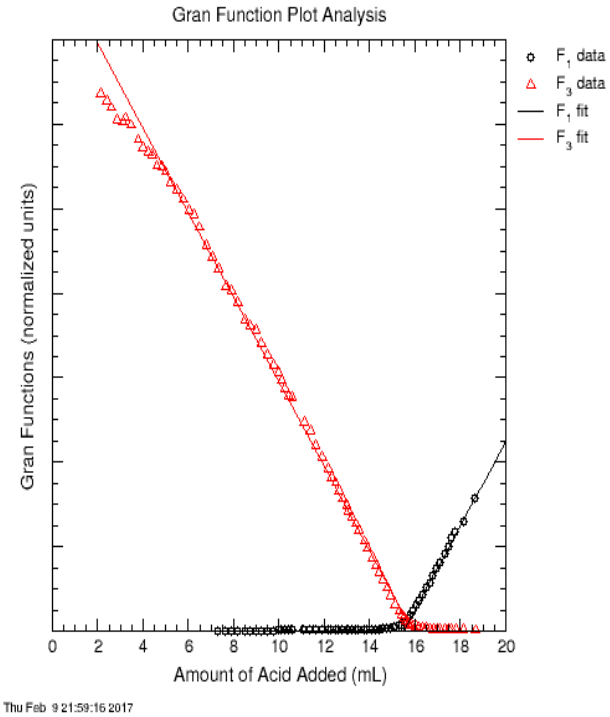

Theoretical Carbonate Titration Curve - 1

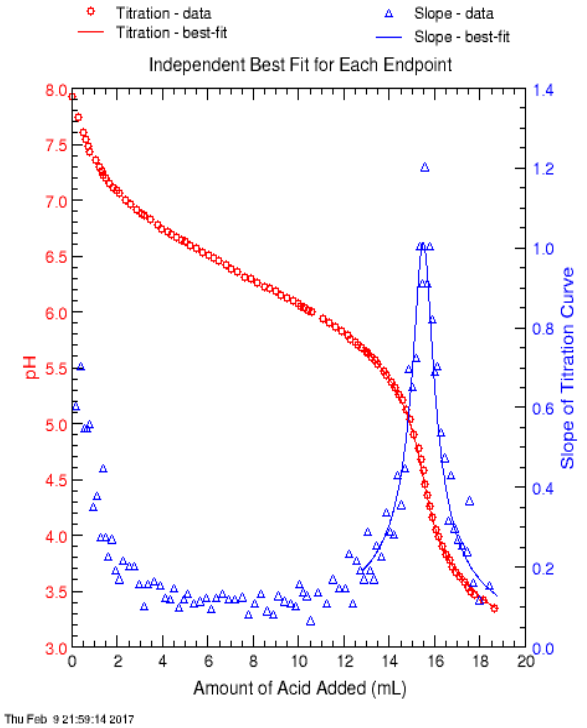

Theoretical Carbonate Titration Curve - 2

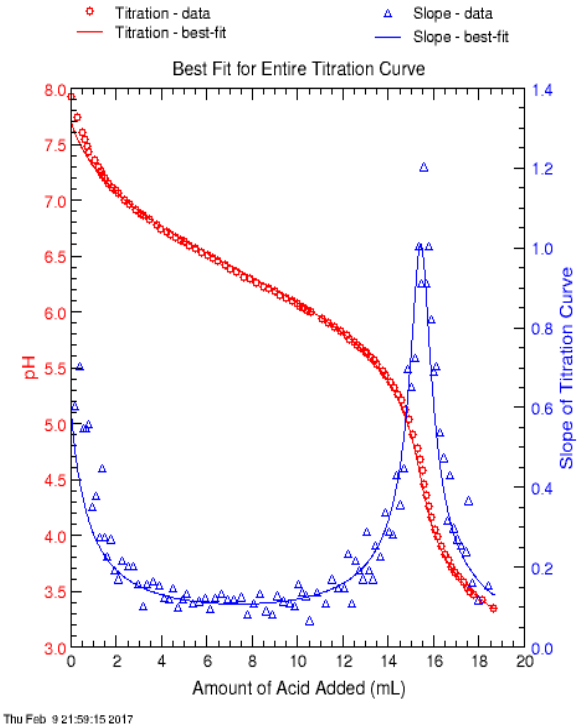

Delaware (DEL) Online Alkalinity Calculator Figures

MAR Graphed Titration & Inflection Point

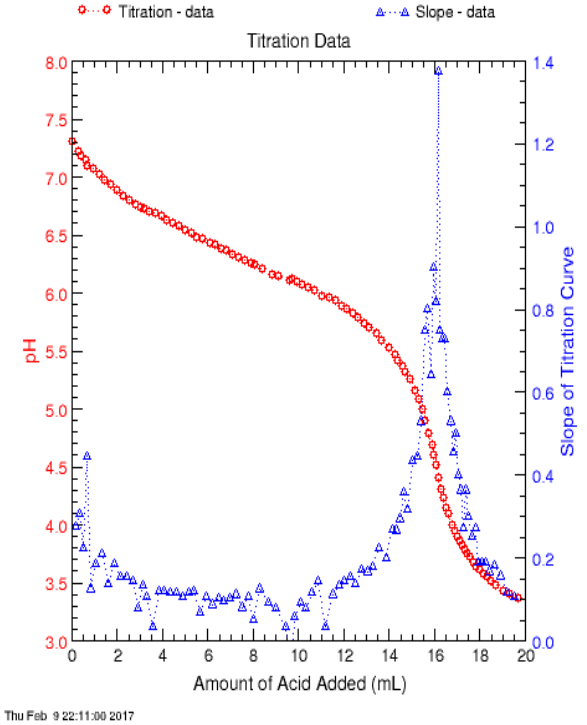

Gran Functions F1 and F3

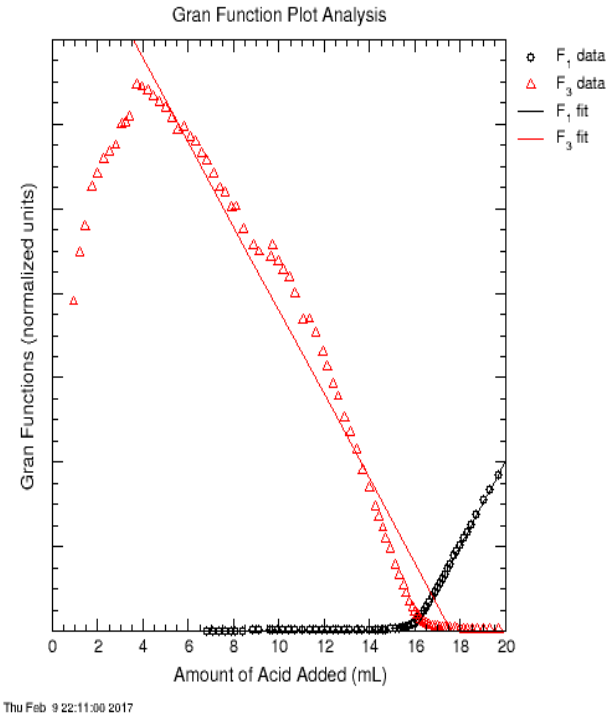

Theoretical Carbonate Titration Curve - 1

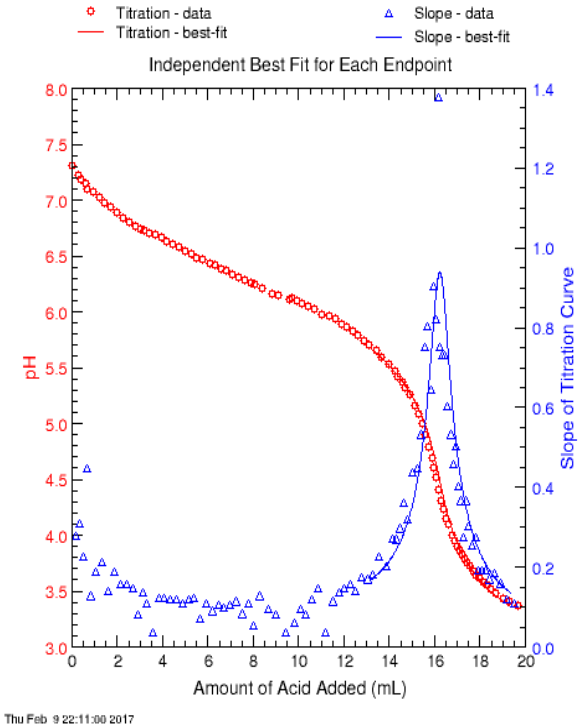

Theoretical Carbonate Titration Curve - 2

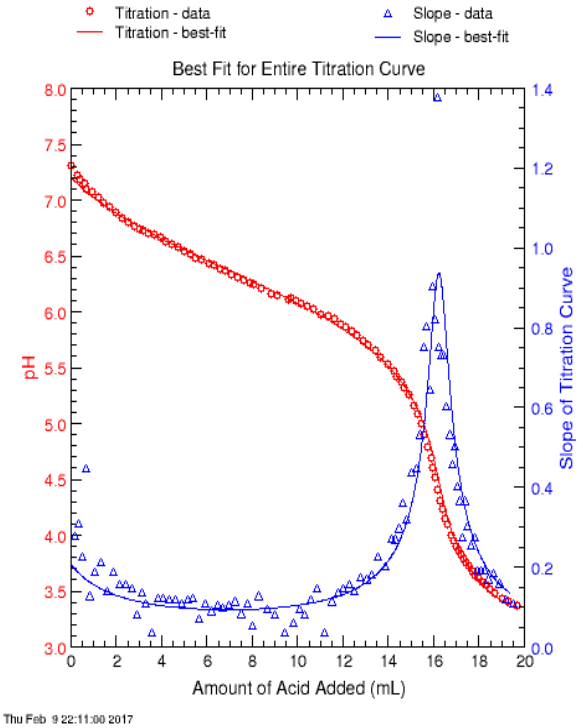

Marysville (MAR) Online Alkalinity Calculator Figures

PIC Graphed Titration & Inflection Point

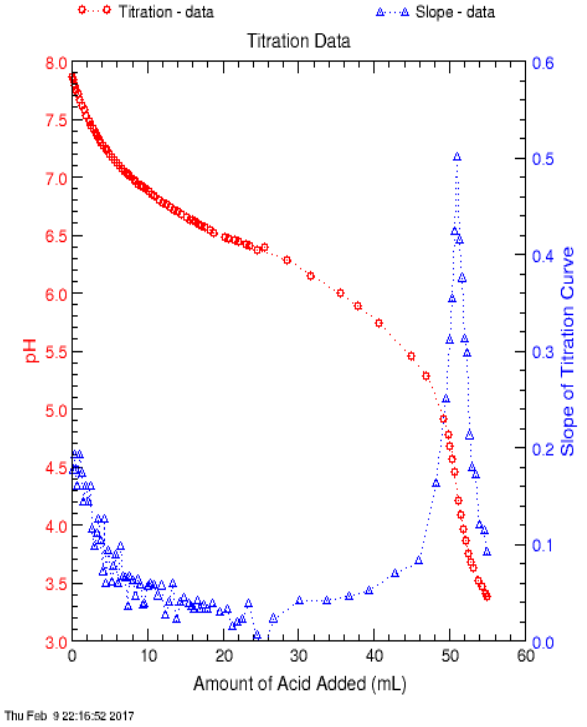

Gran Functions F1 and F3

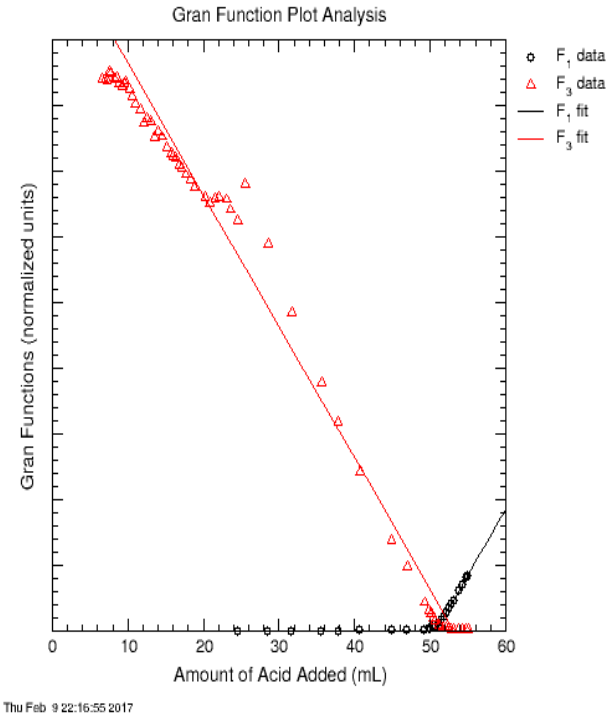

Theoretical Carbonate Titration Curve - 1

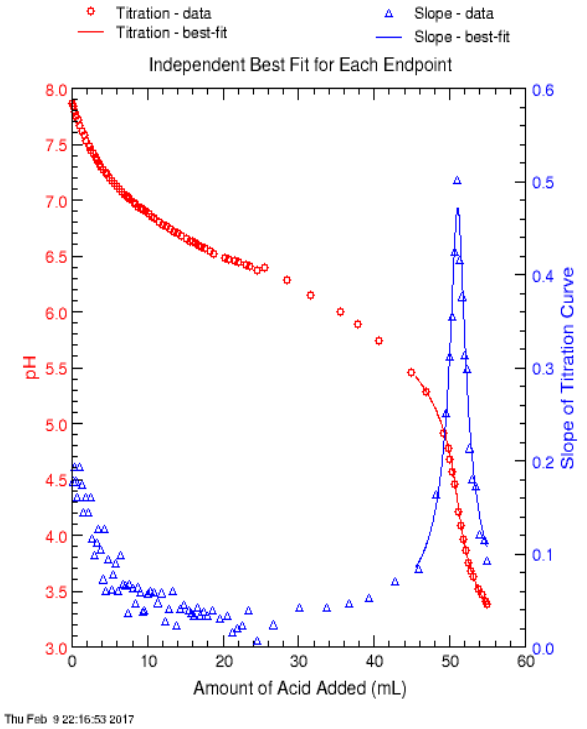

Theoretical Carbonate Titration Curve - 2

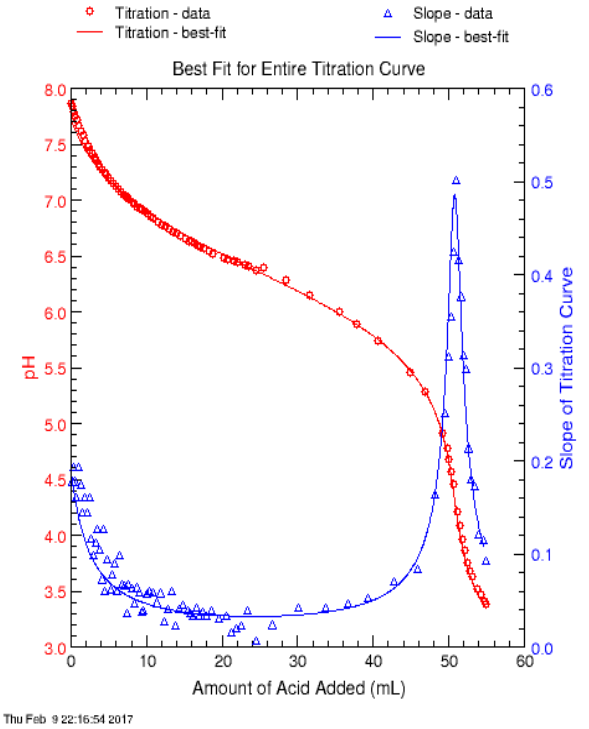

Pickerington (PIC) Online Alkalinity Calculator Figures

NEW Graphed Titration & Inflection Point

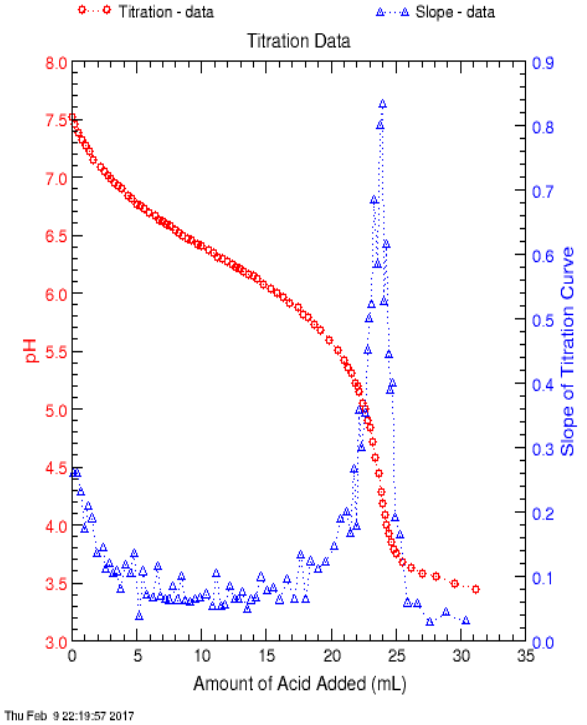

Gran Functions F1 and F3

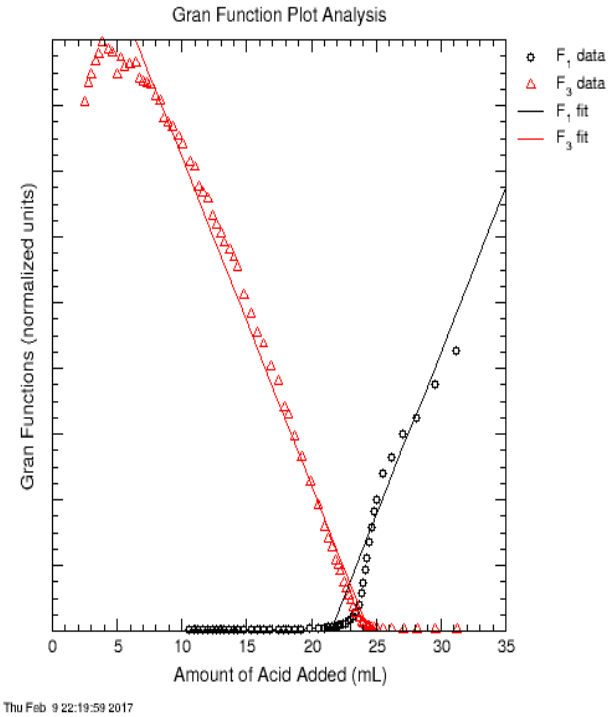

Theoretical Carbonate Titration Curve - 1

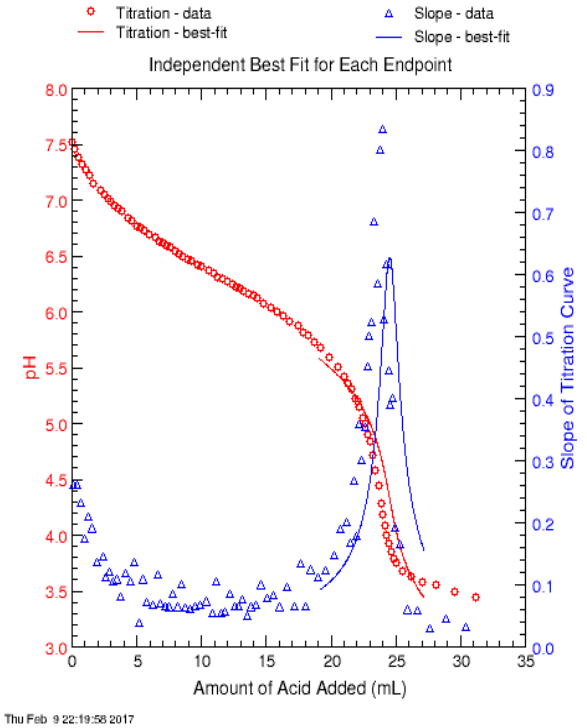

Theoretical Carbonate Titration Curve - 2

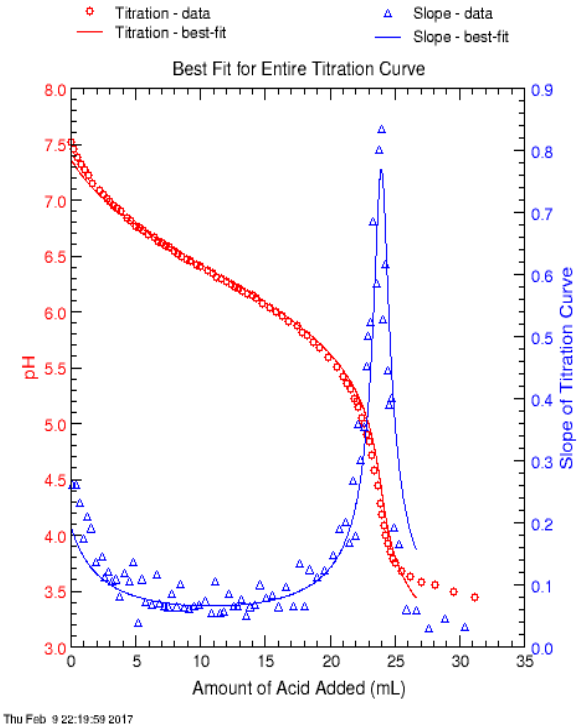

Newark (NEW) Online Alkalinity Calculator Figures

LON Graphed Titration & Inflection Point

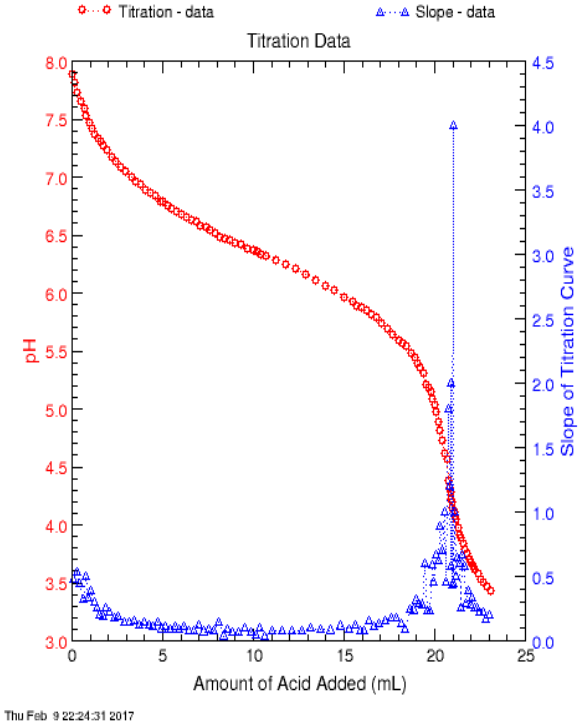

Gran Functions F1 and F3

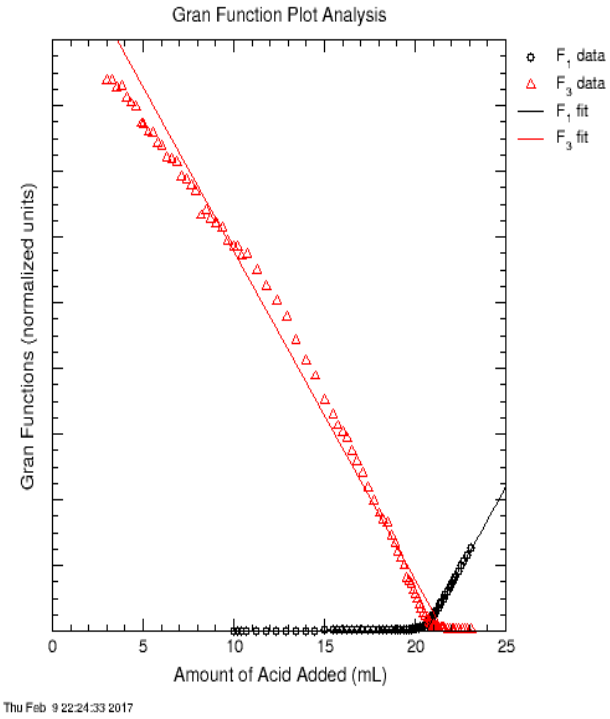

Theoretical Carbonate Titration Curve - 1

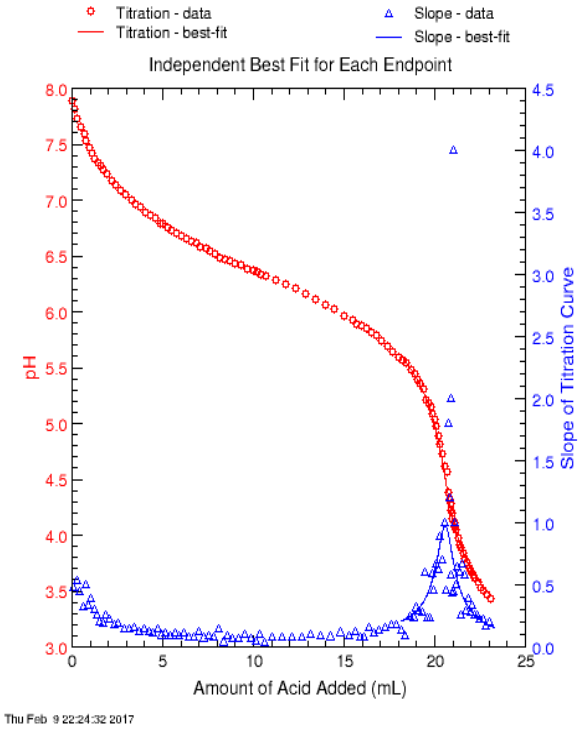

Theoretical Carbonate Titration Curve - 2

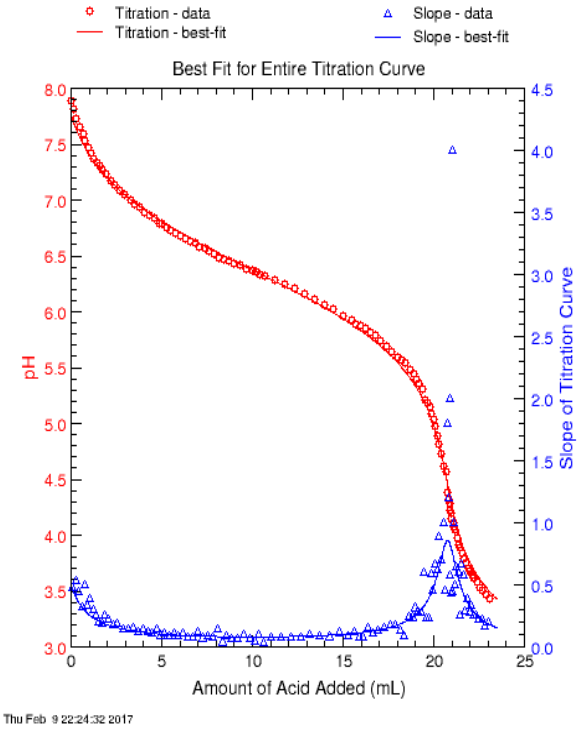

London (LON) Online Alkalinity Calculator Figures

UV-Vis Instrument Settings and Calculation Data

Instrument settings for the Shimadzu UV-1800 Series are shown below:

Wavelength Scanned:	λ = 190 – 800 nm
Wavelength Accuracy:	±0.3nm (190 to 1100nm)
Photometric Accuracy:	±0.002 Abs (0.5Abs)
	±0.004 Abs (1.0Abs)
	±0.006 Abs (2.0Abs)
Scan Speed:	Medium
Interval Measured:	Every 1.0 nm
Spectral Bandwidth:	1.0 nm
Light Source Change:	λ = 340 nm
Measuring:	Absorbance

Data used for SUVA and E_2/E_3 calculations are included below, where MQ for Filtered and MQ for Irradiated were the Milli-Q water blanks before UV-Vis analysis of filtered, non-irradiated effluent for filtered, 8-hr irradiated effluent working solution respectively.

Data for SUVA and E2/E3 Calculations

	DOC (mg_C L^{-1})	Absorbance @ 254 nm (unitless)	UVA @ 254 nm (cm^{-1})	SUVA @ 254 nm (L mg^{-1} m^{-1})	Absorbance @ 280 nm (unitless)	UVA @ 280 nm (cm^{-1})	SUVA @ 280 nm (L mg^{-1} m^{-1})	Absorbance @ 365 nm (unitless)	E2/E3 @ 254 nm / 365 nm	E2/E3 @ 280 nm / 365 nm
Delaware (DEL)										
MQ for Filtered	5.8	0.000	0.000	0.0	0.001	0.001	0.0	0.001	0.0	1.0
Non-Irradiated Effluent	5.8	0.141	0.141	2.4	0.110	0.110	1.9	0.029	4.9	3.8
MQ for Irradiated	5.8	-0.002	-0.002	0.0	-0.001	-0.001	0.0	0.000	0.0	0.0
SUN Irradiated Effluent	5.8	0.112	0.112	1.9	0.081	0.081	1.4	0.018	6.2	4.5
Marysville (MAR)										
MQ for Filtered	7.5	0.004	0.004	0.1	0.003	0.003	0.0	0.002	2.0	1.5
Non-Irradiated Effluent	7.5	0.163	0.163	2.2	0.116	0.116	1.6	0.028	5.8	4.1
MQ for Irradiated	7.5	-0.006	-0.006	-0.1	-0.005	-0.005	-0.1	-0.002	3.0	2.5
SUN Irradiated Effluent	7.5	0.125	0.125	1.7	0.081	0.081	1.1	0.014	8.9	5.8
Pickerington (PIC)										
MQ for Filtered	28.2	-0.006	-0.006	0.0	-0.005	-0.005	0.0	-0.002	3.0	2.5
Non-Irradiated Effluent	28.2	0.099	0.099	0.4	0.075	0.075	0.3	0.018	5.5	4.2
MQ for Irradiated	28.2	-0.004	-0.004	0.0	-0.003	-0.003	0.0	-0.002	2.0	1.5
SUN Irradiated Effluent	28.2	0.077	0.077	0.3	0.052	0.052	0.2	0.008	10.3	6.9
Newark (NEW)										
MQ for Filtered	6.7	-0.002	-0.002	0.0	-0.002	-0.002	0.0	-0.001	2.0	2.0
Non-Irradiated Effluent	6.7	0.177	0.177	2.6	0.131	0.131	2.0	0.036	4.9	3.6
MQ for Irradiated	6.7	-0.004	-0.004	-0.1	-0.003	-0.003	0.0	-0.001	4.0	3.0
SUN Irradiated Effluent	6.7	0.167	0.167	2.5	0.118	0.118	1.8	0.028	6.0	4.2
London (LON)										
MQ for Filtered	4.5	0.006	0.006	0.1	0.006	0.006	0.1	0.004	1.5	1.5
Non-Irradiated Effluent	4.5	0.120	0.120	2.7	0.094	0.094	2.1	0.028	4.3	3.4
MQ for Irradiated	4.5	0.009	0.009	0.2	0.008	0.008	0.2	0.004	2.3	2.0
SUN Irradiated Effluent	4.5	0.097	0.097	2.2	0.071	0.071	1.6	0.016	6.1	4.4

PHOTOLYSIS PROCEDURE: INITIAL RATES

A 1 L Erlenmeyer flask, ~ 300 mL effluent sample, caffeine stock solution, dilute HCl solutions, Milli-Q water, Teflon stir bars, three 150 mL beakers, Teflon tape wrapped o-rings, quartz phototubes with lids, clamps, micropipets to pipet 30-90 µL (DEL), 60-120 µL (all other samples), and 12-40 µL (all samples for calibration curve solutions) volumes, aluminum foil, and quantities of 1 mL borosilicate HPLC autosampling vials were used for photolysis experiments.

Initial Rates

The initial rates method below was used with permission from "Dynamics in the reactivity and photochemical production of hydroxyl radical in treated wastewater effluent and aquatic dissolved organic matter" and has been copied and modified here to detail the algebraic relationships between equations, clarify units, and indicate equation usage in data analysis for experimental data (Semones, 2017).

Initial Rates Method

Assume:

1) Probe concentration does impact $[HO\bullet]_{ss}$

2) Steady state [HO•], where: $d[HO\bullet]/dt=0$ and $P_{\bullet OH}=R_{ns} + R_p$

where $P_{HO\bullet}$ = hydroxyl radical production rate

R_{ns} = consumption of hydroxyl radical by natural scavengers

R_p = consumption of hydroxyl radical by added probe

$P_{HO\bullet}$ is a positive value as it is the generation of hydroxyl radical, and R_{ns} and R_p are positive values as the numbers describe the consumption of hydroxyl radical, so the decrease of hydroxyl radical is implied.

We then have the following equations:

$$P_{HO\bullet}=R_{ns} + R_p \qquad \text{Equation S1}$$

$$R_{ns}=k'_{ns}\,[HO\bullet]'_{ss} \qquad \text{Equation S2}$$

$$R_p=k_p\,[probe]\,[HO\bullet]'_{ss} \qquad \text{Equation S3}$$

where

$P_{HO\bullet}$ = production of hydroxyl radical

$[HO\bullet]'_{ss}$ = the apparent steady state concentration at a given probe concentration

k'_{ns} = the background scavenging rate

k_p = probe second order/bimolecular rate constant

Note that the apparent steady state concentration at a given probe concentration is in the *presence* of probe and that the steady state concentration of hydroxyl radical (without the prime) is in the *absence* of probe.

Rearrange Equation S3 to:

$$[HO\bullet]'_{ss} = R_p/[probe]k_p \qquad \text{Equation S4}$$

Plug Equation S4 into Equation S2:

$$R_{ns}=k'_{ns}\, R_p/([probe]\, k_p) \qquad \text{Equation S5}$$

Plug Equation S5 into Equation S1:

$$P_{HO\bullet} = k'_{ns}\, R_p/([probe]\, k_p) + Rp \qquad \text{Equation S6}$$

Rearrange Equation S6:

$$P_{HO\bullet}= R_p\,(1+ (k'_{ns}/([probe]\, k_p)))$$
$$R_p= P_{HO\bullet}/(1+ (k'_{ns}/([probe]\, k_p)))$$
$$R_p= P_{HO\bullet}\,[probe]\, k_p/ k'_{ns} + P_{HO\bullet}$$
$$1/ R_p =k'_{ns} / (P_{HO\bullet}\, k_p)\,(1 / [probe]) + 1/ P_{HO\bullet} \qquad \text{Equation S7}$$

Equation S7 is a linear equation. Experiments are run at multiple probe concentrations and the results plotted $1/R_p$ vs. 1/[probe]. From this plot $P_{HO\bullet}$, k'_{ns} and $[HO\bullet]_{ss}$ can be determined from plot parameters:

$$m =k'_{ns} / (P_{HO\bullet}\, k_p) \qquad \text{Equation S8}$$
$$b = 1/ P_{HO\bullet} \qquad \text{Equation S9}$$
$$[HO\bullet]_{ss} = P_{HO\bullet}/k'_{ns} = 1/(m\, k_p) \qquad \text{Equation S10}$$
$$k'_{ns} = m\, k_p / b \qquad \text{Equation S11}$$

For each HPLC vial, peak areas of vial injections were averaged to calculate caffeine concentrations from calibration curve data using the Excel-based LINEST function. To obtain the rate of caffeine reaction over time, time in seconds was plotted against the caffeine concentration of each vial, and the consumption of •OH due to added probe (R_p) in units of Ms^{-1} and its associated error were calculated from the slope of the resulting line.

The reaction rate results from each caffeine level were plotted as $1/R_p$ versus 1/[probe] and analyzed using the Excel-based LINEST function, where [probe] is the initial probe

concentration for each caffeine level as determined by using the LINEST function on dark control vials to determine the y-intercept. This plotting of $1/R_p$ versus 1/[probe] results in m (slope) in units of seconds, b (intercept) in units of sM^{-1}, and associated errors. From this plot, $P_{\bullet OH}$, k'_{ns}, and $[\bullet OH]_{ss}$ can be determined, where $[\bullet OH]_{ss}$ is the steady state concentration at a given probe concentration, $P_{\bullet OH}$ is the overall production rate of hydroxyl radical and k'_{ns} is the background scavenging rate of natural scavengers.

$$m = k'_{ns}/(P_{\bullet OH}\, k_p)$$

$$b = 1/P_{\bullet OH}$$

$$[\bullet OH]_{ss} = \frac{P_{\bullet OH}}{k'_{ns}} = \frac{1}{m\, k_p}$$

$$k'_{ns} = \frac{(m\, k_p)}{b}$$

$P_{\bullet OH}$ was found by calculating 1/b (intercept from $1/R_p$ vs 1/[probe]). The variable k_p is a literature constant of 5.9E+9 $M^{-1}s^{-1}$, where k_p is the caffeine probe second order rate constant (Shi & Dalal, 1991). The variable k'_{ns} was calculated by (m * k_p)/b and has units of s^{-1}. The hydroxyl radical steady state concentration can then be calculated either by $P_{\bullet OH}/k'_{ns}$ or by 1/(m * k_p) and has units of molarity.

Additional Photolysis Notes

The spectra provided of the Suntest CPS+ equipped with a solar filter can be compared to the solar irradiance spectrum observed at sea level. An included illustration, denoting the solution making pathway for HPLC analysis of caffeine to measure the initial rates kinetics values, shows the progression of solution preparation from filtered effluent sample to spiked photolysis phototubes and dark control vials. Approximately 300 mL filtered effluent was combined with dilute HCl to adjust to pH 7 to form a working solution. Aliquots of approximately 60 mL working solution were transferred to smaller flasks and spiked with respective 5, 10, 15, or 20 μM caffeine probes. Two phototubes and two borosilicate vials were filled with aliquots of each caffeine-spiked working solution for each time point. Borosilicate vials covered in foil served as dark controls. A phototube containing only working solution was irradiated for the entire duration (time point T3, eight hours) as a control in each experiment. Phototubes and vials were pulled at their respective time points of T1, T2, and T3, corresponding

to one, four, and eight-hour elapsed time respectively. All experiments used 10, 15, and 20 µM caffeine spikes except for Delaware, which used 5, 10, and 15 µM caffeine probe spikes.

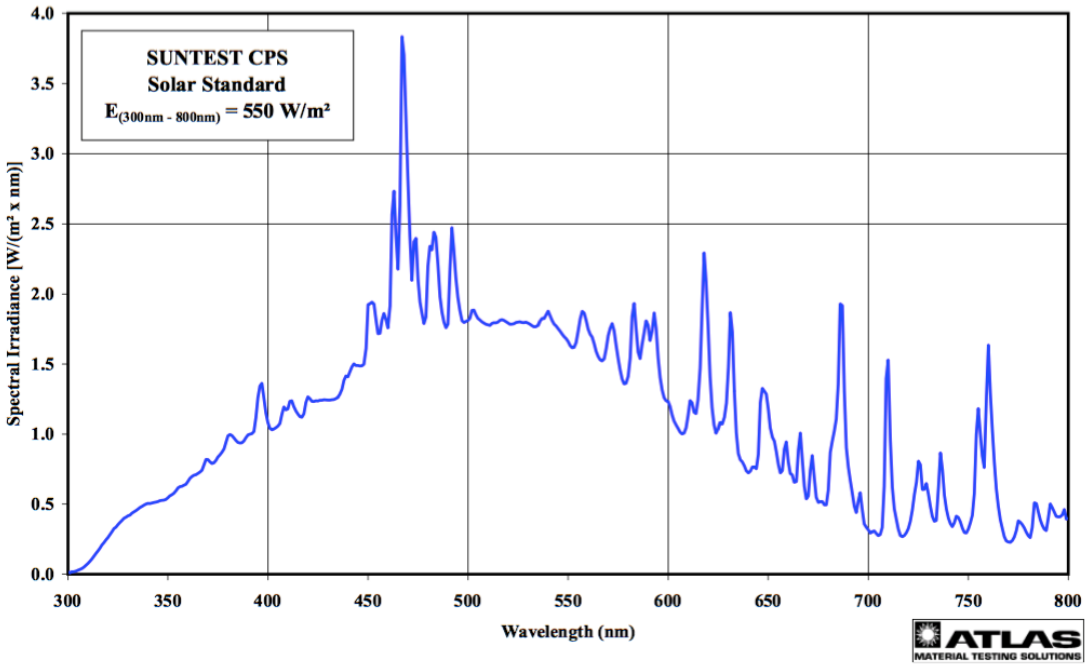

Spectra of the Suntest CPS+ equipped with solar filter. Spectra provided by Atlas Material Testing Solutions, Mount Prospect, Illinois.

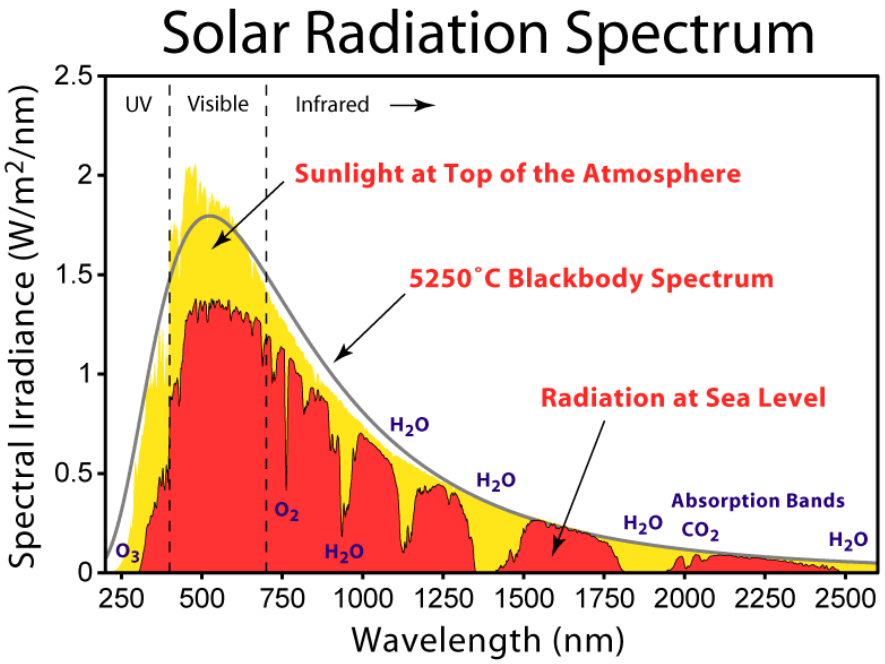

CC BY-SA 3.0, https://commons.wikimedia.org/w/index.php?curid=2623187

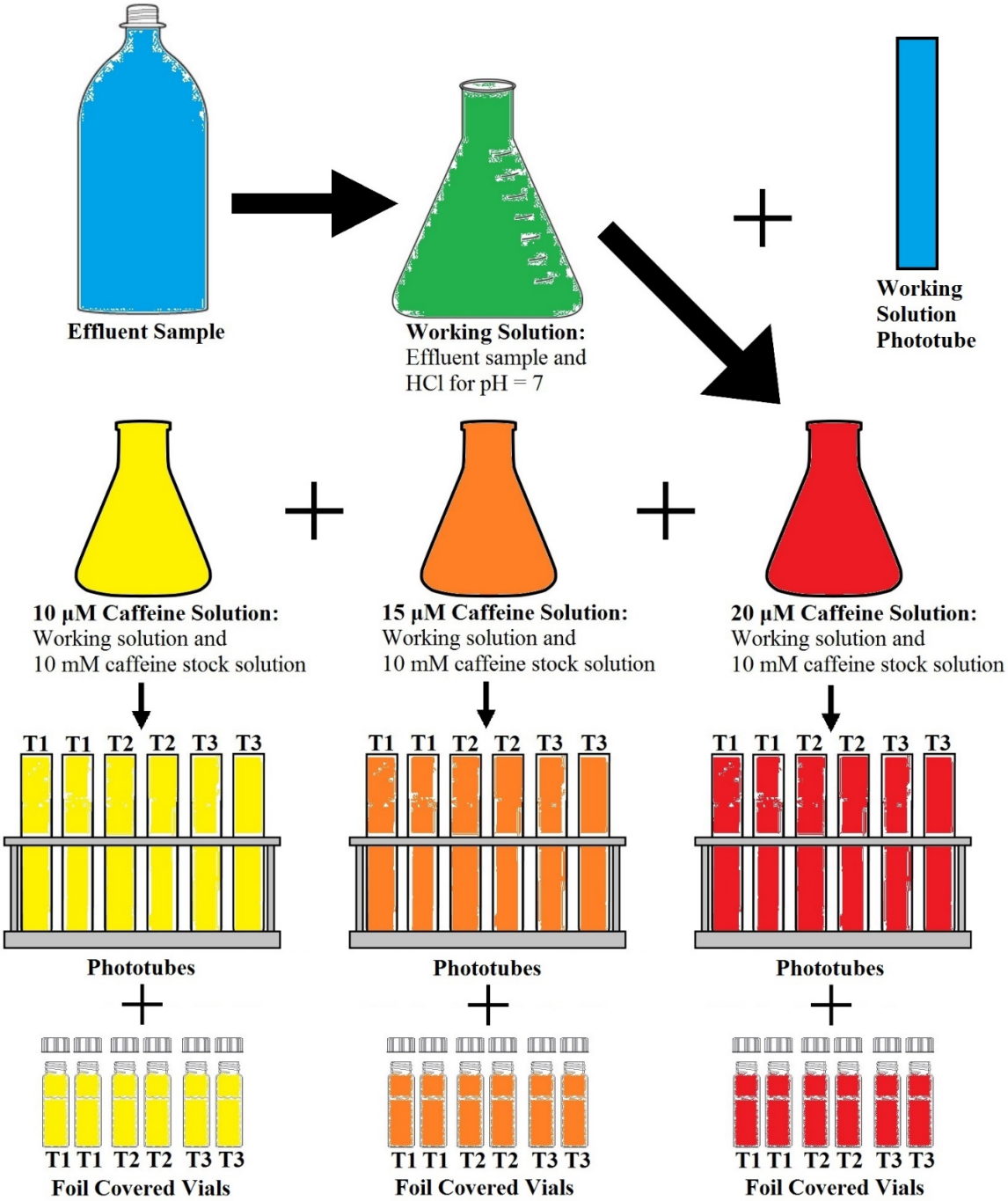

An illustration showing the progression of solution making for HPLC analysis using caffeine probes to measure hydroxyl radical steady state concentration. Foil covered vials served as dark controls for each time point. Two additional foil covered vials not shown in this image served as dark controls for time point T0 for each caffeine level.

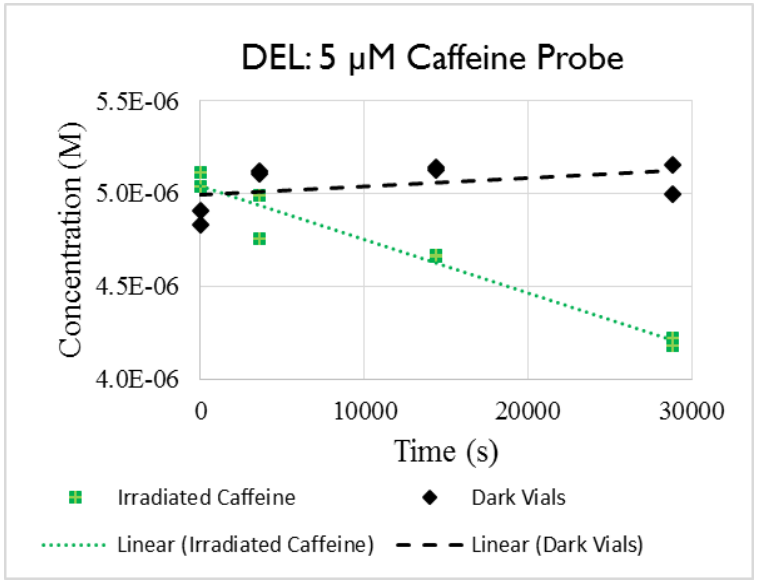
DEL: 5 µM Caffeine Probe
Concentration (M)
5.5E-06
5.0E-06
4.5E-06
4.0E-06
0
10000
20000
30000
Time (s)
Irradiated Caffeine
Dark Vials
Linear (Irradiated Caffeine)
Linear (Dark Vials)

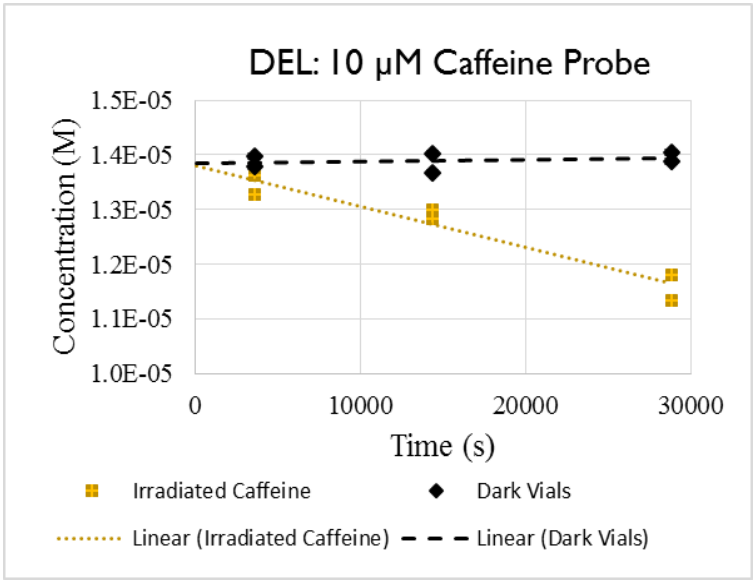
DEL: 10 µM Caffeine Probe
Concentration (M)
1.5E-05
1.4E-05
1.3E-05
1.2E-05
1.1E-05
1.0E-05
0
10000
20000
30000
Time (s)
Irradiated Caffeine
Dark Vials
Linear (Irradiated Caffeine)
Linear (Dark Vials)

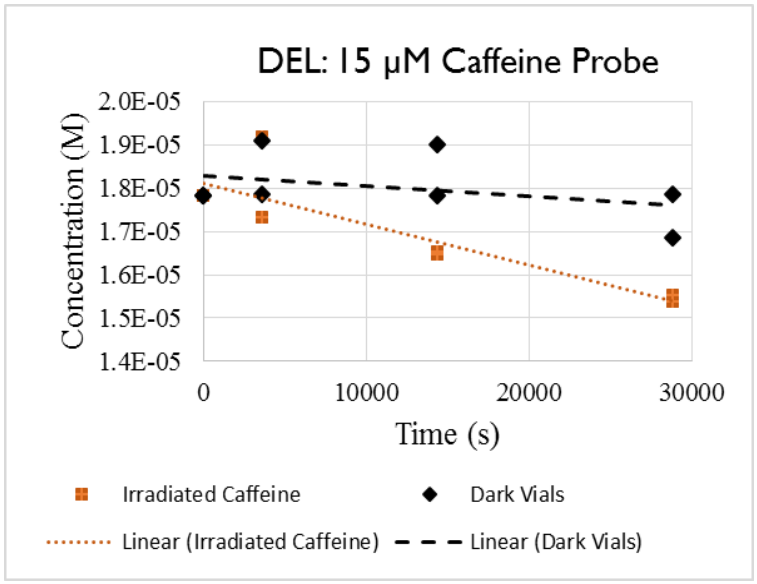
DEL: 15 µM Caffeine Probe
Concentration (M)
2.0E-05
1.9E-05
1.8E-05
1.7E-05
1.6E-05
1.5E-05
1.4E-05
0
10000
20000
30000
Time (s)
Irradiated Caffeine
Dark Vials
Linear (Irradiated Caffeine)
Linear (Dark Vials)

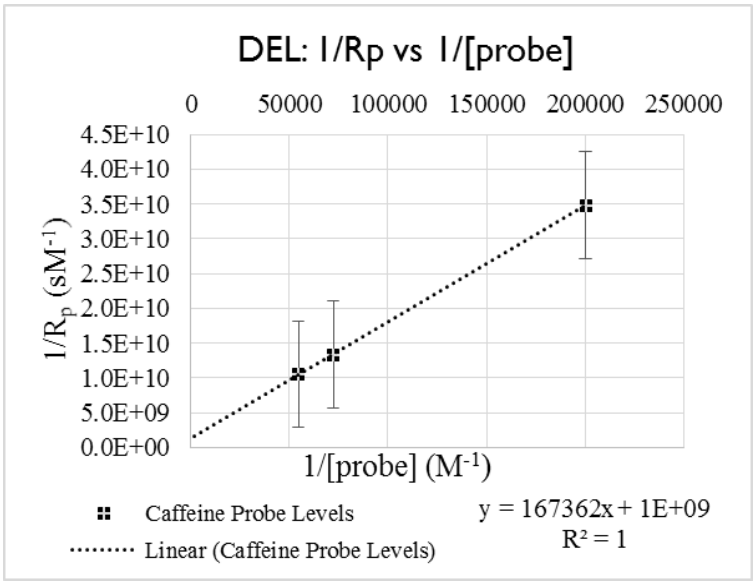
DEL: 1/Rp vs 1/[probe]
0
50000
100000
150000
200000
250000
4.5E+10
4.0E+10
3.5E+10
3.0E+10
2.5E+10
2.0E+10
1.5E+10
1.0E+10
5.0E+09
0.0E+00
1/Rp (sM-1)
1/[probe] (M-1)
Caffeine Probe Levels
Linear (Caffeine Probe Levels)
y = 167362x + 1E+09
R² = 1

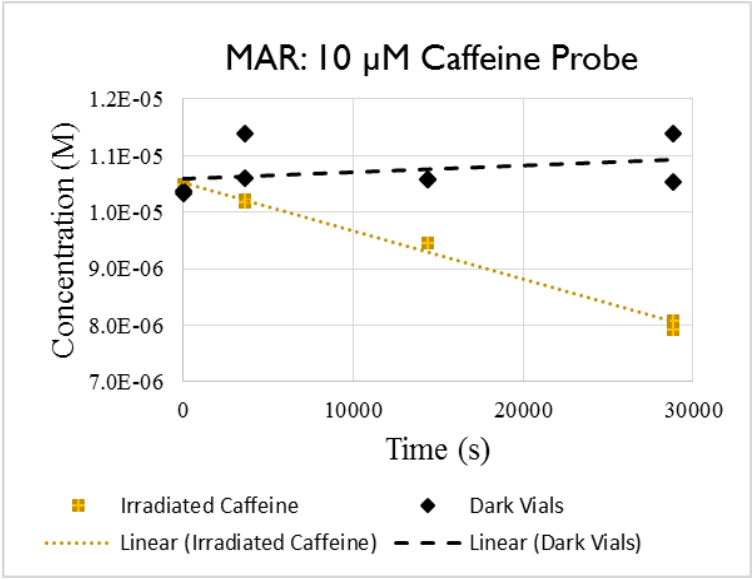
MAR: 10 µM Caffeine Probe
Concentration (M)
1.2E-05
1.1E-05
1.0E-05
9.0E-06
8.0E-06
7.0E-06
0
10000
20000
30000
Time (s)
Irradiated Caffeine
Dark Vials
Linear (Irradiated Caffeine)
Linear (Dark Vials)

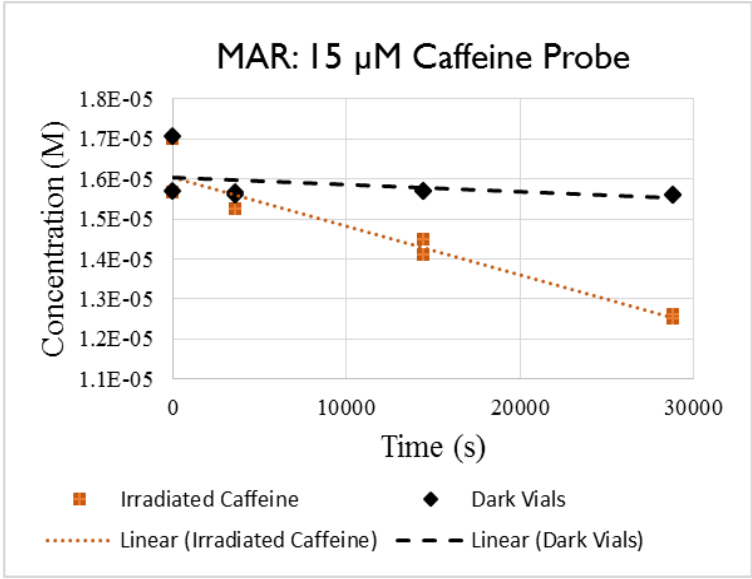
MAR: 15 µM Caffeine Probe
Concentration (M)
1.8E-05
1.7E-05
1.6E-05
1.5E-05
1.4E-05
1.3E-05
1.2E-05
1.1E-05
0
10000
20000
30000
Time (s)
Irradiated Caffeine
Dark Vials
Linear (Irradiated Caffeine)
Linear (Dark Vials)

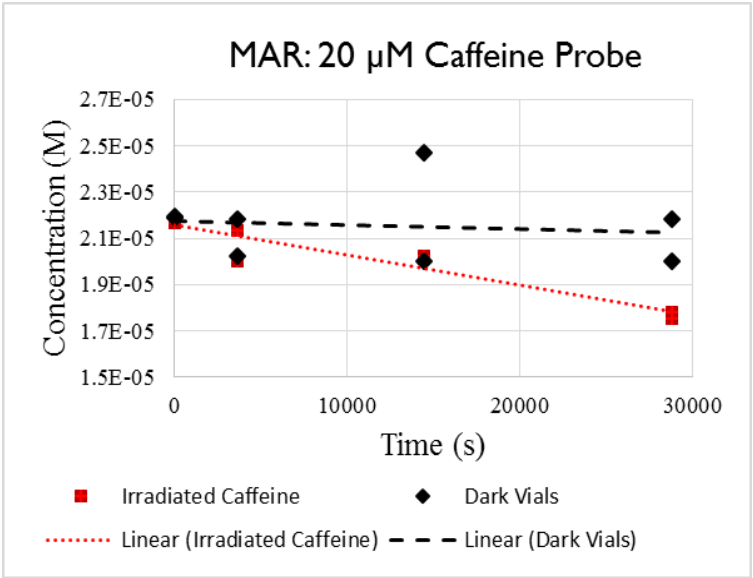
MAR: 20 µM Caffeine Probe
Concentration (M)
2.7E-05
2.5E-05
2.3E-05
2.1E-05
1.9E-05
1.7E-05
1.5E-05
0
10000
20000
30000
Time (s)
Irradiated Caffeine
Dark Vials
Linear (Irradiated Caffeine)
Linear (Dark Vials)

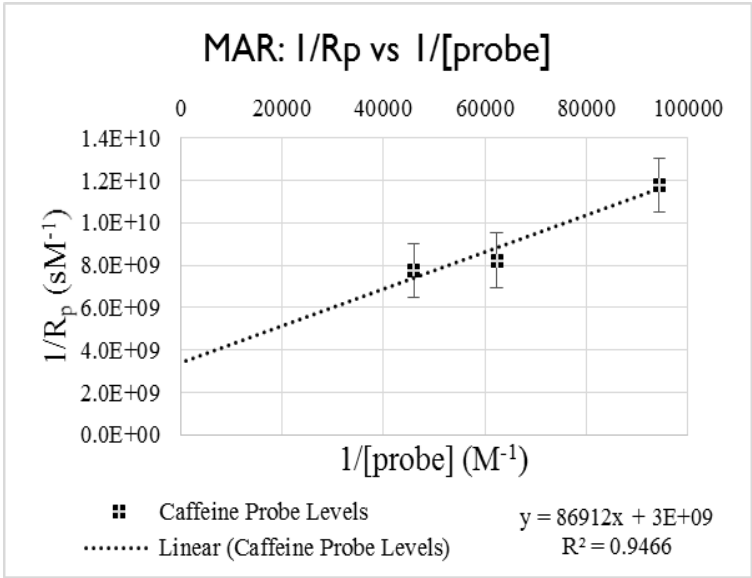
MAR: 1/Rp vs 1/[probe]
0
20000
40000
60000
80000
100000
1.4E+10
1.2E+10
1.0E+10
8.0E+09
6.0E+09
4.0E+09
2.0E+09
0.0E+00
1/Rp (sM-1)
1/[probe] (M-1)
Caffeine Probe Levels
Linear (Caffeine Probe Levels)
y = 86912x + 3E+09
R² = 0.9466

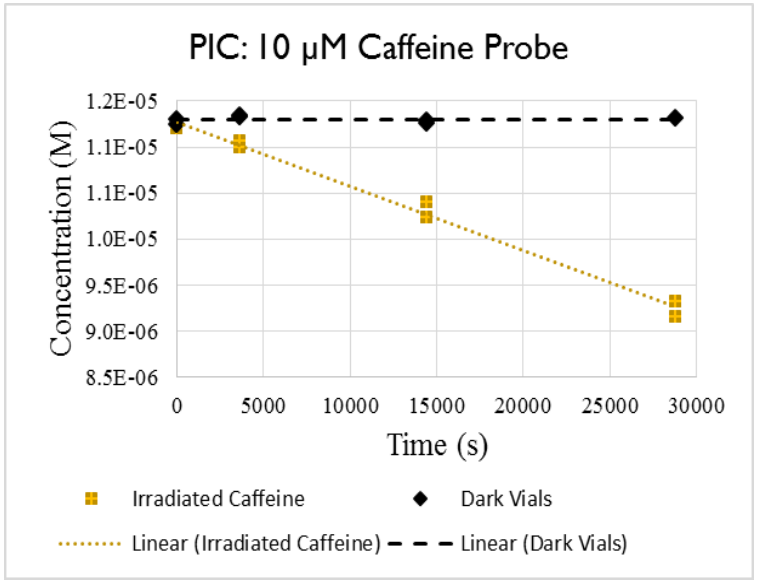
PIC: 10 µM Caffeine Probe
Concentration (M)
1.2E-05
1.1E-05
1.1E-05
1.0E-05
9.5E-06
9.0E-06
8.5E-06
0
5000
10000
15000
20000
25000
30000
Time (s)
Irradiated Caffeine
Dark Vials
Linear (Irradiated Caffeine)
Linear (Dark Vials)

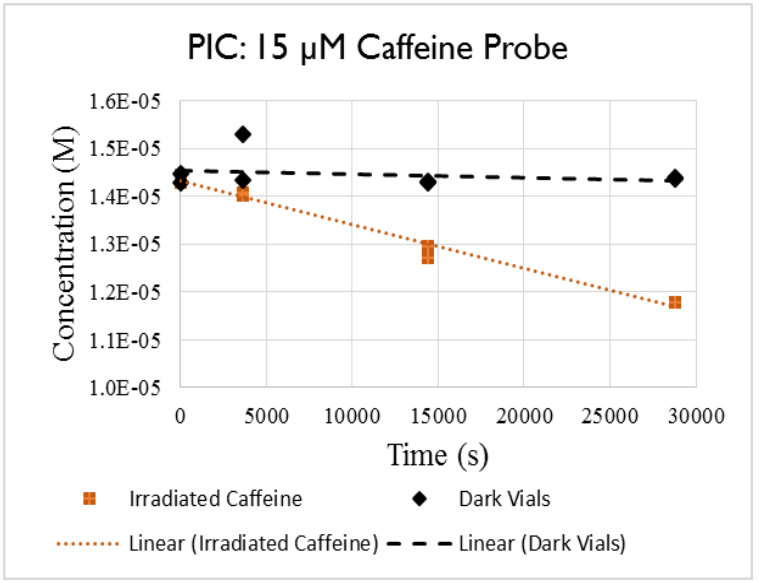
PIC: 15 µM Caffeine Probe
Concentration (M)
1.6E-05
1.5E-05
1.4E-05
1.3E-05
1.2E-05
1.1E-05
1.0E-05
0
5000
10000
15000
20000
25000
30000
Time (s)
Irradiated Caffeine
Dark Vials
Linear (Irradiated Caffeine)
Linear (Dark Vials)

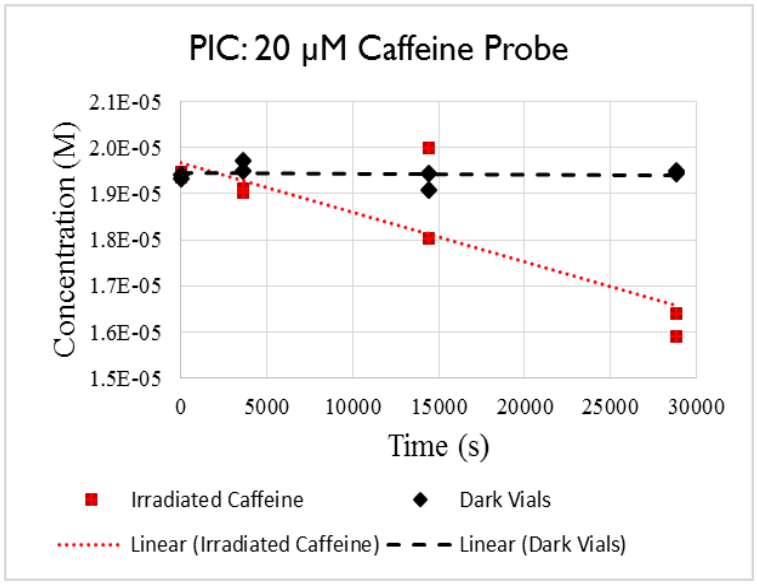
PIC: 20 µM Caffeine Probe
Concentration (M)
2.1E-05
2.0E-05
1.9E-05
1.8E-05
1.7E-05
1.6E-05
1.5E-05
0
5000
10000
15000
20000
25000
30000
Time (s)
Irradiated Caffeine
Dark Vials
Linear (Irradiated Caffeine)
Linear (Dark Vials)

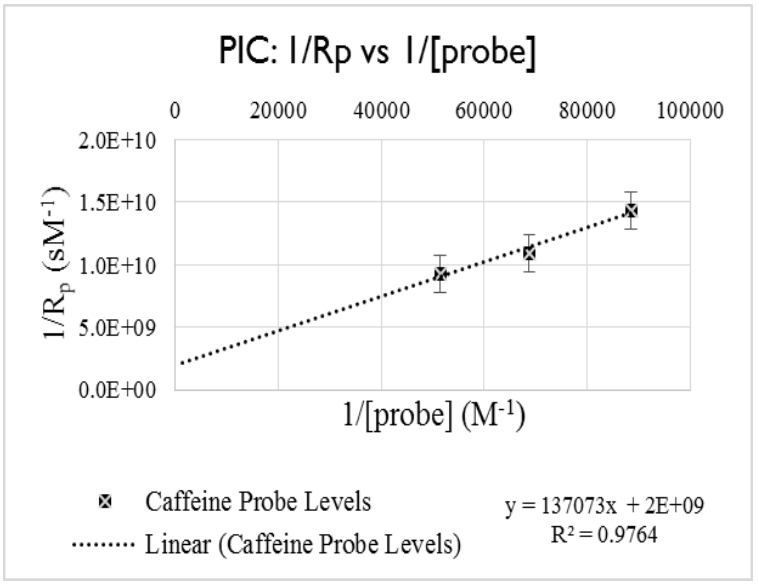
PIC: 1/Rp vs 1/[probe]
0
20000
40000
60000
80000
100000
2.0E+10
1.5E+10
1.0E+10
5.0E+09
0.0E+00
1/Rp (sM-1)
1/[probe] (M-1)
Caffeine Probe Levels
Linear (Caffeine Probe Levels)
y = 137073x + 2E+09
R² = 0.9764

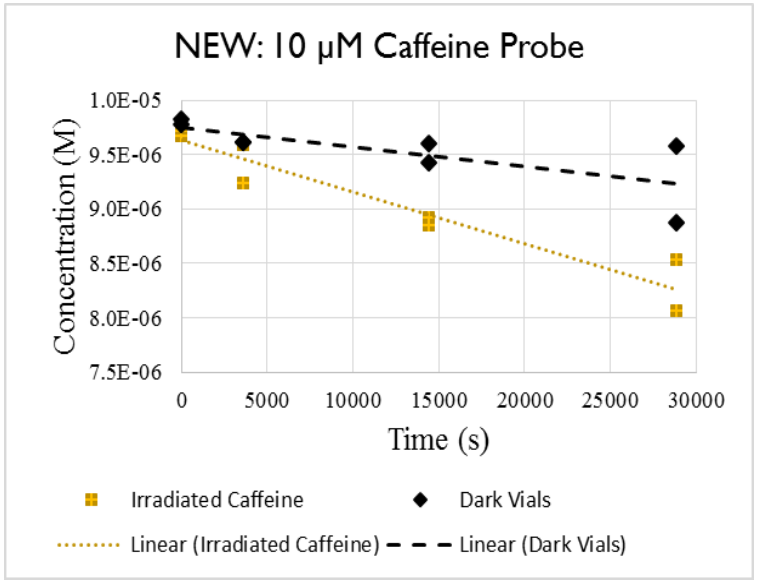
NEW: 10 µM Caffeine Probe
Concentration (M)
1.0E-05
9.5E-06
9.0E-06
8.5E-06
8.0E-06
7.5E-06
0
5000
10000
15000
20000
25000
30000
Time (s)
Irradiated Caffeine
Dark Vials
Linear (Irradiated Caffeine)
Linear (Dark Vials)

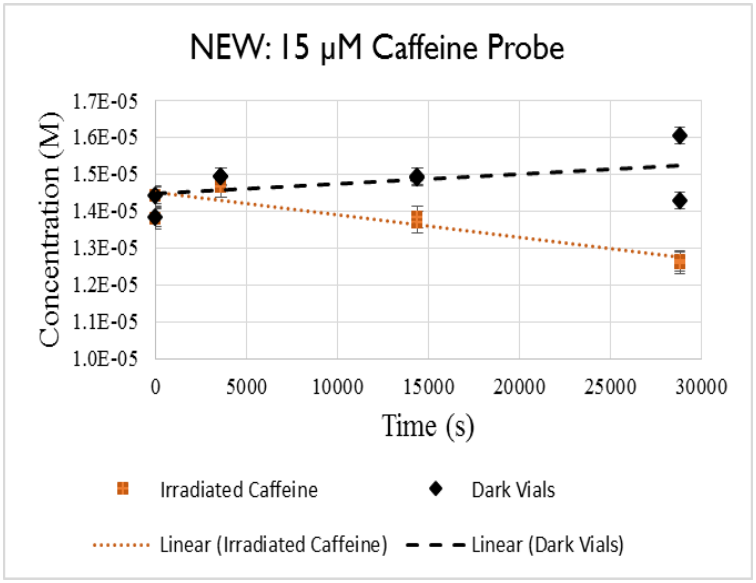
NEW: 15 µM Caffeine Probe
Concentration (M)
1.7E-05
1.6E-05
1.5E-05
1.4E-05
1.3E-05
1.2E-05
1.1E-05
1.0E-05
0
5000
10000
15000
20000
25000
30000
Time (s)
Irradiated Caffeine
Dark Vials
Linear (Irradiated Caffeine)
Linear (Dark Vials)

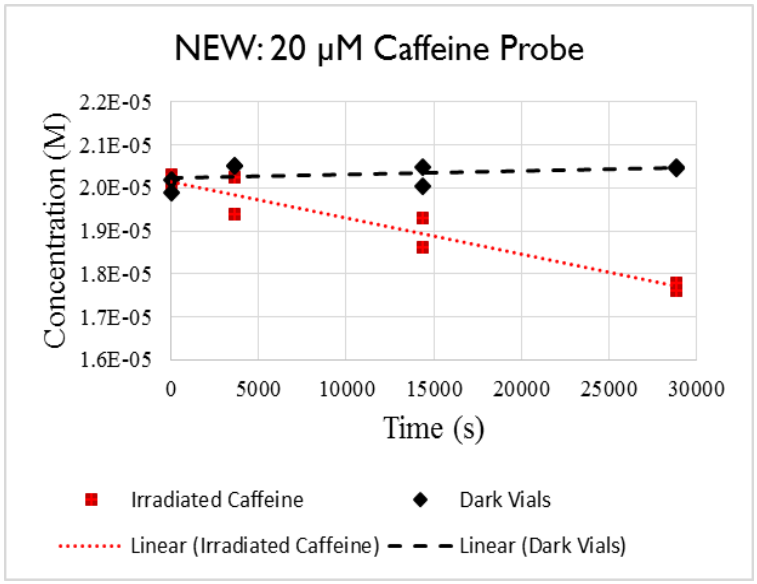
NEW: 20 µM Caffeine Probe
Concentration (M)
2.2E-05
2.1E-05
2.0E-05
1.9E-05
1.8E-05
1.7E-05
1.6E-05
0
5000
10000
15000
20000
25000
30000
Time (s)
Irradiated Caffeine
Dark Vials
Linear (Irradiated Caffeine)
Linear (Dark Vials)

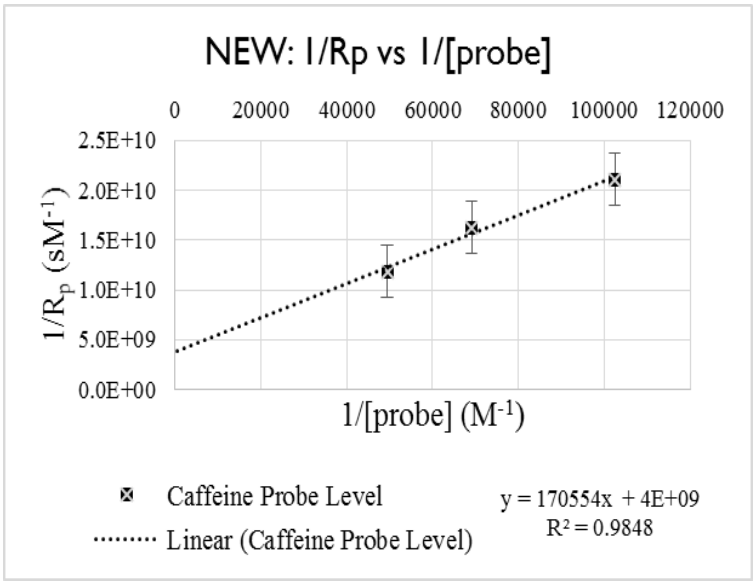
NEW: 1/Rp vs 1/[probe]
0
20000
40000
60000
80000
100000
120000
2.5E+10
2.0E+10
1.5E+10
1.0E+10
5.0E+09
0.0E+00
1/Rp (sM-1)
1/[probe] (M-1)
Caffeine Probe Level
Linear (Caffeine Probe Level)
y = 170554x + 4E+09
R² = 0.9848

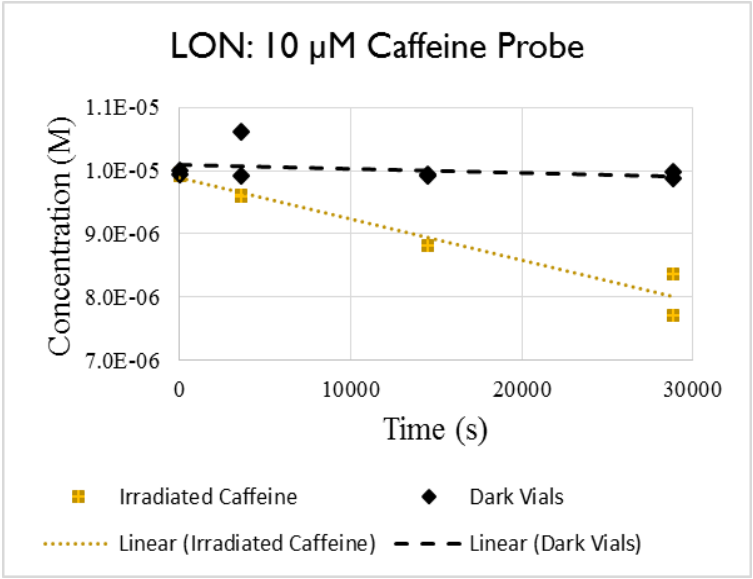
LON: 10 µM Caffeine Probe
Concentration (M)
1.1E-05
1.0E-05
9.0E-06
8.0E-06
7.0E-06
0
10000
20000
30000
Time (s)
Irradiated Caffeine
Dark Vials
Linear (Irradiated Caffeine)
Linear (Dark Vials)

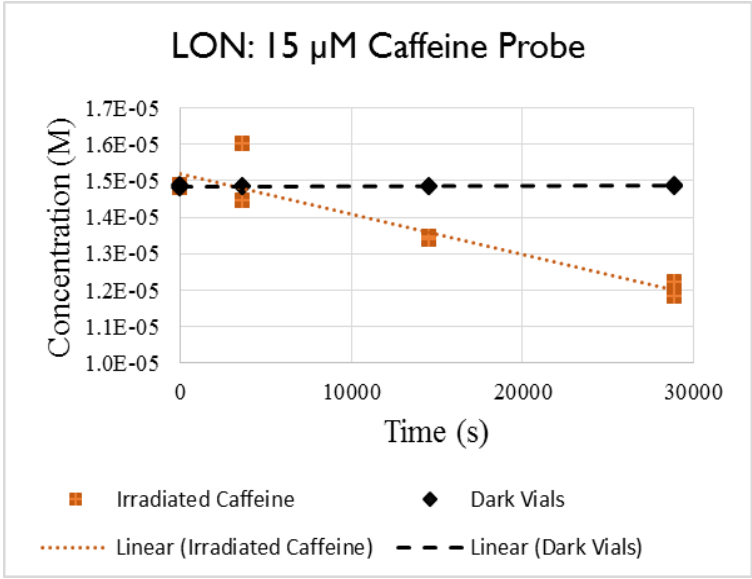
LON: 15 µM Caffeine Probe
Concentration (M)
1.7E-05
1.6E-05
1.5E-05
1.4E-05
1.3E-05
1.2E-05
1.1E-05
1.0E-05
0
10000
20000
30000
Time (s)
Irradiated Caffeine
Dark Vials
Linear (Irradiated Caffeine)
Linear (Dark Vials)

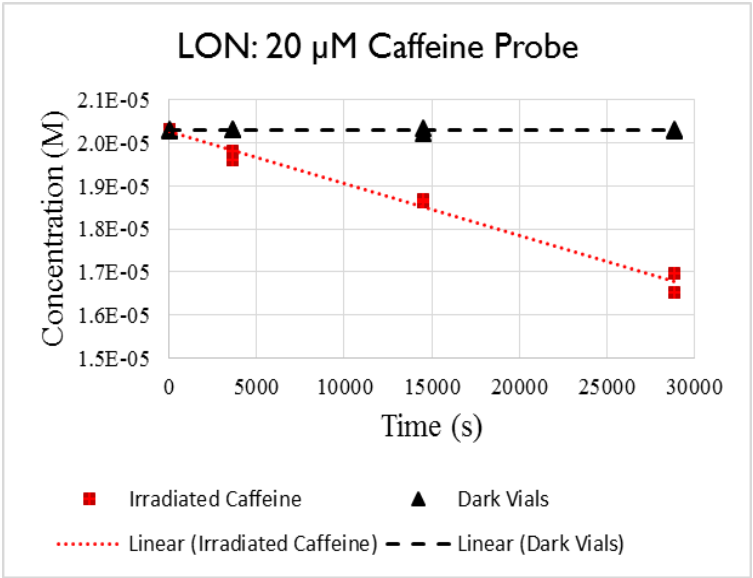
LON: 20 µM Caffeine Probe
Concentration (M)
2.1E-05
2.0E-05
1.9E-05
1.8E-05
1.7E-05
1.6E-05
1.5E-05
0
5000
10000
15000
20000
25000
30000
Time (s)
Irradiated Caffeine
Dark Vials
Linear (Irradiated Caffeine)
Linear (Dark Vials)

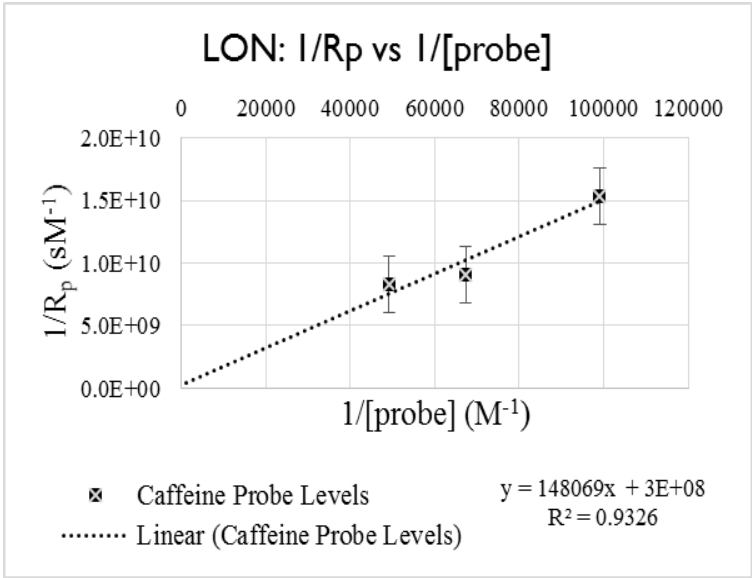
LON: 1/Rp vs 1/[probe]
0
20000
40000
60000
80000
100000
120000
2.0E+10
1.5E+10
1.0E+10
5.0E+09
0.0E+00
1/Rp (sM-1)
1/[probe] (M-1)
Caffeine Probe Levels
Linear (Caffeine Probe Levels)
y = 148069x + 3E+08
R² = 0.9326

GLASSWARE DECONTAMINATION

Glassware were cleaned and sterilized through the following methods:

Plastics

Caps, stoppers, o-rings, and other plastics were rinsed with tap water and stored in a 5% HCl solution overnight. Plastics were rinsed with three rinses of reverse osmosis water (RO) followed by three rinses of Milli-Q water and let air dry before storage. Plastics were stored in sealed bags or glass containers.

Small Glassware

Glassware small enough to fit inside of a muffle furnace were scrubbed with tap water and Alconox. Glassware were rinsed with three rinses of RO and three rinses of Milli-Q water before preliminary drying at high heat before transfer to a muffle furnace for at least four hours at 400°C. Glassware such as bottles, flasks, and beakers were sealed with laboratory grade aluminum foil before storage.

Large Glassware

Glassware too large to fit inside of a muffle furnace were rinsed with tap water and filled with Nochromix solution for a minimum of one hour. Nochromix solution was removed from glassware, and glassware were then rinsed with tap water to dilute any lingering Nochromix solution. Glassware were then rinsed with three rinses of RO and three rinses of Milli-Q water and either let air dry or were dried at a high heat setting before storage. Glassware such as bottles, flasks, and beakers were sealed with laboratory grade aluminum foil before storage.

Transfer Pipettes

Transfer pipettes were rinsed with Milli-Q water and dried in a muffle furnace for at least four hours at 400°C before use. Transfer pipettes were not reused in laboratory experiments.

APPENDIX C

RAW DATA

ALKALINITY TITRATION DATA

Raw data for alkalinity titrations for Delaware (analysis date on 10/17/16), Marysville (10/24/16), Pickerington (10/31/16), Newark (11/7/16), and London (11/14/16) wastewater treatment facility effluent samples is shown (Rounds & Wilde, 2002). Bolded values indicate data used for the Excel-based F1 Gran Function analysis.

DEL		MAR		PIC		NEW		LON	
pH	**Titrant (mL)**	**pH**	**Titrant (mL)**	**pH**	**Titrant (mL)**	**pH**	**Titrant (mL)**	**pH**	**Titrant (mL)**
7.92	0.00	7.30	0.00	7.86	0.00	7.52	0.00	7.89	0.00
7.74	0.30	7.22	0.29	7.83	0.17	7.45	0.27	7.81	0.17
7.60	0.50	7.18	0.42	7.78	0.43	7.38	0.54	7.73	0.32
7.54	0.61	7.14	0.60	7.75	0.60	7.32	0.80	7.65	0.50
7.48	0.72	7.10	0.69	7.71	0.85	7.27	1.09	7.59	0.69
7.43	0.81	7.07	0.93	7.66	1.11	7.22	1.33	7.53	0.81
7.35	1.04	7.02	1.20	7.61	1.40	7.15	1.70	7.47	0.99
7.29	1.20	6.97	1.44	7.57	1.68	7.08	2.22	7.42	1.12
7.26	1.31	6.93	1.73	7.53	1.93	7.04	2.50	7.37	1.29
7.22	1.40	6.88	2.00	7.48	2.28	7.01	2.77	7.33	1.45
7.19	1.51	6.84	2.26	7.44	2.53	6.98	3.02	7.30	1.60
7.15	1.69	6.80	2.52	7.41	2.79	6.95	3.31	7.27	1.76
7.11	1.84	6.76	2.80	7.38	3.10	6.92	3.59	7.23	1.92
7.08	2.00	6.74	3.06	7.35	3.37	6.90	3.84	7.17	2.20
7.06	2.12	6.72	3.21	7.32	3.61	6.84	4.35	7.13	2.43
7.00	2.40	6.70	3.40	7.29	3.90	6.81	4.64	7.08	2.70
6.96	2.60	6.69	3.53	7.27	4.18	6.76	5.01	7.04	2.99
6.91	2.85	6.69	3.70	7.24	4.42	6.75	5.28	7.00	3.28
6.87	3.11	6.66	3.95	7.23	4.59	6.72	5.56	6.96	3.55
6.86	3.21	6.63	4.20	7.19	5.02	6.69	5.99	6.93	3.81
6.82	3.47	6.60	4.46	7.17	5.35	6.66	6.44	6.89	4.09
6.77	3.78	6.57	4.72	7.15	5.61	6.63	6.70	6.86	4.34
6.74	3.98	6.54	5.00	7.12	5.95	6.61	6.99	6.83	4.62
6.71	4.23	6.51	5.26	7.10	6.29	6.59	7.30	6.79	4.90
6.69	4.40	6.48	5.51	7.07	6.60	6.57	7.62	6.78	5.01
6.66	4.61	6.46	5.80	7.05	6.90	6.54	7.98	6.75	5.28
6.64	4.82	6.43	6.08	7.03	7.21	6.52	8.30	6.73	5.52
6.62	4.99	6.41	6.31	7.02	7.50	6.49	8.60	6.70	5.80
6.59	5.22	6.38	6.60	7.01	7.65	6.47	8.93	6.68	6.03
6.56	5.50	6.36	6.81	6.97	8.30	6.45	9.27	6.65	6.31
6.53	5.77	6.33	7.10	6.96	8.52	6.42	9.74	6.63	6.58
6.50	6.02	6.30	7.37	6.94	8.84	6.40	10.04	6.61	6.86
6.48	6.24	6.28	7.62	6.92	9.19	6.36	10.60	6.58	7.11
6.45	6.49	6.25	7.90	6.91	9.46	6.34	10.98	6.56	7.40
6.41	6.80	6.24	8.10	6.90	9.72	6.31	11.27	6.54	7.64
6.38	7.06	6.20	8.42	6.87	10.26	6.29	11.65	6.52	7.91
6.35	7.32	6.16	8.85	6.85	10.60	6.27	12.02	6.48	8.19
6.31	7.65	6.14	9.11	6.83	10.95	6.24	12.38	6.47	8.48
6.29	7.91	6.12	9.40	6.80	11.60	6.22	12.69	6.45	8.71
6.26	8.19	6.11	9.62	6.77	12.13	6.20	13.00	6.43	9.02
6.22	8.50	6.12	9.71	6.76	12.52	6.18	13.27	6.41	9.35
6.20	8.73	6.09	9.96	6.74	13.02	6.16	13.68	6.38	9.67
6.18	8.99	6.07	10.18	6.71	13.53	6.14	14.00	6.36	9.99
6.15	9.23	6.05	10.44	6.70	14.00	6.12	14.30	6.35	10.22
6.12	9.50	6.02	10.70	6.68	14.51	6.07	14.81	6.33	10.43

6.09	9.78	5.97	11.05	6.65	15.19	6.03	15.33	6.32	10.74
6.07	9.87	5.96	11.35	6.63	15.71	5.99	15.82	6.28	11.29
6.07	9.98	5.93	11.62	6.62	16.00	5.96	16.30	6.24	11.81
6.05	10.11	5.89	11.92	6.61	16.31	5.91	16.83	6.20	12.38
6.03	10.26	5.86	12.13	6.59	16.80	5.87	17.45	6.16	12.92
6.01	10.42	5.82	12.39	6.58	17.11	5.81	17.90	6.11	13.43
6.00	10.58	5.79	12.61	6.56	17.65	5.79	18.21	6.06	14.00
5.96	10.58	5.74	12.90	6.54	18.28	5.73	18.70	6.02	14.50
5.93	11.10	5.70	13.14	6.52	18.80	5.67	19.24	5.96	15.03
5.90	11.38	5.65	13.42	6.48	20.20	5.59	19.90	5.92	15.48
5.86	11.62	5.59	13.69	6.46	20.83	5.50	20.52	5.89	15.73
5.82	11.90	5.53	13.99	6.45	21.55	5.41	21.00	5.87	16.00
5.78	12.18	5.46	14.25	6.44	22.10	5.35	21.30	5.85	16.26
5.75	12.31	5.42	14.40	6.42	22.52	5.30	21.60	5.81	16.52
5.73	12.50	5.37	14.57	6.42	23.04	5.22	21.90	5.78	16.80
5.70	12.64	5.32	14.71	6.40	23.56	5.19	22.07	5.74	17.10
5.67	12.80	5.26	14.90	6.37	24.56	5.14	22.21	5.69	17.43
5.64	12.98	5.16	15.13	6.39	25.55	5.05	22.51	5.64	17.72
5.62	13.05	5.08	15.31	6.28	28.56	4.99	22.68	5.59	18.01
5.59	13.21	4.99	15.48	6.15	31.70	4.90	22.88	5.56	18.24
5.56	13.39	4.90	15.60	5.99	35.61	4.83	23.02	5.54	18.48
5.53	13.51	4.78	15.75	5.89	37.81	4.71	23.25	5.48	18.73
5.47	13.78	4.69	15.89	5.74	40.70	4.58	23.44	5.44	18.90
5.43	13.90	4.60	15.99	5.45	44.90	4.44	23.68	5.39	19.06
5.37	14.11	4.51	16.10	5.28	46.97	**4.28**	**23.88**	5.35	19.20
5.32	14.29	4.40	16.18	4.91	49.24	**4.18**	**24.00**	5.30	19.38
5.26	14.43	4.31	16.30	4.77	49.80	**4.08**	**24.19**	5.21	19.53
5.20	14.60	4.23	16.41	4.68	50.09	**4.00**	**24.32**	5.18	19.66
5.12	14.78	**4.15**	**16.52**	4.56	50.43	**3.92**	**24.50**	5.15	19.79
5.03	14.91	**4.09**	**16.62**	4.45	50.69	**3.85**	**24.68**	5.08	19.91
4.90	15.11	**4.00**	**16.79**	4.20	51.19	**3.79**	**24.83**	5.03	20.02
4.77	15.29	**3.95**	**16.90**	**4.08**	**51.48**	**3.75**	**25.04**	4.97	20.11
4.67	15.39	**3.90**	**17.00**	**3.96**	**51.80**	3.67	25.53	4.89	20.24
4.57	15.50	**3.86**	**17.10**	**3.86**	**52.12**	3.63	26.22	4.81	20.33
4.45	15.60	**3.82**	**17.21**	**3.75**	**52.49**	3.58	27.10	4.72	20.46
4.35	15.71	**3.79**	**17.32**	**3.68**	**52.82**	3.55	28.16	4.61	20.57
4.25	15.81	**3.75**	**17.43**	**3.63**	**53.10**	3.49	29.55	4.56	20.68
4.16	**15.92**	**3.72**	**17.53**	**3.52**	**53.74**	3.44	31.24	4.38	20.78
4.05	**16.08**	**3.67**	**17.73**	**3.46**	**54.24**			4.32	20.83
3.98	**16.18**	**3.64**	**17.84**	**3.40**	**54.77**			**4.28**	**20.90**
3.90	**16.33**	**3.61**	**18.00**	**3.38**	**54.99**			**4.22**	**20.93**
3.82	**16.50**	**3.58**	**18.16**					**4.19**	**21.00**
3.77	**16.66**	**3.55**	**18.32**					**4.15**	**21.01**
3.71	**16.80**	**3.52**	**18.50**					**4.11**	**21.10**
3.66	**16.97**	**3.48**	**18.72**					**4.07**	**21.14**
3.62	**17.12**	**3.43**	**19.04**					**4.04**	**21.20**
3.57	**17.32**	**3.40**	**19.30**					**3.97**	**21.31**
3.53	**17.49**	**3.36**	**19.68**					**3.91**	**21.41**
3.49	17.60							**3.89**	**21.49**
3.46	17.79							**3.83**	**21.58**
3.42	18.14							**3.79**	**21.65**
3.34	18.67							**3.75**	**21.79**
								3.70	**21.92**
								3.67	**22.03**
								3.64	**22.12**
								3.61	**22.24**
								3.57	**22.40**
								3.53	**22.58**
								3.50	**22.72**
								3.47	**22.90**
								3.43	**23.10**

UV-Vis Optical Spectra

Full absorbance data were included graphically due to the volume of data generated. Each graph represents six measurements – two aliquots of filtered effluent sample, two aliquots of filtered effluent sample working solution (filtered effluent + HCl to reach pH 7) that were exposed to eight hours irradiation in the Suntest CPS+, and two Milli-Q water blanks for one blank per sample type. The two graphs below illustrate the non-irradiated samples and irradiated samples for relative comparison.

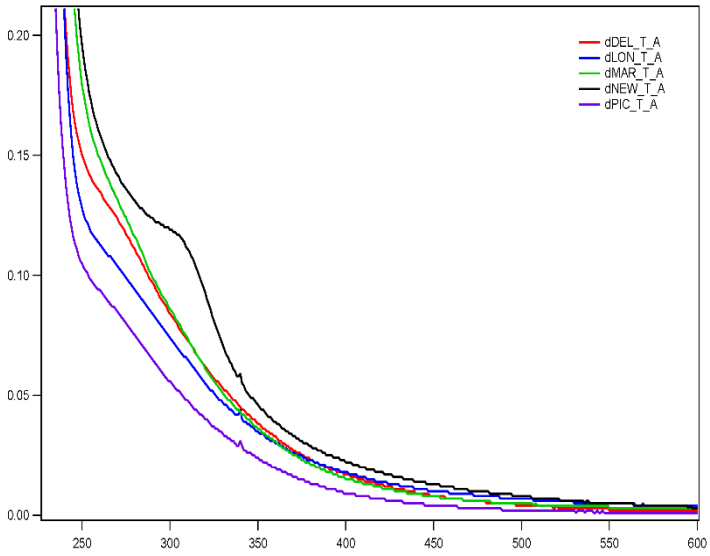

Non-irradiated effluent samples

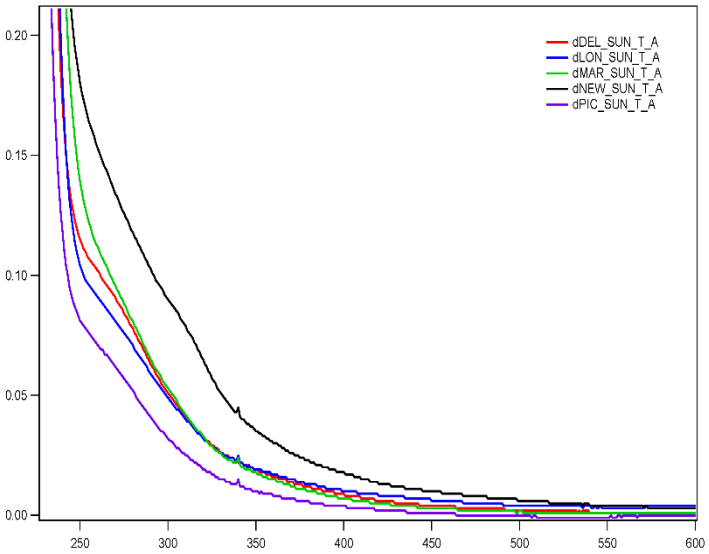

Irradiated effluent samples

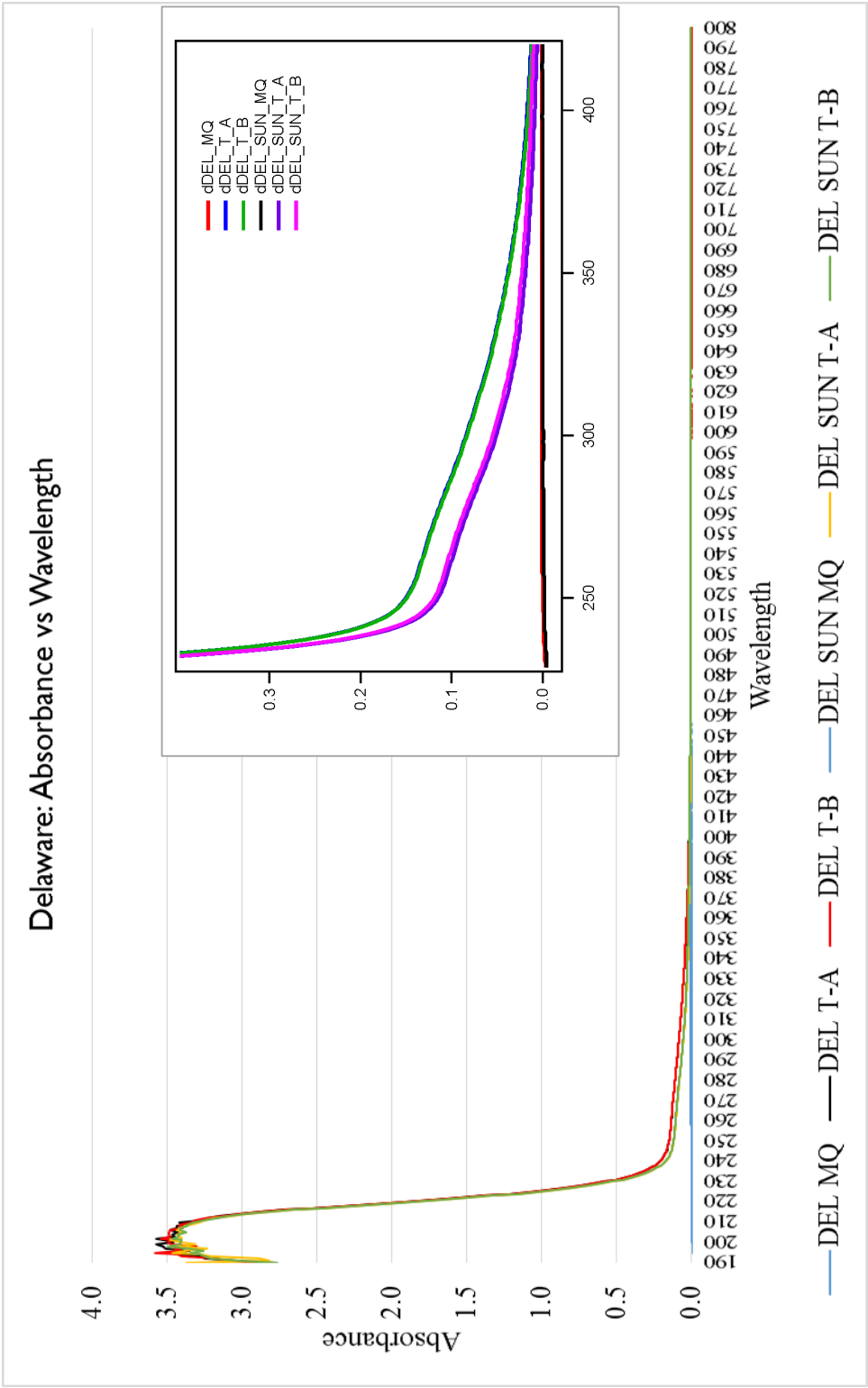

UV-Vis for Delaware (DEL) filtered effluent, 8-hour irradiated working solution filtered effluent samples (SUN), and Milli-Q water (MQ) blanks. T-A and T-B indicate replicates of each type of effluent sample. Insert graph shows zoomed in range from 250 to 400 nm.

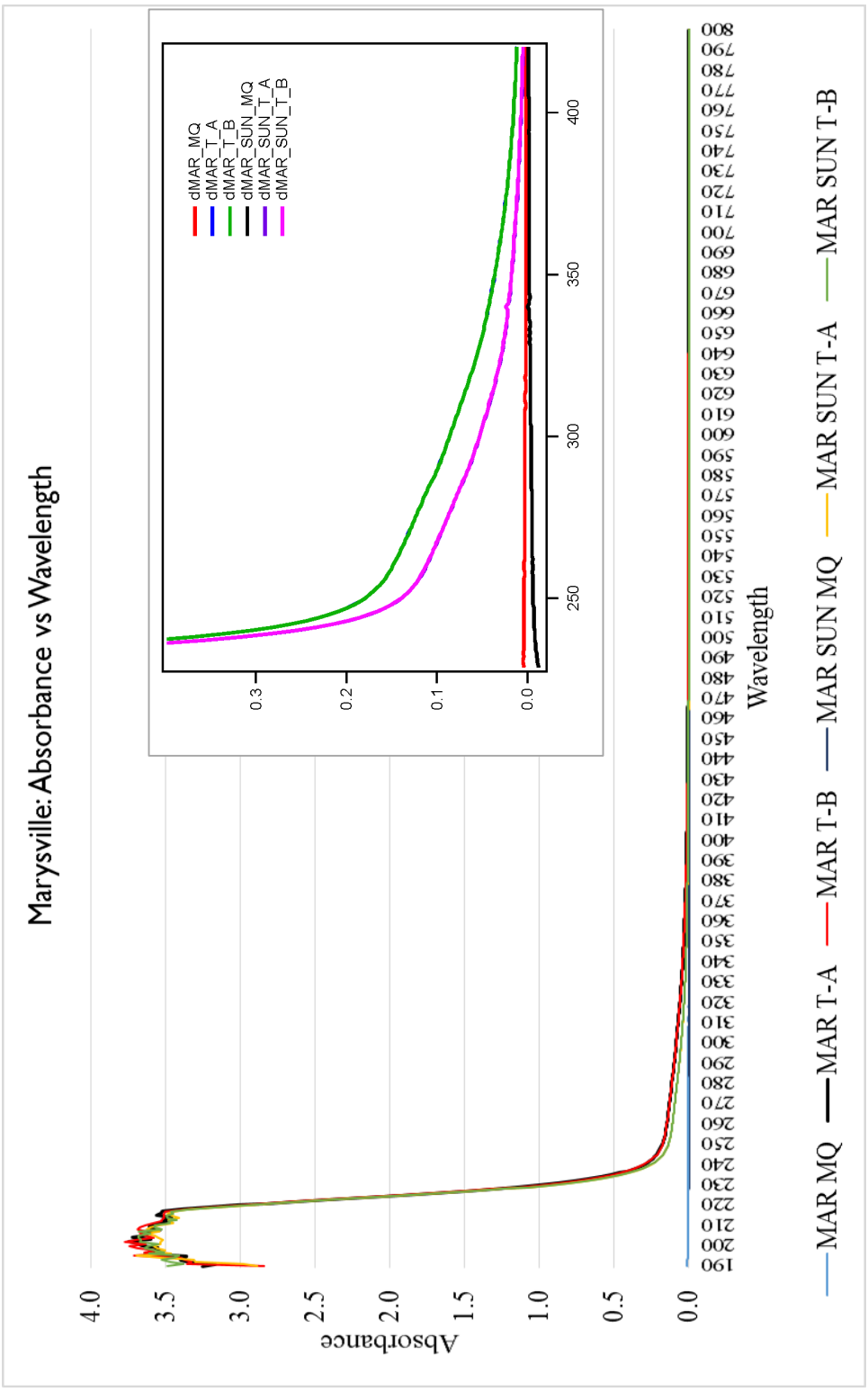

UV-Vis for Marysville (MAR) filtered effluent, 8-hour irradiated working solution filtered effluent samples (SUN), and Milli-Q water (MQ) blanks. T-A and T-B indicate replicates of each type of effluent sample. Insert graph shows zoomed in range from 250 to 400 nm.

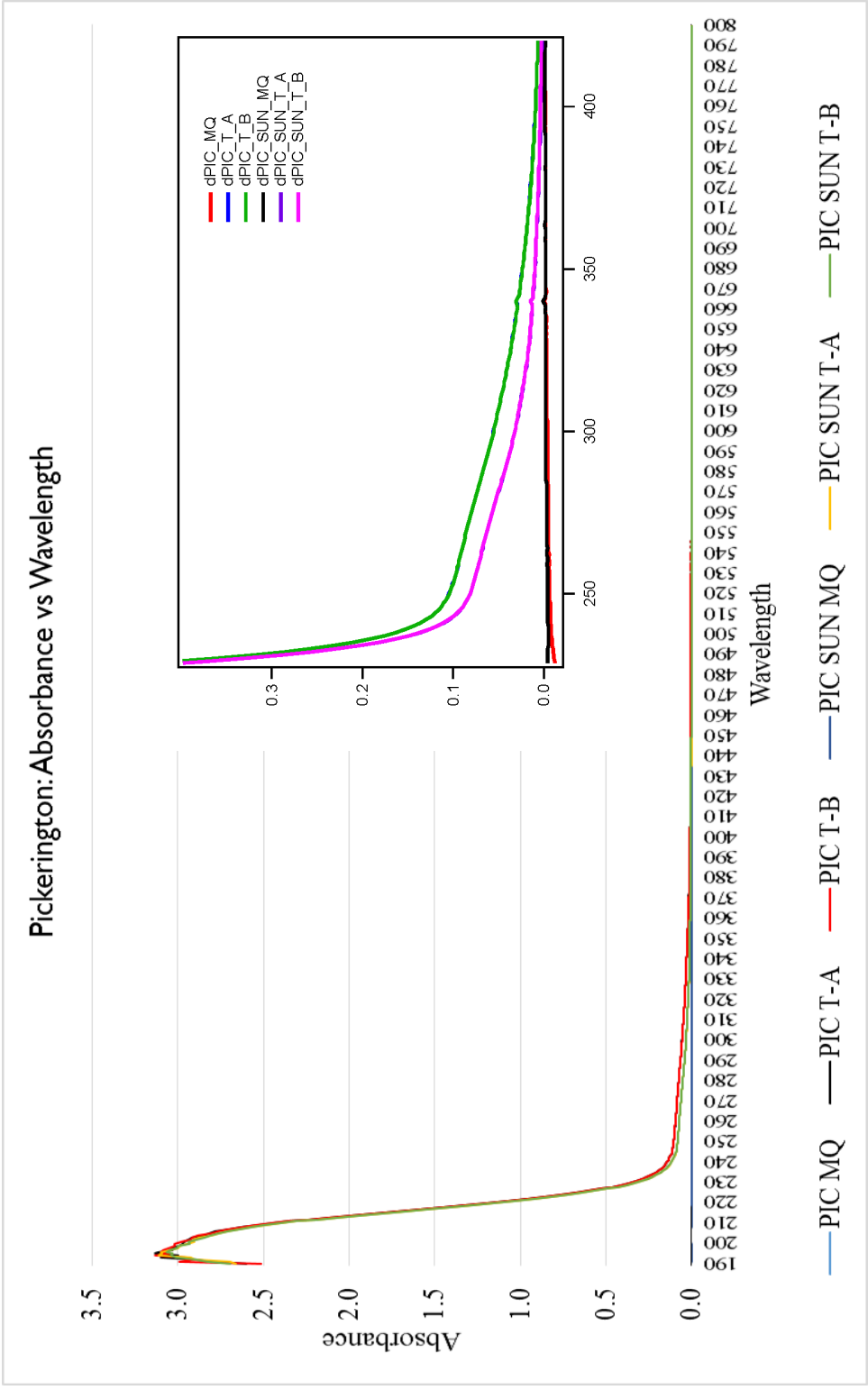

UV-Vis of Pickerington (PIC) filtered effluent, 8-hour irradiated working solution filtered effluent samples (SUN), and Milli-Q water (MQ) blanks. T-A and T-B indicate replicates of each type of effluent sample. Insert graph shows zoomed in range from 250 to 400 nm.

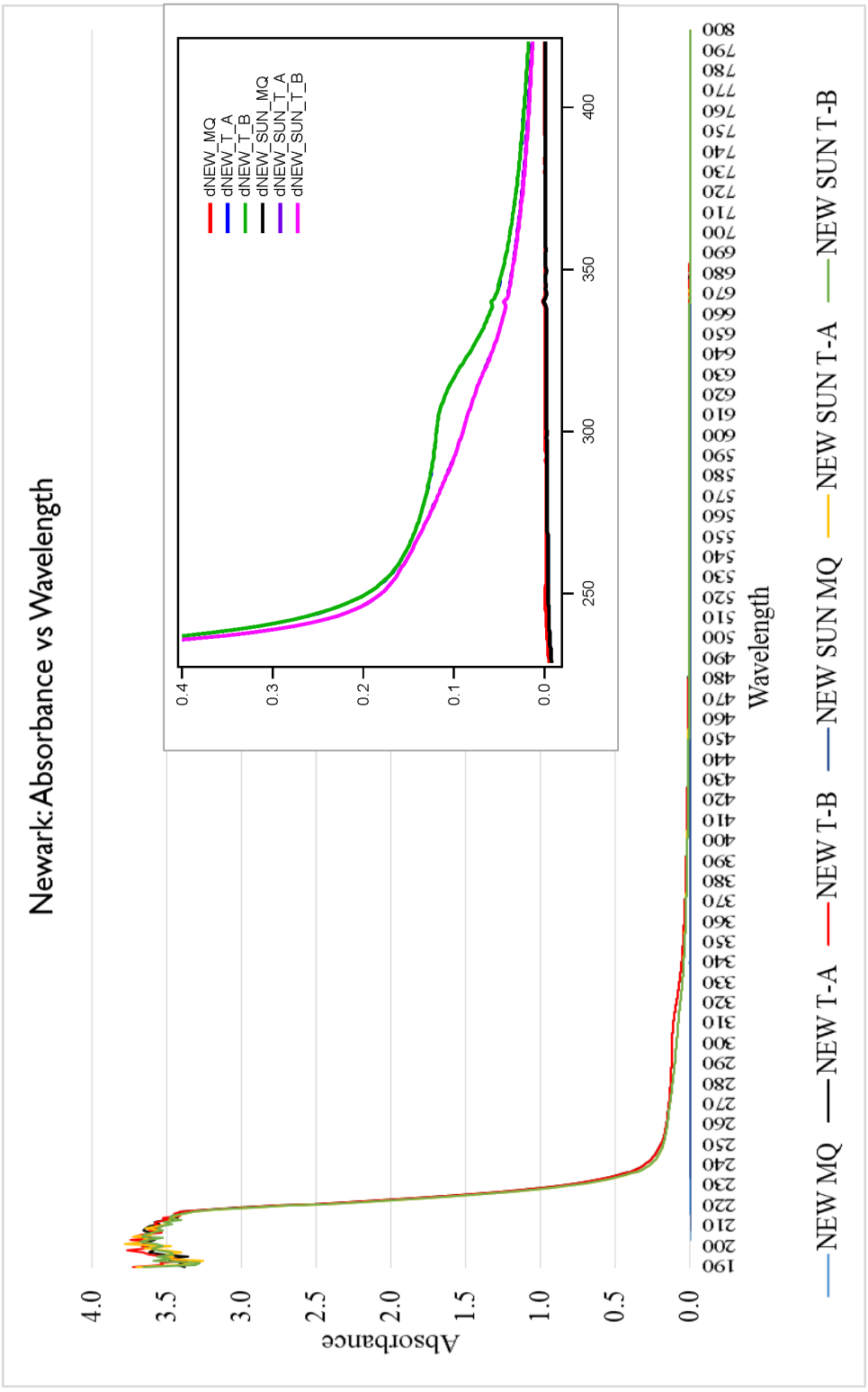

UV-Vis for Newark (NEW) filtered effluent, 8-hour irradiated working solution filtered effluent samples (SUN), and Milli-Q water (MQ) blanks. T-A and T-B indicate replicates of each type of effluent sample. Insert graph shows zoomed in range from 250 to 400 nm.

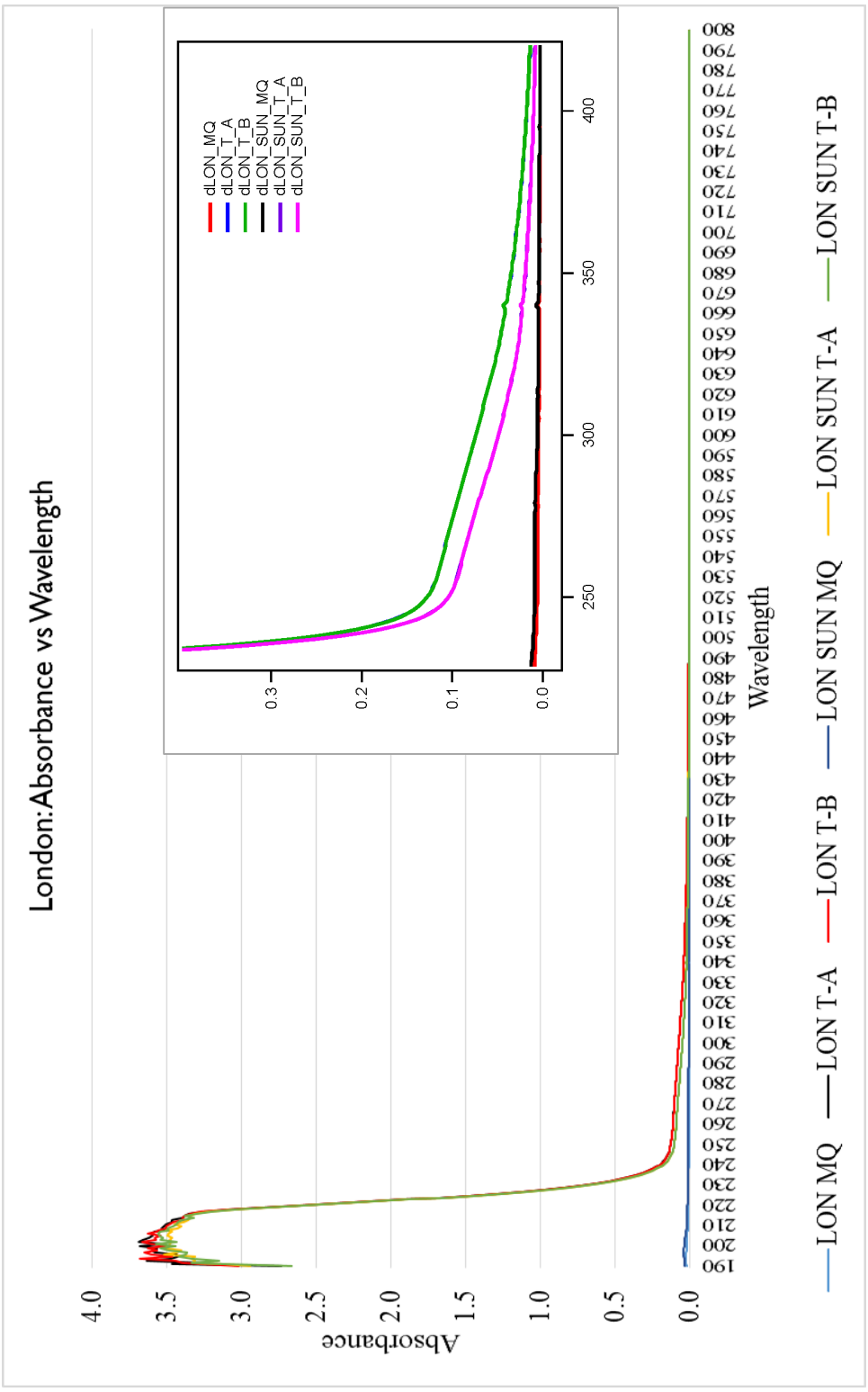

UV-Vis for London (LON) filtered effluent, 8-hour irradiated working solution filtered effluent samples (SUN), and Milli-Q water (MQ) blanks. T-A and T-B indicate replicates of each type of effluent sample. Insert graph shows zoomed in range from 250 to 400 nm.

NITRATE AND NITRITE ANALYSIS

The detection of nitrate and nitrite is based on the cadmium reduction method to reduce nitrate to nitrite; diazonium compounds form from chemical reactions between nitrite, sulfanilamide, and N-(1-naphthyl)ethylenediamine dihydrochloride, which produces a reddish-purple color that can be measured at 540 nm (———, Analysis: Nitrate+Nitrite, 2008). The detection of nitrite follows a similar chemical reaction path, but does not proceed through a cadmium reduction column (———, Analysis: Nitrite, 2008).

Raw data obtained from Skalar San^{++} System for nitrite and nitrate+nitrite analysis of effluent samples stored at 4°C and samples that were kept frozen at 0°C since collection have been included for reference. For nitrite analysis, standard solutions of 0, 100, 200, and 500 ppb nitrogen (N) as nitrite were used. For nitrate-nitrite analysis, standard solutions of 0, 500, 1000, and 2000 ppb N measured as nitrate-nitrite converted to nitrite were used. For nitrite analysis, reported NO_2^- concentrations were determined by Skalar San^{++} System internal software. For nitrate-nitrite analysis, the Skalar internal software calibration curve was not used. Instead the LINEST function in Excel was used to re-calculate nitrate+nitrite concentrations from standard solution data using y=846.21x, intercept = 0, error in slope of 5.8, and error in s(y) of 13419.

Notes:

The Delaware frozen effluent sample storage container was damaged during frozen storage and evaporated. As such, no f-DEL measurements were taken for either nitrite or nitrate-nitrite analysis. Effluent samples from all five locations exhibited varying degrees of a transparent yellow tint, likely due to treatment processes, such as use of ferric chloride. It was assumed that this yellow tint would not affect the absorbance readings taken by the Skalar San++ System instrumentation, which scans at a wavelength of 540 nm.

Legend:

UD = undiluted effluent sample aliquot

d10x = effluent aliquot diluted by a factor of 10; reported results were readjusted by a factor of 10 to reflect undiluted nitrite-nitrate concentration

f- = denotes a frozen effluent sample aliquot

T1 & T2 = tests on two separate aliquots of the same sample

A & B = replicates of the same aliquot

Series# = indicates each of the four measurements for each effluent sample

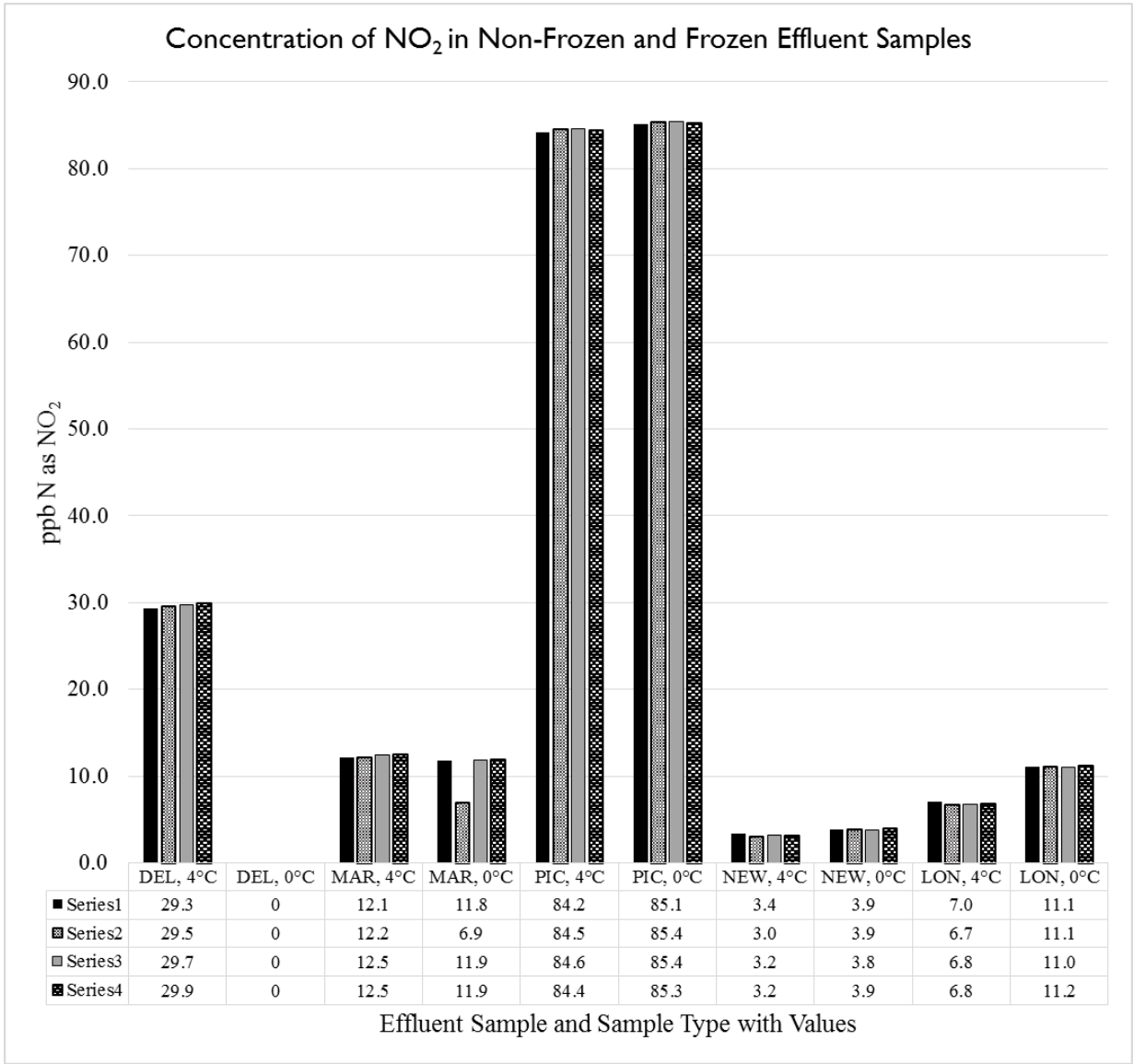

	DEL, 4°C	DEL, 0°C	MAR, 4°C	MAR, 0°C	PIC, 4°C	PIC, 0°C	NEW, 4°C	NEW, 0°C	LON, 4°C	LON, 0°C
Series1	29.3	0	12.1	11.8	84.2	85.1	3.4	3.9	7.0	11.1
Series2	29.5	0	12.2	6.9	84.5	85.4	3.0	3.9	6.7	11.1
Series3	29.7	0	12.5	11.9	84.6	85.4	3.2	3.8	6.8	11.0
Series4	29.9	0	12.5	11.9	84.4	85.3	3.2	3.9	6.8	11.2

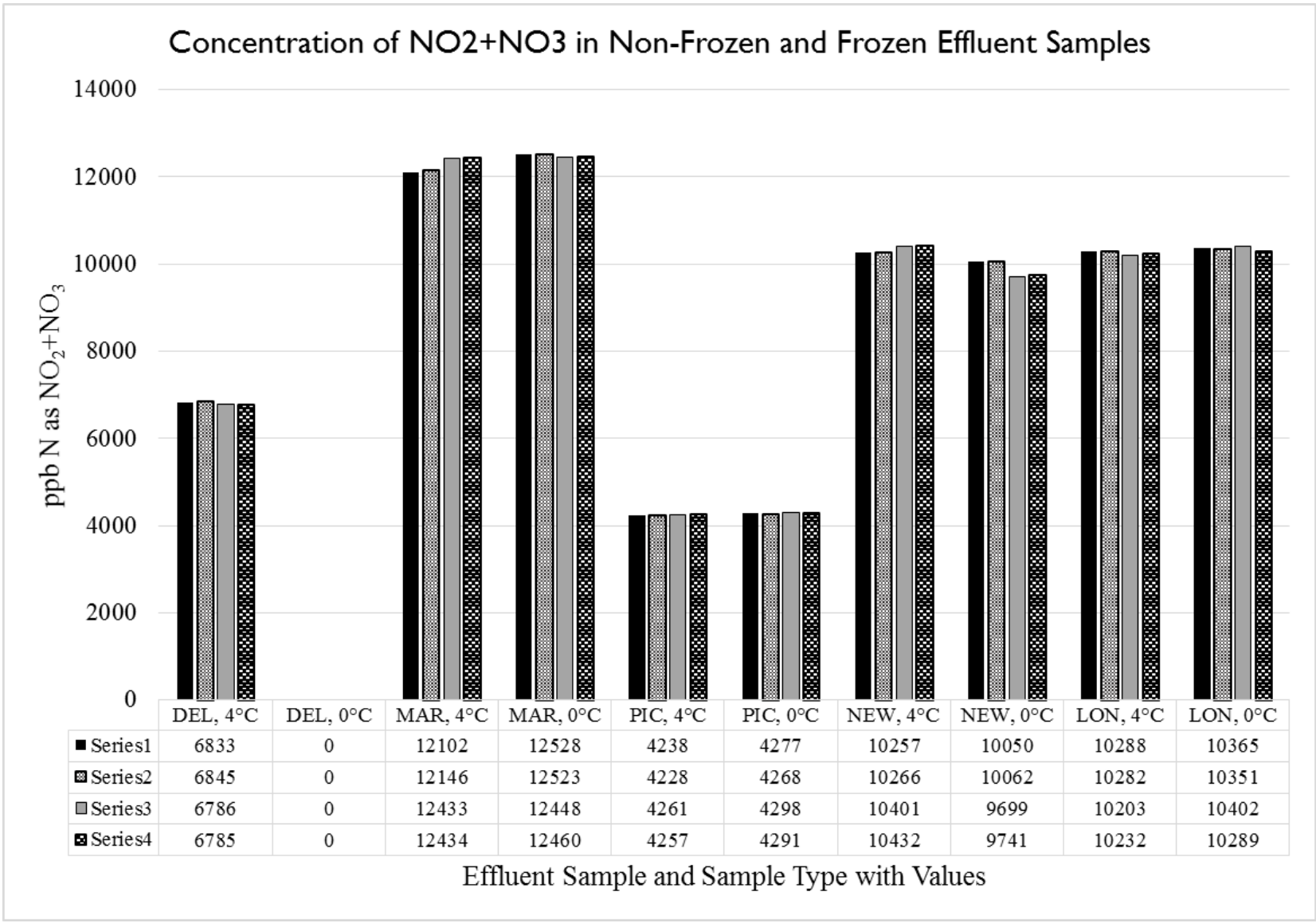

	DEL, 4°C	DEL, 0°C	MAR, 4°C	MAR, 0°C	PIC, 4°C	PIC, 0°C	NEW, 4°C	NEW, 0°C	LON, 4°C	LON, 0°C
Series1	6833	0	12102	12528	4238	4277	10257	10050	10288	10365
Series2	6845	0	12146	12523	4228	4268	10266	10062	10282	10351
Series3	6786	0	12433	12448	4261	4298	10401	9699	10203	10402
Series4	6785	0	12434	12460	4257	4291	10432	9741	10232	10289

Skalar Data for Nitrite Analysis			
Sample Identity	**NO2 ppb**	**Corr. Ht NO2**	**Description**
0 ppb N as NO2	0.48449109	1744	Calibration Curve Standards for N as NO2 in ppb
100 ppb N NO2	105.860113	381103	
200 ppb N NO2	214.429568	771961	
500 ppb N NO2	493.05615	1775035	
0 ppb N as NO2	0.6790153	2444	
100 ppb N NO2	109.065219	392642	
200 ppb N NO2	218.87084	787950	
500 ppb N NO2	497.293364	1790289	
DEL UD T1 - A	29.305078	105500	Undiluted
rep DEL UD T1 - B	29.5437628	106360	Stored as Liquid at 4°C for NO2 analysis
MAR UD T1 - A	12.1210121	43636	Trial Run 1 + duplicates
rep MAR UD T1 - B	12.188665	43880	
PIC UD T1 - A	84.2009184	303129	
rep PIC UD T1 - B	84.4928922	304180	
NEW UD T1 - A	3.41169649	12282	
rep NEW UD T1 - B	3.00397259	10814	
LON UD T1 - A	7.02780275	25301	
rep LON UD T1 - B	6.71728382	24183	
DEL UD T2 - A	29.7479257	107094	Undiluted
rep DEL UD T2 - B	29.8873676	107596	Stored as Liquid at 4°C for NO2 analysis
MAR UD T2 - A	12.4682432	44886	Trial Run 2 + duplicates
rep MAR UD T2 - B	12.4817151	44935	
PIC UD T2 - A	84.6112234	304606	
rep PIC UD T2 - B	84.4277545	303946	
NEW UD T2 - A	3.20230228	11528	
rep NEW UD T2 - B	3.15077545	11343	
LON UD T2 - A	6.80265281	24490	
rep LON UD T2 - B	6.79756013	24472	
f-MAR UD T1 - A	11.8228384	42563	Undiluted
rep f-MAR UD T1 - B	6.91667849	24900	Stored as Frozen Sample, frozen on day of collection,
f-PIC UD T1 - A	85.0731593	306269	at 0°C for NO2 analysis
rep f-PIC UD T1 - B	85.3516265	307272	Trial Run 1 + duplicates
f-NEW UD T1 - A	3.85534584	13880	
rep f-NEW UD T1 - B	3.86923447	13930	
f-LON UD T1 - A	11.1118792	40004	
rep f-LON UD T1 - B	11.1257212	40053	
f-MAR UD T2 - A	11.895337	42824	Undiluted
rep f-MAR UD T2 - B	11.9418639	42992	Stored as Frozen Sample, frozen on day of collection,
f-PIC UD T2 - A	85.3996811	307444	at 0°C for NO2 analysis
rep f-PIC UD T2 - B	85.2869054	307038	Trial Run 2 + duplicates
f-NEW UD T2 - A	3.83715173	13814	
rep f-NEW UD T2 - B	3.93020558	14149	
f-LON UD T2 - A	10.9978535	39593	
rep f-LON UD T2 - B	11.2438679	40479	
NO2 ppb calculated by Skalar San++ System			
Corrected height calculated by Skalar San++ System			

Skalar Data for Nitrate+Nitrite Analysis				
Sample Identity	**N+N ppb**	**Corr.Ht N+N**	**Manually Corrected N+N ppb**	**Description**
0 ppb N as NO3	-20.6120599	820	0.96902767	Calibration Curve Standards for N as nitrite for
500 ppb N NO3	505.1178577	439390	519.245206	analysis of NO3+NO2 in ppb
1000 ppb N NO3	1033.547333	880212	1040.18267	
2000 ppb N NO3	1981.946869	1671376	1975.13365	
0 ppb N as NO3	-20.6345362	802	0.94775633	
500 ppb N NO3	511.0366265	444328	525.080644	
1000 ppb N NO3	1038.254478	884138	1044.82218	
2000 ppb N NO3	1984.665906	1673645	1977.81502	
DEL d10x T1 - A	671.5470429	578227	683.31459	Diluted by a factor of 10
rep DEL d10x T1 - B	672.7110175	579198	684.462061	Stored as Liquid at 4°C for NO3+NO2 analysis
MAR d10x T1 - A	1205.991186	1024066	1210.18084	Trial Run 1 + duplicates
rep MAR d10x T1 - B	1210.510428	1027836	1214.63601	
PIC d10x T1 - A	408.331753	358650	423.831433	
rep PIC d10x T1 - B	407.3128257	357800	422.826953	
NEW d10x T1 - A	1018.895758	867989	1025.73824	
rep NEW d10x T1 - B	1019.733676	868688	1026.56428	
LON d10x T1 - A	1021.964527	870549	1028.7635	
rep LON d10x T1 - B	1021.362761	870047	1028.17027	
DEL d10x T2 - A	666.7731439	574245	678.608897	Diluted by a factor of 10
rep DEL d10x T2 - B	666.6396344	574133	678.476542	Stored as Liquid at 4°C for NO3+NO2 analysis
MAR d10x T2 - A	1239.541165	1052054	1243.25541	Trial Run 2 + duplicates
rep MAR d10x T2 - B	1239.701347	1052187	1243.41259	
PIC d10x T2 - A	410.6068453	360548	426.074377	
rep PIC d10x T2 - B	410.2575256	360256	425.729309	
NEW d10x T2 - A	1033.491667	880165	1040.12712	
rep NEW d10x T2 - B	1036.570775	882734	1043.16302	
LON d10x T2 - A	1013.386658	863393	1020.30696	
rep LON d10x T2 - B	1016.297868	865822	1023.17741	
f-MAR d10x T1 - A	1249.252142	1060155	1252.8287	Diluted by a factor of 10
rep f-MAR d10x T1 - B	1248.727844	1059717	1252.3111	Stored as Frozen Sample, frozen on day of
f-PIC d10x T1 - A	412.2936944	361955	427.737087	collection, at 0°C for NO3+NO2 analysis
rep f-PIC d10x T1 - B	411.324777	361147	426.78224	Trial Run 2 + duplicates
f-NEW d10x T1 - A	997.9028593	850476	1005.04241	
rep f-NEW d10x T1 - B	999.0496769	851433	1006.17334	
f-LON d10x T1 - A	1029.835291	877115	1036.52281	
rep f-LON d10x T1 - B	1028.35455	875880	1035.06336	
f-MAR d10x T2 - A	1241.158263	1053403	1244.84958	Diluted by a factor of 10
rep f-MAR d10x T2 - B	1242.318192	1054370	1245.99233	Stored as Frozen Sample, frozen on day of
f-PIC d10x T2 - A	414.3735048	363690	429.787408	collection, at 0°C for NO3+NO2 analysis
rep f-PIC d10x T2 - B	413.63954	363078	429.064182	Trial Run 2 + duplicates
f-NEW d10x T2 - A	962.2523917	820736	969.897434	
rep f-NEW d10x T2 - B	966.5051394	824284	974.090251	
f-LON d10x T2 - A	1021.894851	870491	1028.69496	
rep f-LON d10x T2 - B	1022.061176	870630	1028.85922	
NO3+NO2 (N+N) ppb calculated by Skalar San++ System				
Corrected height calculated by Skalar San++ System				
Manually corrected N+N ppb calculated by LINEST Excel-based function with intercept = 0				

PHOTOLYSIS: HPLC DATA

Raw HPLC data, initial calibration curve concentrations and averaged peak areas, elapsed time, and Suntest CPS+ monitoring data were recorded for use in the initial rates method. A vial containing non-irradiated working solution and a vial of eight hour irradiated working solution were run through the HPLC as controls to verify a lack of peaks with no caffeine present. No peaks were recorded for these vials in any of the experiments, indicating that caffeine was the only chemical registering a peak area in the retention time as measured.

Legend:

RT = Retention Time

PA = Peak Area

Peak areas in bold and italics were discarded for analysis during this study as they were the result of instrumental error or were not otherwise reproducible. The colors highlighting these peak areas help identify peak areas grouped together based on caffeine level. Colored peak areas that are not bolded and italicized were not discarded.

Vial Name Guide:

D = Delaware (DEL) effluent sample

MV = Marysville (MAR) effluent sample

P = Pickerington (PIC) effluent sample

N = Newark (NEW) effluent sample

L = London (LON) effluent sample

G = Caffeine level 5 μM

Y = Caffeine level 10 μM

O = Caffeine level 15 μM

R = Caffeine level 20 μM

D = Dark controls of caffeine and working solution wrapped in foil during irradiation

A/B = Aliquots from phototubes of the same caffeine level

WS = Working Solution: composed of effluent sample and adjusted to pH = 7

CC = Calibration Curve solution at concentrations of 5, 10, 15, and 20 μM

T# = Phototube or vial removed from irradiation at time point 1, 2, or 3, corresponding to elapsed times of 1, 4, and 8 hours respectively

Delaware (DEL) Effluent HPLC Raw Data									
Vial Name	**Vial #**	**Inj. #**	**RT (min)**	**PA (uV*sec)**		**Vial Name**	**Vial #**	**Inj. #**	**RT (min)**	**PA (uV*sec)**
D WS	1	1	-	-		D GB-T2	25	1	3.900	133599
		2	-	-				2	3.900	133469
D CC5	2	1	3.891	153278		D YA-T2	26	1	3.893	358047
		2	3.895	153745				2	3.898	387166
D CC10	3	1	3.895	292245		D YB-T2	27	1	3.893	367433
		2	3.893	289456				2	3.901	367505
D CC15	4	1	3.899	436589		D OA-T2	28	1	3.900	472314
		2	3.903	437173				2	3.901	472427
D CC20	5	1	3.903	569742		D OB-T2	29	1	3.902	473797
		2	3.901	581850				2	3.907	473455
D GA-T0	6	1	3.906	142172		D GAD-T2	30	1	3.916	146937
		2	3.904	146403				2	3.916	147036
D GB-T0	7	1	3.900	146823		D GBD-T2	31	1	3.914	147458
		2	3.899	146174				2	3.916	147151
D YA-T0	8	1	3.898	***150801***		D YAD-T2	32	1	3.913	383162
		2	3.889	***130890***				2	3.914	400444
D YB-T0	9	1	3.896	***146942***		D YBD-T2	33	1	3.916	401231
		2	3.896	***339748***				2	3.916	401892
D OA-T0	10	1	3.878	511094		D OAD-T2	34	1	3.922	***603559***
		2	3.879	510761				2	3.916	544315
D OB-T0	11	1	3.882	511013		D OBD-T2	35	1	3.920	511362
		2	3.883	510949				2	3.916	510902
D GA-T1	12	1	3.887	135877		D GA-T3	36	1	3.919	118900
		2	3.886	136887				2	3.923	120511
D GB-T1	13	1	3.892	142788		D GB-T3	37	1	3.925	120951
		2	3.893	143024				2	3.924	121068
D YA-T1	14	1	3.891	390277		D YA-T3	38	1	3.920	338359
		2	3.889	390186				2	3.920	338662
D YB-T1	15	1	3.887	375779		D YB-T3	39	1	3.918	324645
		2	3.883	384404				2	3.916	325452
D OA-T1	16	1	3.894	567552		D OA-T3	40	1	3.915	440412
		2	3.896	531500				2	3.917	440239
D OB-T1	17	1	3.887	494931		D OB-T3	41	1	3.915	443956
		2	3.890	498748				2	3.915	445880
D GAD-T1	18	1	3.898	146175		D GAD-T3	42	1	3.918	147727
		2	3.898	146436				2	3.921	147861
D GBD-T1	19	1	3.894	146786		D GBD-T3	43	1	3.907	***95775***
		2	3.898	146748				2	3.916	143108
D YAD-T1	20	1	3.901	391082		D YAD-T3	44	1	3.921	403166
		2	3.889	398823				2	3.915	392170
D YBD-T1	21	1	3.891	400909		D YBD-T3	45	1	3.923	404524
		2	3.893	400333				2	3.920	400716
D OAD-T1	22	1	3.891	512385		D OAD-T3	46	1	3.916	460347
		2	3.891	511398				2	3.918	505611
D OBD-T1	23	1	3.898	543513		D OBD-T3	47	1	3.921	511419
		2	3.899	551089				2	3.923	511761
D GA-T2	24	1	3.896	132721		D WS+8hr	48	1	-	-
		2	3.897	134761				2	-	-

Marysville (MAR) Effluent HPLC Raw Data									
Vial Name	**Vial #**	**Inj. #**	**RT (min)**	**PA (uV*sec)**		**Vial Name**	**Vial #**	**Inj. #**	**RT (min)**	**PA (uV*sec)**
MV WS	1	1	-	-		MV YB-T2	25	1	3.873	251262
		2	-	-				2	3.872	251049
MV CC5	2	1	3.877	144181		MV OA-T2	26	1	3.873	386869
		2	3.881	143955				2	3.827	384346
MV CC10	3	1	3.896	***87345***		MV OB-T2	27	1	3.878	376138
		2	3.880	260477				2	3.875	374740
MV CC15	4	1	3.879	401383		MV RA-T2	28	1	3.877	537870
		2	3.883	399680				2	3.877	537386
MV CC20	5	1	3.888	492830		MV RB-T2	29	1	3.875	534604
		2	3.878	505091				2	3.879	536696
MV YA-T0	6	1	3.882	278861		MV YAD-T2	30	1	3.879	281243
		2	3.885	278917				2	3.890	281223
MV YB-T0	7	1	3.886	275842		MV YBD-T2	31	1	3.891	281614
		2	3.885	279661				2	3.884	280981
MV OA-T0	8	1	3.883	415572		MV OAD-T2	32	1	3.883	417875
		2	3.894	417674				2	3.884	417830
MV OB-T0	9	1	3.908	460079		MV OBD-T2	33	1	3.887	417831
		2	3.897	443792				2	3.884	417201
MV RA-T0	10	1	3.890	578677		MV RAD-T2	34	1	3.883	582486
		2	3.887	576994				2	3.883	482860
MV RB-T0	11	1	3.883	577194		MV RBD-T2	35	1	3.901	710210
		2	3.880	576207				2	3.887	602558
MV YA-T1	12	1	3.873	271861		MV YA-T3	36	1	3.887	209523
		2	3.872	271586				2	3.885	212345
MV YB-T1	13	1	3.871	270691		MV YB-T3	37	1	3.886	215042
		2	3.866	270762				2	3.883	214958
MV OA-T1	14	1	3.866	406100		MV OA-T3	38	1	3.883	333385
		2	3.876	405837				2	3.886	333048
MV OB-T1	15	1	3.881	404306		MV OB-T3	39	1	3.882	335048
		2	3.881	407602				2	3.884	336015
MV RA-T1	16	1	3.886	572624		MV RA-T3	40	1	3.861	466326
		2	3.883	492484				2	3.881	466112
MV RB-T1	17	1	3.878	566785		MV RB-T3	41	1	3.881	473702
		2	3.878	566952				2	3.880	473754
MV YAD-T1	18	1	3.880	281277		MV YAD-T3	42	1	3.882	280461
		2	3.879	282911				2	3.882	279895
MV YBD-T1	19	1	3.895	308938		MV YBD-T3	43	1	3.882	***142256***
		2	3.882	296535				2	3.890	303003
MV OAD-T1	20	1	3.873	415568		MV OAD-T3	44	1	3.881	414761
		2	3.873	417480				2	3.879	414837
MV OBD-T1	21	1	3.873	415231		MV OBD-T3	45	1	3.878	413339
		2	3.872	414433				2	3.882	416607
MV RAD-T1	22	1	3.881	438331		MV RAD-T3	46	1	3.881	581349
		2	3.877	637903				2	3.878	481697
MV RBD-T1	23	1	3.869	580846		MV RBD-T3	47	1	3.883	580866
		2	3.870	581635				2	3.881	579843
MV YA-T2	24	1	3.870	251241		MV WS+8h	48	1	-	-
		2	3.873	251285				2	-	-

Pickerington (PIC) Effluent HPLC Raw Data									
Vial Name	**Vial #**	**Inj. #**	**RT (min)**	**PA (uV*sec)**		**Vial Name**	**Vial #**	**Inj. #**	**RT (min)**	**PA (uV*sec)**
PWS	1	1	-	-		P YB-T2	25	1	3.919	***381264***
		2	-	-				2	3.905	293950
P CC5	2	1	3.880	151409		P OA-T2	26	1	3.906	372023
		2	3.883	141074				2	3.907	371697
P CC10	3	1	3.880	296728		P OB-T2	27	1	3.900	361898
		2	3.881	296536				2	3.902	368715
P CC15	4	1	3.878	436195		P RA-T2	28	1	3.915	602155
		2	3.877	440405				2	3.907	546235
P CC20	5	1	3.880	572085		P RB-T2	29	1	3.905	517556
		2	3.874	573429				2	3.905	518042
P YA-T0	6	1	3.883	322035		P YAD-T2	30	1	3.909	324023
		2	3.880	324675				2	3.907	323908
P YB-T0	7	1	3.882	322332		P YBD-T2	31	1	3.911	323859
		2	3.875	321461				2	3.909	322764
P OA-T0	8	1	3.879	415148		P OAD-T2	32	1	3.907	410036
		2	3.889	414690				2	3.909	409663
P OB-T0	9	1	3.894	409967		P OBD-T2	33	1	3.910	410600
		2	3.897	409646				2	3.912	410728
P RA-T0	10	1	3.892	556078		P RAD-T2	34	1	3.915	567204
		2	3.893	555621				2	3.901	528347
P RB-T0	11	1	3.894	557114		P RBD-T2	35	1	3.909	557890
		2	3.894	559797				2	3.908	557916
P YA-T1	12	1	3.894	316132		P YA-T3	36	1	3.910	262820
		2	3.889	315699				2	3.907	262835
P YB-T1	13	1	3.893	317352		P YB-T3	37	1	3.912	267775
		2	3.895	317777				2	3.911	267452
P OA-T1	14	1	3.896	403632		P OA-T3	38	1	3.912	338035
		2	3.896	404655				2	3.914	338076
P OB-T1	15	1	3.895	402116		P OB-T3	39	1	3.913	338191
		2	3.899	403537				2	3.912	338463
P RA-T1	16	1	3.899	547216		P RA-T3	40	1	3.912	470805
		2	3.897	544764				2	3.913	470631
P RB-T1	17	1	3.895	548968		P RB-T3	41	1	3.917	445642
		2	3.897	548250				2	3.907	467160
P YAD-T1	18	1	3.900	325570		P YAD-T3	42	1	3.911	325146
		2	3.903	325261				2	3.912	324488
P YBD-T1	19	1	3.904	325321		P YBD-T3	43	1	3.885	***159597***
		2	3.904	326248				2	3.888	***194582***
P OAD-T1	20	1	3.905	411507		P OAD-T3	44	1	3.909	411569
		2	3.904	411801				2	3.912	412854
P OBD-T1	21	1	3.867	***11717***		P OBD-T3	45	1	3.911	412049
		2	3.910	438943				2	3.912	414345
P RAD-T1	22	1	3.914	558406		P RAD-T3	46	1	3.911	559382
		2	3.904	561123				2	3.911	559664
P RBD-T1	23	1	3.900	575332		P RBD-T3	47	1	3.912	557724
		2	3.901	557031				2	3.913	557426
P YA-T2	24	1	3.906	298609		P WS+8h	48	1	-	-
		2	3.904	298754				2	-	-

Newark (NEW) Effluent HPLC Raw Data									
Vial Name	**Vial #**	**Inj. #**	**RT (min)**	**PA (uV*sec)**		**Vial Name**	**Vial #**	**Inj. #**	**RT (min)**	**PA (uV*sec)**
NWS	1	1	-	-		N YB-T2	25	1	3.840	257354
		2	-	-				2	3.834	257410
N CC5	2	1	3.839	148285		N OA-T2	26	1	3.832	396051
		2	3.849	147900				2	3.827	393332
N CC10	3	1	3.850	284872		N OB-T2	27	1	3.836	399226
		2	3.852	283434				2	3.830	399459
N CC15	4	1	3.848	428754		N RA-T2	28	1	3.825	555878
		2	3.842	432738				2	3.829	556586
N CC20	5	1	3.847	577368		N RB-T2	29	1	3.833	522055
		2	3.849	578079				2	3.828	552393
N YA-T0	6	1	3.848	280409		N YAD-T2	30	1	3.833	270352
		2	3.846	280428				2	3.827	273167
N YB-T0	7	1	3.841	279203		N YBD-T2	31	1	3.834	276805
		2	3.845	278819				2	3.835	277323
N OA-T0	8	1	3.846	367678		N OAD-T2	32	1	3.832	430846
		2	3.840	428241				2	3.834	430594
N OB-T0	9	1	3.852	411756		N OBD-T2	33	1	3.835	430551
		2	3.822	419153				2	3.834	430134
N RA-T0	10	1	3.821	584605		N RAD-T2	34	1	3.833	590211
		2	3.830	586571				2	3.830	590605
N RB-T0	11	1	3.835	577696		N RBD-T2	35	1	3.839	***664138***
		2	3.834	575279				2	3.830	578076
N YA-T1	12	1	3.837	262967		N YA-T3	36	1	3.834	232629
		2	3.840	270074				2	3.840	232329
N YB-T1	13	1	3.853	285486		N YB-T3	37	1	3.848	246570
		2	3.841	267989				2	3.835	245715
N OA-T1	14	1	3.841	423347		N OA-T3	38	1	3.840	364958
		2	3.842	422867				2	3.837	364450
N OB-T1	15	1	3.839	422782		N OB-T3	39	1	3.842	361760
		2	3.835	422876				2	3.837	363933
N RA-T1	16	1	3.839	543181		N RA-T3	40	1	3.843	507882
		2	3.837	575047				2	3.852	507642
N RB-T1	17	1	3.839	583340		N RB-T3	41	1	3.852	512988
		2	3.839	583528				2	3.853	512474
N YAD-T1	18	1	3.844	277194		N YAD-T3	42	1	3.854	276550
		2	3.847	277602				2	3.853	276184
N YBD-T1	19	1	3.839	277511		N YBD-T3	43	1	3.856	268259
		2	3.859	277036				2	3.847	243864
N OAD-T1	20	1	3.846	430771		N OAD-T3	44	1	3.859	393307
		2	3.835	431116				2	3.853	430451
N OBD-T1	21	1	3.840	431408		N OBD-T3	45	1	3.860	497781
		2	3.833	430452				2	3.848	427827
N RAD-T1	22	1	3.831	591125		N RAD-T3	46	1	3.856	593726
		2	3.836	591975				2	3.850	586160
N RBD-T1	23	1	3.837	592042		N RBD-T3	47	1	3.852	590301
		2	3.833	591037				2	3.849	590562
N YA-T2	24	1	3.834	255415		N WS+8hr	48	1	-	-
		2	3.840	255264				2	-	-

London (LON) Effluent HPLC Raw Data									
Vial Name	**Vial #**	**Inj. #**	**RT (min)**	**PA (uV*sec)**		**Vial Name**	**Vial #**	**Inj. #**	**RT (min)**	**PA (uV*sec)**
LWS	1	1	-	-		L YB-T2	25	1	3.867	234647
		2	-	-				2	3.861	254597
L CC5	2	1	3.820	***57511***		L OA-T2	26	1	3.863	381726
		2	3.851	138761				2	3.867	391762
L CC10	3	1	3.852	298292		L OB-T2	27	1	3.865	389164
		2	3.848	293365				2	3.866	389562
L CC15	4	1	3.850	429752		L RA-T2	28	1	3.865	539624
		2	3.849	429513				2	3.866	539139
L CC20	5	1	3.845	572932		L RB-T2	29	1	3.865	537435
		2	3.874	572580				2	3.865	537551
L YA-T0	6	1	3.849	286740		L YAD-T2	30	1	3.868	286702
		2	3.845	289102				2	3.869	286918
L YB-T0	7	1	3.843	286435		L YBD-T2	31	1	3.869	286801
		2	3.841	286335				2	3.869	286463
L OA-T0	8	1	3.842	430822		L OAD-T2	32	1	3.867	428799
		2	3.841	429600				2	3.868	429008
L OB-T0	9	1	3.838	427966		L OBD-T2	33	1	3.867	429417
		2	3.832	427138				2	3.869	429146
L RA-T0	10	1	3.834	587209		L RAD-T2	34	1	3.868	586048
		2	3.827	586667				2	3.865	582910
L RB-T0	11	1	3.828	586161		L RBD-T2	35	1	3.852	***147629***
		2	3.822	587190				2	3.866	587423
L YA-T1	12	1	3.840	277289		L YA-T3	36	1	3.884	246759
		2	3.854	276991				2	3.873	236376
L YB-T1	13	1	3.858	277458		L YB-T3	37	1	3.868	221968
		2	3.862	277815				2	3.870	223097
L OA-T1	14	1	3.862	417148		L OA-T3	38	1	3.869	341390
		2	3.865	417552				2	3.870	341566
L OB-T1	15	1	3.880	483146		L OB-T3	39	1	3.876	343061
		2	3.880	442586				2	3.874	362758
L RA-T1	16	1	3.884	572491		L RA-T3	40	1	3.871	477130
		2	3.888	571667				2	3.872	476798
L RB-T1	17	1	3.899	563542		L RB-T3	41	1	3.873	490145
		2	3.887	568724				2	3.874	490051
L YAD-T1	18	1	3.890	322674		L YAD-T3	42	1	3.872	290481
		2	3.878	289942				2	3.870	286058
L YBD-T1	19	1	3.874	286214		L YBD-T3	43	1	3.874	285345
		2	3.876	286157				2	3.870	285489
L OAD-T1	20	1	3.887	428373		L OAD-T3	44	1	3.871	428656
		2	3.879	428694				2	3.871	429535
L OBD-T1	21	1	3.872	429365		L OBD-T3	45	1	3.871	429702
		2	3.866	429372				2	3.872	429312
L RAD-T1	22	1	3.863	585975		L RAD-T3	46	1	3.869	586342
		2	3.865	587105				2	3.871	586136
L RBD-T1	23	1	3.866	586898		L RBD-T3	47	1	3.871	586062
		2	3.868	586522				2	3.872	585399
L YA-T2	24	1	3.803	***1707***		L WS+8hr	48	1	-	-
		2	3.821	***5502***				2	-	-

Delaware (DEL) HPLC Data			
Calibration Curve			
Level	Vial Name	[caffeine] (M)	Ave PA (uV*sec)
5 µM	D CC5	5.1086E-06	153512
10µM	D CC10	1.0105E-05	290851
15 µM	D CC15	1.5280E-05	436881
20 µM	D CC20	2.0153E-05	575796
Suntest Data			
Time Name	Temperature (°C)	Radiometer	Elapsed Time (s)
T0	Not recorded	Not recorded	0
R1	24.3	Not recorded	1800.34
T1	25.0	6.109	3600.60
R2	22.1	6.253	7288.61
T2	23.4	6.195	14400.56
T3	23.2	6.276	28811.19

Marysville (MAR) HPLC Data			
Calibration Curve			
Level	Vial Name	[caffeine] (M)	Ave PA (uV*sec)
5 µM	MV CC5	5.0687E-06	144068
10µM	MV CC10	1.0328E-05	260477
15 µM	MV CC15	1.4220E-05	400532
20 µM	MV CC20	1.9190E-05	498961
Suntest Data			
Time Name	Temperature (°C)	Radiometer	Elapsed Time (s)
T0	20.8	6.149	0
R1	23.4	6.206	1921.84
T1	25.0	6.252	3607.49
R2	24.8	6.277	7283.64
T2	24.3	6.327	14401.51
T3	24.3	6.583	28800.20

Pickerington (PIC) HPLC Data			
Calibration Curve			
Level	Vial Name	[caffeine] (M)	Ave PA (uV*sec)
5 µM	P CC5	5.2253E-06	146242
10µM	P CC10	1.0316E-05	296632
15 µM	P CC15	1.5296E-05	438300
20 µM	P CC20	1.9907E-05	572757
Suntest Data			
Time Name	Temperature (°C)	Radiometer	Elapsed Time (s)
T0	19.0	5.629	0
R1	23.3	5.613	1800.07
T1	22.6	5.782	3600.33
R2	23.1	5.779	7200.67
T2	23.3	6.008	14400.23
T3	23.2	5.915	28800.08

Newark (NEW) HPLC Data			
Calibration Curve			
Level	Vial Name	[caffeine] (M)	Ave PA (uV*sec)
5 µM	N CC5	5.1546E-06	148093
10µM	N CC10	1.0184E-05	284153
15 µM	N CC15	1.5023E-05	430746
20 µM	N CC20	1.9790E-05	577724
Suntest Data			
Time Name	Temperature (°C)	Radiometer	Elapsed Time (s)
T0	20.5	5.910	0
R1	24.7	5.887	1800.65
T1	24.9	5.944	3600.13
R2	24.3	6.044	7200.11
T2	24.0	6.030	14399.97
T3	23.8	6.059	28849.07

London (LON) HPLC Data			
Calibration Curve			
Level	Vial Name	[caffeine] (M)	Ave PA (uV*sec)
5 µM	L CC5	4.8700E-06	138761
10µM	L CC10	1.0232E-05	295829
15 µM	L CC15	1.4877E-05	429633
20 µM	L CC20	1.9825E-05	572756
Suntest Data			
Time Name	Temperature (°C)	Radiometer	Elapsed Time (s)
T0	20.8	5.879	0.00
R1	23.8	5.751	1811.19
T1	23.5	5.917	3603.26
R2	25.2	5.948	7250.03
T2	24.3	6.022	14512.51
T3	24.2	6.055	28856.13

Caffeine Level	(g) caffeine	(g) Soln. Mass	(M) Initial [ ]
DEL-Green	0.0308	60.03	5.123E-06
DEL-Yellow	0.0844	60.03	1.404E-05
DEL-Orange	0.1103	61.24	1.799E-05
MAR-Yellow	0.0591	59.99	9.837E-06
MAR-Orange	0.0884	60.05	1.470E-05
MAR-Red	0.1241	60.04	2.064E-05
PIC-Yellow	0.0688	60.01	1.145E-05
PIC-Orange	0.0869	60.08	1.444E-05
PIC-Red	0.1183	60.04	1.968E-05
NEW-Yellow	0.0586	60.11	9.735E-06
NEW-Orange	0.0904	60.03	1.504E-05
NEW-Red	0.1258	60.11	2.090E-05
LON-Yellow	0.0605	60.18	1.004E-05
LON-Orange	0.0913	60.17	1.515E-05
LON-Red	0.1252	60.17	2.078E-05

Initial concentration of probe as noted in the table above was calculated from the physical addition of solid caffeine to Milli-Q water or working solution. Initial concentrations used for calculations in this project were obtained by finding the initial concentration of probe (caffeine) at time T0 via back-calculation using the LINEST function in Excel based on experimentally obtained values from dark vial controls for each experiment.